

INFORMATION TO USERS

This manuscript has been reproduced from the microfilm master. UMI films the text directly from the original or copy submitted. Thus, some thesis and dissertation copies are in typewriter face, while others may be from any type of computer printer.

The quality of this reproduction is dependent upon the quality of the copy submitted. Broken or indistinct print, colored or poor quality illustrations and photographs, print bleedthrough, substandard margins, and improper alignment can adversely affect reproduction.

In the unlikely event that the author did not send UMI a complete manuscript and there are missing pages, these will be noted. Also, if unauthorized copyright material had to be removed, a note will indicate the deletion.

Oversize materials (e.g., maps, drawings, charts) are reproduced by sectioning the original, beginning at the upper left-hand corner and continuing from left to right in equal sections with small overlaps.

Photographs included in the original manuscript have been reproduced xerographically in this copy. Higher quality 6" x 9" black and white photographic prints are available for any photographs or illustrations appearing in this copy for an additional charge. Contact UMI directly to order.

Bell & Howell Information and Learning
300 North Zeeb Road, Ann Arbor, MI 48106-1346 USA

UMI[®]
800-521-0600



**GLYCOPROTEIN IIb-IIIa-LIPOSOMES BIND
FIBRINOGEN BUT DO NOT UNDERGO FIBRINOGEN-
MEDIATED AGGREGATION**

by

Stephen Michael Sloan
Department of Physiology
McGill University
Montreal, Quebec

August 1997

A thesis submitted to the Faculty of Graduate Studies and Research in partial fulfillment
of the degree of Master of Science.

© Stephen Sloan, 1997





National Library
of Canada

Acquisitions and
Bibliographic Services

395 Wellington Street
Ottawa ON K1A 0N4
Canada

Bibliothèque nationale
du Canada

Acquisitions et
services bibliographiques

395, rue Wellington
Ottawa ON K1A 0N4
Canada

Your file *Votre référence*

Our file *Notre référence*

The author has granted a non-exclusive licence allowing the National Library of Canada to reproduce, loan, distribute or sell copies of this thesis in microform, paper or electronic formats.

The author retains ownership of the copyright in this thesis. Neither the thesis nor substantial extracts from it may be printed or otherwise reproduced without the author's permission.

L'auteur a accordé une licence non exclusive permettant à la Bibliothèque nationale du Canada de reproduire, prêter, distribuer ou vendre des copies de cette thèse sous la forme de microfiche/film, de reproduction sur papier ou sur format électronique.

L'auteur conserve la propriété du droit d'auteur qui protège cette thèse. Ni la thèse ni des extraits substantiels de celle-ci ne doivent être imprimés ou autrement reproduits sans son autorisation.

0-612-44281-0

Canada

ABSTRACT

Platelet aggregation is mediated primarily by the binding of fibrinogen to its membrane receptor, GPIIb-IIIa, but such an interaction may not be sufficient to support aggregation. This question could potentially be resolved by reconstituting GPIIb-IIIa into a model membrane system.

A protocol was developed for the generation of liposomes containing purified GPIIb-IIIa. Flow cytometric techniques confirmed that the receptor was present in the lipid bilayer and were used to evaluate the characteristics of fibrinogen binding to the liposomes, which like fibrinogen-platelet interactions exhibited specificity, saturability, time-dependence, and calcium-dependence.

No fibrinogen-specific aggregation of GPIIb-IIIa-liposomes with stir or shear was observed, as determined by flow cytometric cell counting and microscopic examination of particles. In contrast, platelets rapidly formed large aggregates in the presence of fibrinogen. It thus appears that elements other than fibrinogen and GPIIb-IIIa play an important role in platelet aggregation.

RÉSUMÉ

L'agrégation des plaquettes arrive principalement grâce à la reliure de fibrinogène à son récepteur de la membrane, GPIIb-IIIa, mais il n'est pas clair si cette interaction est suffisante pour soutenir l'agrégation. On pourrait peut-être résoudre cette question en reconstituant GPIIb-IIIa dans une membrane modèle.

Un protocole a été développé pour la formation de liposomes qui contenaient de la GPIIb-IIIa purifiée. Des techniques de cytomètre en flu ont confirmé que le récepteur se trouvait bien dans la membrane. Ces techniques ont aussi montré que, comme pour l'interaction de fibrinogène avec les plaquettes, la reliure de fibrinogène aux liposomes était spécifique et saturable, et dépendait sur le temps ainsi que sur le calcium.

Les liposomes qui contenaient GPIIb-IIIa ne se sont pas spécifiquement agrégés en la présence de fibrinogène après agitation ou cisaillement; ceci a été conclu en comptant les cellules avec le cytomètre en flu et en les observant par microscope. Par contre, les plaquettes ont rapidement formé de grands agrégats en la présence de fibrinogène. Il paraît donc que des éléments à part le fibrinogène et la GPIIb-IIIa jouent un grand rôle dans l'agrégation des plaquettes.

TO ANDREA

Thank you for believing in me, for all your encouragement and support, and above all, for your love. This thesis would not have been possible without your inspiration and motivation.

ACKNOWLEDGEMENTS

I would like to express my most sincere appreciation to my supervisor, Dr. Mony Frojmovic, for his guidance, support, and patience throughout the course of this project. I am particularly indebted to him for taking me on as a Master's student part way through my degree, and for having confidence in my abilities when preliminary experiments were less than encouraging.

The advice and assistance given to me by the "Blood Lab" research associate, Bobbi Brown, and my fellow graduate students, Qingde Liu, Ana Kasirer-Friede, and Esther Levine, has been invaluable and is truly appreciated. In addition to your numerous helpful suggestions, I am grateful for your ongoing friendship and encouragement. I would especially like to thank Bobbi for having isolated and purified the GPIIb-IIIa, and Liu for preparing the activated, fixed platelets.

A kind thank you goes to Drs. J. Silvius, H. Goldsmith, R. Sipehia, and T.M.S. Chang, for your helpful advice and suggestions. As well, I am grateful to the other members of the Artificial Cells and Organs Research Centre for their technical assistance.

To Lawrence Le and Amole Khadilkar, thank you for your friendship.

Last but not least, I would like to express my deepest appreciation to my parents for their love, guidance, and encouragement throughout my studies. Thank you also to my siblings and grandparents, and to Jorge and Marina Gutman, for your support.

TABLE OF CONTENTS

ABSTRACT	i
RÉSUMÉ	ii
ACKNOWLEDGEMENTS	iv
TABLE OF CONTENTS	v
LIST OF FIGURES	vii
LIST OF TABLES	viii
INTRODUCTION	1
BACKGROUND	6
Part 1	
The integrin superfamily	6
Platelet membrane glycoproteins	9
The GPIIb-IIIa complex	11
Glanzmann's thrombasthenia and GPIIb-IIIa polymorphisms	15
Platelet activation and aggregation	16
Activation of GPIIb-IIIa and ligand binding	18
GPIIb-IIIa ligands	23
Fibrinogen (Fg)	23
von Willebrand Factor (vWF)	29
Thrombospondin-1 (TSP-1)	30
Fibronectin (Fn)	32
Vitronectin (Vn)	33
Collagen type I (Col I)	34
GPIIb-IIIa antagonists	35
Post-occupancy events	35
Platelet lipids	36
Part 2	
Liposomes	41
Preparation of liposomes	42
Reconstitution of membrane proteins into liposomes	43
Liposome-liposome interactions	47
Liposome adhesion to surfaces	48

MATERIALS	49
EXPERIMENTAL METHODS	51
Preparation of liposomes	51
Quantitative analysis of liposome lipid	51
Characterization of liposomes and platelets	53
Solubilization of liposomes by octyl glucoside	54
Flow cytometry	54
Spectrophotometry	54
Preparation of GPIIb-IIIa-liposomes	55
Fluorescent labelling of Fg and mAb's	56
Calibration of FACScan fluorescence	57
Test for the presence of GPIIb-IIIa in the liposomes	57
FITC-Fg binding to liposomes or platelets	58
Stir-induced aggregation studies	59
Shear-induced aggregation studies	60
Binding of liposomes or platelets to Fg immobilized on latex beads	62
Binding of mAb's to GPIIb-IIIa-bound Fg	63
RESULTS AND DISCUSSION	65
Characterization of control-liposomes	65
Liposome solubilization by octyl glucoside	69
Flow cytometry	69
Spectrophotometry	69
Characterization of FITC-Fg	73
Calibration of FACScan fluorescence	73
Preparation and characterization of GPIIb-IIIa-liposomes	75
Fg binding to GPIIb-IIIa-liposomes	80
Aggregation studies	90
Characterization of Fg- and Alb-beads	99
Co-aggregation of beads with liposomes or platelets	101
Binding of mAb's to GPIIb-IIIa-bound Fg	104
CONCLUSIONS	108
REFERENCES	111

LIST OF FIGURES

Figure I:	Hemostasis	2
Figure II:	Hemostasis versus thrombosis	2
Figure III:	Fibrinogen binding to platelets and reversible aggregation	4
Figure IV:	Irreversible platelet aggregation	4
Figure V:	The GPIIb-IIIa complex	14
Figure VI:	Integrin-mediated inside-out signalling	20
Figure VII:	Fibrinogen	24
Figure VIII:	Platelet crosslinking by Fg	26
Figure IX:	Integrin-mediated outside-in signalling	37
Figure X:	Lipid structures	39
Figure XI:	Common detergents	45
Figure XII:	Membrane protein reconstitution	46
Figure XIII:	Preparation of liposomes by reverse phase evaporation	52
Figure XIV:	Micro-couette	61
Figure 1:	FACScan scatter profiles of control-liposomes and fixed platelets	68
Figure 2:	Liposome and platelet FACScan histograms	68
Figure 3:	FACScan scatter profile of liposomes in the presence of octyl glucoside	71
Figure 4:	Effect of octyl glucoside concentration on number of liposomes	71
Figure 5:	Effect of octyl glucoside concentration on liposome turbidity	72
Figure 6:	FACScan fluorescence calibration curve	74
Figure 7:	FSC and SSC histograms for GPIIb-IIIa-liposomes	78
Figure 8:	Fluorescence histogram of FITC-AP-2 binding to liposomes and platelets	78
Figure 9:	Contour plot of FITC-AP-2 binding to GPIIb-IIIa-liposomes and platelets	79
Figure 10a:	Fluorescence histogram of FITC-Fg binding to liposomes and platelets	84
Figure 10b:	Specificity of FITC-Fg binding to liposomes and platelets	84
Figure 11a:	Saturability of FITC-Fg binding to liposomes and platelets	86
Figure 11b:	Concentration-dependence of GPIIb-IIIa*-liposome receptor occupancy by FITC-Fg	86
Figure 11c:	Scatchard plot of FITC-Fg binding to GPIIb-IIIa*-liposomes	87
Figure 12a:	Time-dependence of FITC-Fg binding to liposomes and platelets	87
Figure 12b:	Time-dependence of FITC-Fg binding to GPIIb-IIIa*-liposomes for two different Fg concentrations	88
Figure 12c:	Time-dependence of GPIIb-IIIa*-liposome receptor occupancy by FITC-Fg	88
Figure 13:	Calcium-dependence of FITC-Fg binding to liposomes and platelets	89
Figure 14:	Specificity of FITC-PAC-1 binding to liposomes and platelets	89

Figure 15a:	Change in liposome # with stir at 1000 rpm in the presence or absence of 500 nM Fg	95
Figure 15b:	Change in liposome # with stir at 250 rpm in the presence of 500 nM Fg \pm Ro	95
Figure 15c:	Change in platelet # for AFP with stir at 1000 rpm	96
Figure 16a:	Singlet-aggregate distribution of GPIIb-IIIa*-liposomes with stir at 250 rpm	97
Figure 16b:	Singlet-aggregate distribution of platelets with stir at 1000 rpm	97
Figure 17:	Change in liposome # with stir at 1000 rpm in the presence of 100 nM Fg \pm Ro	98
Figure 18:	Change in liposome # with shear at 50 s ⁻¹ in the presence or absence of 500 nM Fg \pm Ro	98
Figure 19a:	FACScan Fg-bead scatter profile	100
Figure 19b:	Fluorescence histograms of Fg- and Alb-beads	100
Figure 20a:	Change in liposome # with stir at 1000 rpm in the presence of Fg- or Alb-beads	102
Figure 20b:	Change in Fg- or Alb-bead # after 1000 rpm stir in the presence of liposomes	102
Figure 21a:	Change in platelet # after 1000 rpm stir in the presence of Fg- or Alb-beads	103
Figure 21b:	Change in Fg- or Alb-bead # after 1000 rpm stir in the presence of platelets	103
Figure 22a:	Specificity of FITC-4A5 binding to Fg immobilized on liposomes and platelets	106
Figure 22b:	Specificity of FITC-anti-Fg-RIBS-I binding to Fg immobilized on liposomes and platelets	106
Figure 23:	Time-dependence of FITC-4A5 binding to Fg immobilized on liposomes and platelets	107

LIST OF TABLES

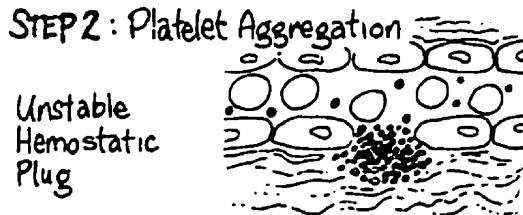
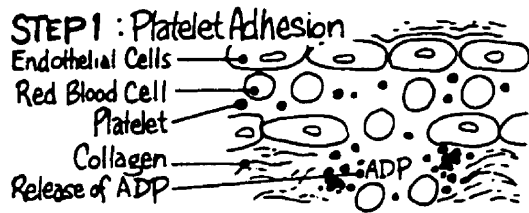
Table I:	Phospholipid:cholesterol and phosphatidylcholine:phosphatidylserine ratios in platelet membranes and REV liposomes	67
Table II:	Theoretical and experimental values of R_{sat} and R_{sol} for three lipid concentrations in the presence of octyl glucoside	72
Table III:	Estimated GPIIb-IIIa surface density on platelets and liposomes	79
Table IV:	B_{max} and # of Fg/GPIIb-IIIa for GPIIb-IIIa-liposomes	85
Table V:	B_{max} and # of Fg/GPIIb-IIIa for activated, fixed platelets	85

INTRODUCTION

Platelet aggregation is an essential component of both hemostasis and thrombosis. **Hemostasis** refers to the normal physiological mechanism for arresting local blood flow at a site of vessel wall damage [Hirsh & Brain 1979]. Within seconds of injury platelets adhere to the exposed subendothelial matrix and become activated: they change shape by spreading out and forming pseudopods, and secrete **lysosomal, dense, and α -granules** [Gerrard 1988; Holmsen 1994]. These granules release many different types of molecules into the surrounding environment, including adhesive proteins, coagulation and growth factors, acid hydrolases, and platelet agonists such as **adenosine diphosphate (ADP)**. Increased plasma levels of ADP and generation of the lipid metabolite **thromboxane A₂** will recruit additional platelets to the site of injury, where they aggregate to form a **primary hemostatic plug**. After a few minutes this becomes a **secondary hemostatic plug** due to stabilization by a network of insoluble fibrin polymers, which are the final products of the coagulation cascade. However, the abnormal activation of platelets and/or the clotting factors, known as **thrombosis**, may lead to the formation of an intravascular platelet plug (**thrombus**). Thrombi often break away from the vessel wall and are transported through the circulation to a distant site such as the heart or brain, where they can become lodged in small or atherosclerotic vessels, severely restricting blood flow and eventually provoking a myocardial infarction or stroke. The three steps of hemostasis are illustrated in Figure I, while a brief comparison of hemostasis and thrombosis is shown in Figure II.

Figure I: Hemostasis (from Hirsh & Brain 1979, p. 4)

Formation of Unstable Platelet Plug



Stabilization of Plug with Fibrin

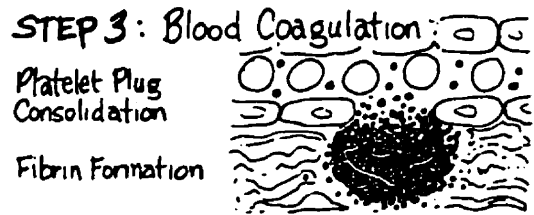
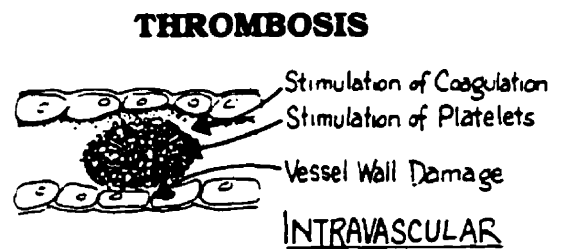
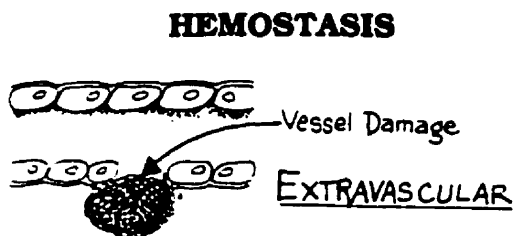


Figure II: Hemostasis versus thrombosis (from Hirsh & Brain 1979, p. 83)



In both hemostasis and thrombosis, platelet aggregation is mediated primarily by the binding of **fibrinogen (Fg)** to its platelet membrane receptor, **the glycoprotein (GP) IIb-IIIa complex** [Bennett & Vilaire 1979; Marguerie et al. 1979]. GPIIb-IIIa on resting platelets is unable to bind Fg, but after platelet activation by ADP or other weak agonists the receptor undergoes a conformational change which allows it to interact with plasma fibrinogen [Leung & Nachman 1986]. Another site on the same Fg can then bind to a GPIIb-IIIa receptor on an adjacent platelet, crosslinking the two platelets to induce reversible microaggregation; this is illustrated by Figure III. Stronger activators such as thrombin or collagen will also cause platelets to secrete α -granules, which release - among other molecules - the adhesive proteins Fg, **thrombospondin-1 (TSP-1)**, and **von Willebrand Factor (vWF)** [Gerrard 1988]. As depicted in Figure IV, TSP-1 binds directly to Fg as well as to one or more platelet receptors, helping to form stable, irreversible macroaggregates which can be detected by changes in light transmission. Platelet aggregation is further enhanced by the progressive irreversibility of Fg binding over time and the expression of various neoepitopes on Fg and GPIIb-IIIa [Shattil 1993], as well as by clustering of the receptor in the membrane, association with membrane proteins like **p24**, and attachment to the actin cytoskeleton [Nurden 1994]. In the absence of Fg and/or under the high flow conditions of the microcirculation, vWF can also bind to GPIIb-IIIa and mediate platelet aggregation [Peterson et al. 1987; Ikeda et al. 1991].

Figure III: Fibrinogen binding to platelets and reversible aggregation (from Leung & Nachman 1986, Fig. 2)

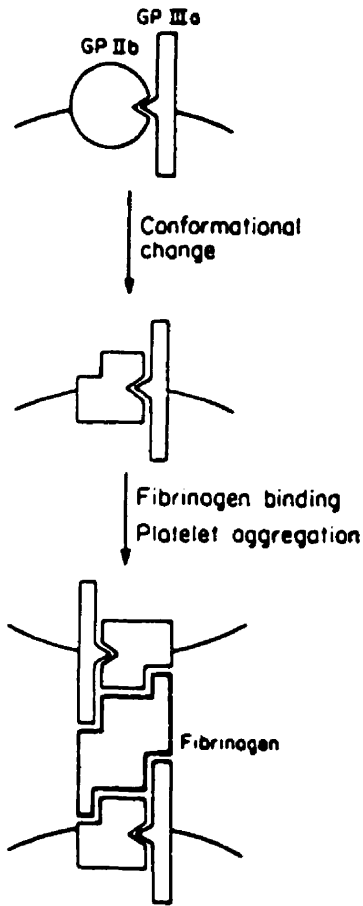
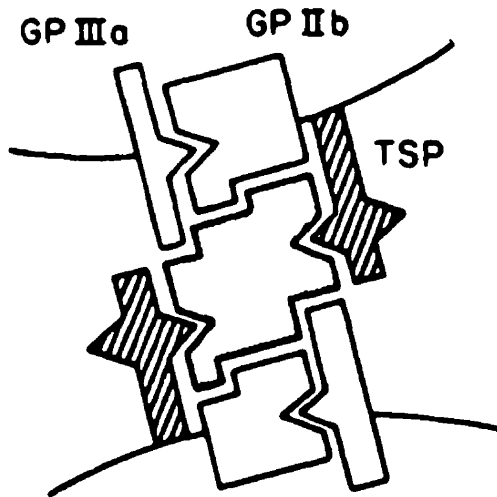


Figure IV: Irreversible platelet aggregation (from Leung & Nachman 1986, Fig. 3)



Despite extensive research into the mechanisms of platelet aggregation, it is still not clear whether under normal physiological conditions the interaction between Fg and GPIIb-IIIa is sufficient to support this process. This question has been addressed through the use of systems less complex than the native platelet, such as latex beads coupled to purified GPIIb-IIIa or intact platelet membranes [Gawaz et al. 1996; E Brown & M Frojmovic, unpublished experiments], but this setup does not adequately mimic the flexibility of the platelet membrane. These investigators have also developed a cell line expressing recombinant GPIIb-IIIa [Frojmovic et al. 1991a]; however, this receptor may have different characteristics than the platelet protein, such as a lack of glycosylation. Other groups have studied the Fg-GPIIb-IIIa interaction by incorporating the purified receptor into the bilayer of artificial lipid vesicles known as **liposomes**, which are commonly used as model membrane systems [Baldassare et al. 1985; Parise & Phillips 1985; Pytela et al. 1986; Rybak 1986]. Previous work has shown that liposomes containing GPIIb-IIIa are able to bind fibrinogen and other ligands, but only one study has looked at the ability of such liposomes to be crosslinked by Fg, with inconclusive results. In addition, the relative contributions to platelet aggregation of proteins other than GPIIb-IIIa, receptor mobility within the membrane, and phospholipid composition, could all be potentially evaluated through the use of liposomes.

The objectives of this study were fourfold: to prepare phospholipid/cholesterol vesicles of a size similar to platelets; to insert purified GPIIb-IIIa into the lipid membrane; to investigate the Fg-binding characteristics of these liposomes; and to determine whether the vesicles were capable of undergoing Fg-mediated aggregation. It will be shown that GPIIb-IIIa-liposomes are able to bind Fg in a manner similar to platelets, but cannot specifically aggregate in the presence of Fg.

BACKGROUND PART 1

The integrin superfamily

Glycoprotein IIb-IIIa belongs to the **integrin superfamily of cell adhesion receptors**. The members of this family are found in a wide variety of organisms, where they are involved in diverse biological processes such as survival, proliferation, differentiation, morphogenesis, and migration [Hynes 1992]. Integrins function as important links between the cell interior and exterior, helping to transmit information across the membrane in both directions: they mediate cell adhesion to the **extracellular matrix (ECM)** and other cells, and anchor the cytoskeleton to the plasma membrane [Dedhar & Hannigan 1996]. In addition, integrins are significant players in cellular events like changes in cell shape and intracellular pH, induction of protein phosphorylation, and gene transcription. All integrins consist of two noncovalently associated subunits, of which the higher molecular weight component is referred to as the **α -subunit** and the lower molecular weight one as the **β -subunit** [Plow & Ginsberg 1989]. Within the integrin superfamily there exist three main subfamilies which each share a common β -subunit (β_1 , β_2 , or β_3), but other heterodimers have distinct β -chains (β_4 to β_8) [Gille & Swerlick 1996]. Seventeen different α -chains have been identified, some of which can associate with more than one β -subunit, giving a total of twenty-three known integrins.

The largest integrin subfamily is the **β_1 (CD29) or Very Late Antigen (VLA) receptor** subfamily, which is made up of ten members, having α -chains α_{1-9} and α_v [Plow & Ginsberg 1989; Gille & Swerlick 1996]. These molecules are expressed on almost all cells, where they are indispensable in promoting adherence to the ECM; many β_1 integrins are receptors for matrix proteins such as laminin (Ln), fibronectin (Fn), and various types of collagen (Col). Unlike its fellow β_1 integrins **VLA-4 ($\alpha_4\beta_1$)** is restricted to blood and tumour cells, where it helps to mediate attachment to the vessel wall via interactions with endothelial cell (EC) vascular cell adhesion molecule-1 (VCAM-1) [Hynes 1992]. Other VLA integrins appear to play a role in leukocyte extravasation and migration into inflamed tissues.

The four members of the β_2 (CD18) or leukocyte adhesion receptor (Leu-CAM) subfamily were thought to be specific to leukocytes, but β_2 integrins have recently been detected on platelets and on several megakaryocyte (MK) cell lines [Gille & Swerlick 1996; Philippeaux et al. 1996]. **LFA-1** ($\alpha_L\beta_2$ or **CD11a/CD18**) is present on various leukocytes, where its main function is mediating cell adhesion to and migration through the endothelium; it binds to intercellular adhesion molecule (ICAM)-1, -2, and -3¹. **MAC-1** ($\alpha_M\beta_2$, **CD11b/CD18**, or **CR3**) and **p150,95** ($\alpha_X\beta_2$, **CD11c/CD18**, or **CR4**) are found on monocytes/macrophages and neutrophils (PMN); they both bind to fibrinogen (Fg) and the inactivated form of the complement protein C3b (C3bi), helping to mediate phagocytosis and leukocyte adherence, while MAC-1 also interacts with Fn, ICAM-1, and one of the coagulation factors, Factor X. $\alpha_D\beta_2$ (**CD11d/CD18**) is expressed on PMN, T-cells, and macrophages; it binds to ICAM-3 [Van der Vieren et al. 1995].

A number of adhesion molecules, including Fg, Fn, von Willebrand Factor (vWF), and vitronectin (Vn), bind to the three members of the β_3 (CD61) or cytoadhesin subfamily [Gille & Swerlick 1996]. **Glycoprotein IIb-IIIa** ($\alpha_{IIb}\beta_3$ or **CD41/CD61**) is well known as a platelet receptor for Fg and other adhesive proteins, but has also been found on monocytes and various tumour cells; on the latter it helps to mediate interactions with platelets, EC, and the subendothelium [Prieto et al. 1994; Trikha et al. 1996]. The **Vn receptor** ($\alpha_V\beta_3$ or **CD51/CD61**), is expressed by many cells and has been implicated in adhesion, angiogenesis, and inhibition of apoptosis. The **leukocyte response integrin** (**LRI** or $\alpha_R\beta_3$) is found on PMN and macrophages, where it plays a role in phagocytosis, adhesion, and chemotaxis [Gresham et al. 1992]. All three cytoadhesins can recognize and bind to a particular sequence on their ligands, **Arg-Gly-**

¹ ICAM-1 (CD54) is found on a variety of cells, ICAM-2 (CD102) is present on EC, leukocytes, and platelets, and ICAM-3 (CD50) is expressed exclusively on leukocytes [Haskard 1994; Diacovo et al. 1994].

Asp-X (RGDX or RGD)², where X could be any amino acid but is often a serine, phenylalanine, or valine [Plow & Ginsberg 1989]. GPIIb-IIIa and the LRI - but not $\alpha_v\beta_3$ - also interact with the **H12** dodecapeptide found at the carboxyl-terminus of the Fg γ chain, which does not contain the RGD sequence [Savage et al. 1995]. In addition to the cytoadhesins, five members of the β_1 subfamily ($\alpha_3\beta_1$, $\alpha_5\beta_1$, $\alpha_8\beta_1$, $\alpha_9\beta_1$, and $\alpha_v\beta_1$) and three other integrins with an α_v subunit ($\alpha_v\beta_5$, $\alpha_v\beta_6$, and $\alpha_v\beta_8$) participate in RGD-mediated ligand binding [Schnapp et al. 1995].

As mentioned above, the α_v subunit can pair with the β_5 , β_6 , and β_8 chains to form heterodimers which bind RGD-containing proteins. There are also three other integrins which do not fit into one of the major subfamilies: $\alpha_4\beta_7$, which is found on lymphocytes and is involved in T-cell homing to lymph nodes as well as B-cell interactions with Fn and VCAM-1; $\alpha_E\beta_7$, which mediates the binding of gut and skin T-cells to epithelial tissue E-cadherin; and $\alpha_6\beta_4$, which binds to Ln and is present on EC, epithelial cells, and Schwann cells [Gille & Swerlick 1996].

The eight integrin β -subunits are transmembrane glycoproteins - with a single transmembrane domain - and have 40-48% amino acid homology [Hynes 1992]. Except for β_4 , all these proteins have short cytoplasmic tails of 50 amino acids (a.a.) or less and molecular weights of 90-110 kDa; β_4 has a very large cytoplasmic domain of over 1000 a.a. and thus a much higher molecular weight (M_r) [Gille & Swerlick 1996]. Each chain has four cysteine-rich tandem repeats within the extracellular domain, with the consensus sequence X-Cys-X-X-Cys-X-Cys [Phillips et al. 1988]. Similar sequences have been found in other cell membrane receptors, such as the low-density lipoprotein (LDL) receptor, the epidermal growth factor (EGF) receptor, and the insulin receptor, and may represent a ligand binding site. Another highly conserved extracellular region contains the

² The RGD sequence is found in more than one hundred proteins; a number of these - Fg, vWF, Fn, Vn, thrombospondin-1 (TSP-1), Ln, Col types I and IV, and entactin, among others - serve as adhesion molecules [Yamada & Kleinman 1992; Gille & Swerlick 1996].

metal ion-dependent adhesion site (MIDAS) motif, Arg-X-Ser-X-Ser, which has been implicated in cation-dependent ligand binding.

The α -chains are more heterogeneous than their heterodimer partners, but like the β -subunits they are primarily extracellular [Hynes 1992]. Some consist of a single chain which passes once through the membrane, while others are made up of two chains linked by one or more disulfide bonds: a heavy chain which is entirely extracellular, and a light chain with one transmembrane domain. However, all α -subunits have a seven-fold repeat of homologous domains, three or four of which contain sequences of twelve amino acids resembling the calcium-binding domains of proteins such as calmodulin and troponin C, known as **EF hands** [Phillips et al. 1988]. In several α -chains, such as those which pair with the β_2 subunits, an additional sequence of around 200 a.a. - known as the **inserted or I domain** - is found between the second and third repeats [Schwartz et al. 1995; Gille & Swerlick 1996]. This sequence contains a MIDAS motif and shares significant homology with complement proteins as well as the collagen-binding domains of vWF.

Platelet membrane glycoproteins

Two integrins from the β_3 subfamily are platelet membrane receptors for a number of adhesive proteins. **GPIIb-IIIa** - the most abundant platelet integrin - mediates adhesion and aggregation primarily via interactions with vWF and Fg, respectively, and will be discussed in detail below. The role of platelet $\alpha_v\beta_3$ is uncertain, as only 50-100 copies exist per cell, but it likely participates in adhesion to the subendothelium and may be important in the absence of functional GPIIb-IIIa [Coller et al. 1991]. Platelets also have three β_1 integrins which promote attachment to the ECM: **GPIa-IIa** ($\alpha_2\beta_1$ or **VLA-2**), a receptor for Col; **GPIc-IIa** ($\alpha_5\beta_1$ or **VLA-5**), a receptor for Fn; and **GPIc'-IIa** ($\alpha_6\beta_1$ or **VLA-6**), a receptor for Ln [Charo et al. 1994; Gille & Swerlick 1996]. Approximately 1000 copies of each of these three integrins exist on the platelet surface [Coller et al. 1995].

Another prominent group of glycoproteins makes up the **GPIb-IX-V complex**, with about 25 000 copies per platelet [Charo et al. 1994]. The complex is composed of

four non-covalently associated subunits - disulfide-linked **GPIb α (CD42b)** and **GPIb β (CD42c)**, **GPIX (CD42a)**, and **GPV (CD42d)** - which are all members of the leucine-rich glycoprotein (LRG) gene family. Binding of GPIb to ECM-immobilized vWF is essential for platelet adhesion and aggregation, particularly under the high flow conditions found in small vessels [Nurden 1994]. In patients with a bleeding disorder known as **Bernard-Soulier syndrome (BSS)** the GPIb-IX-V complex is absent or dysfunctional, leading to a marked reduction in platelet attachment to the subendothelium [George & Nurden 1994]. Other functions of GPIb include helping to maintain platelet shape via a cytoplasmic association with actin-binding protein (linked to a network of actin filaments), and acting as a high affinity receptor for thrombin on the platelet surface. GPV is a substrate for thrombin on resting platelets and may act as a low affinity thrombin receptor.

Many other glycoproteins are present in the plasma membrane of unactivated platelets. **GPIV (GPIIb or CD36)** is a Ca^{2+} -dependent platelet receptor for TSP-1 and collagen which is additionally expressed on monocytes, EC and melanoma cells [Charo et al. 1994; Nurden 1994]. Col appears to interact with **GPVI (P62)** and an 85-90 kDa glycoprotein as well, while besides $\alpha_6\beta_1$ Ln can bind to a 67 kDa receptor also found on various tumour cells [Tandon et al. 1991; Sixma 1994; Kehrel 1995]. **Integrin-associated protein (IAP or CD47)** and **platelet endothelial cell adhesion molecule-1 (PECAM-1 or CD31)** are members of the immunoglobulin superfamily³ [Haskard 1994]. IAP is linked to $\alpha_v\beta_3$ in platelets and to $\alpha_r\beta_3$ in leukocytes, where it modulates integrin activity; this glycoprotein is a cation-independent receptor for TSP-1 on platelets, and may help to regulate activation and aggregation [Brown et al. 1990; Dorahy et al. 1997]. PECAM-1 is found on platelets, EC, monocytes, and PMN; after platelet activation it is redistributed in the membrane and becomes associated with the cytoskeleton. **p24 (CD9)** associates with GPIIb-IIIa upon platelet stimulation, and may play a role in Ca^{2+} -dependent platelet activation and aggregation [Slupsky et al. 1989]. It belongs to the

³ VCAM-1 (CD106) and the three ICAM's are also members of this family

quadraspanin family of membrane proteins and in addition to platelets is present on other cells such as EC, smooth muscle cells (SMC), and fibroblasts. Other platelet glycoproteins important in aggregation are receptors for various agonists such as **thrombin⁴**, **ADP**, **serotonin**, **thromboxane A₂**, **platelet-activating factor (PAF)**, and **epinephrine** [Hawiger et al. 1994].

Several of the above glycoproteins - like GPIIb-IIIa, GPIV, PECAM-1, and p24 - are found in α -granule membranes [Cramer et al. 1994]. Upon platelet activation the granules fuse with the plasma membrane, leading to increased surface levels of these proteins. However, platelet granules also contain other glycoproteins which are virtually absent from resting platelets, and are only expressed on the surface once the platelet becomes activated. **P-selectin (GMP-140, PADGEM, or CD62P)** is a member of the selectin superfamily which is found in platelet α - and dense granules as well as the Weibel-Palade bodies of EC [Nurden 1994]. This glycoprotein regulates PAF synthesis and phagocytosis by monocytes, helps to mediate the adhesion of leukocytes to activated platelets and EC at sites of inflammation or thrombosis, and serves as a useful marker for platelet activation [Elstad 1995]. The latter is also true of the lysosome-associated membrane proteins **LAMP-1 (CD107a)**, **LAMP-2 (CD107b)**, and **LAMP-3 (CD63)**, which are found in lysosomal granule membranes of platelets, macrophages, fibroblasts, and lymphocytes; LAMP-2 and -3 are present in platelet dense granules as well [Metzelaar & Clevers 1992; Israels et al. 1996]. As LAMP's are rich in polylectosaminoglycans they may serve as platelet ligands for molecules such as endothelial cell P- and E-selectin. This heavy glycosylation could also help to protect the plasma membrane from degradation by released lysosomal enzymes.

The GPIIb-IIIa complex

The glycoprotein IIb-IIIa complex is the most abundant protein in the platelet plasma membrane, accounting for 3% of all platelet proteins and 17% of membrane

⁴ this receptor is distinct from GPIb and GPV

protein by weight [Calvete 1995]. Like other integrins GPIIb-IIIa is a heterodimer composed of an α -subunit (GPIIb or α_{IIb}) and a β -subunit (GPIIIa or β_3), which self-assemble in a 1:1 ratio in the presence of calcium [Phillips et al. 1992]. Sodium dodecyl sulfate (SDS) electrophoresis determined the molecular weights of GPIIb and GPIIIa to be 136 and 95 kDa respectively, with the M_r of the entire complex around 265 kDa; both proteins are approximately 15% carbohydrate by weight (14% for GPIIb and 16% for GPIIIa). β_3 - as mentioned above - also associates with α_v and α_R on various cells, but α_{IIb} has no other integrin partners.

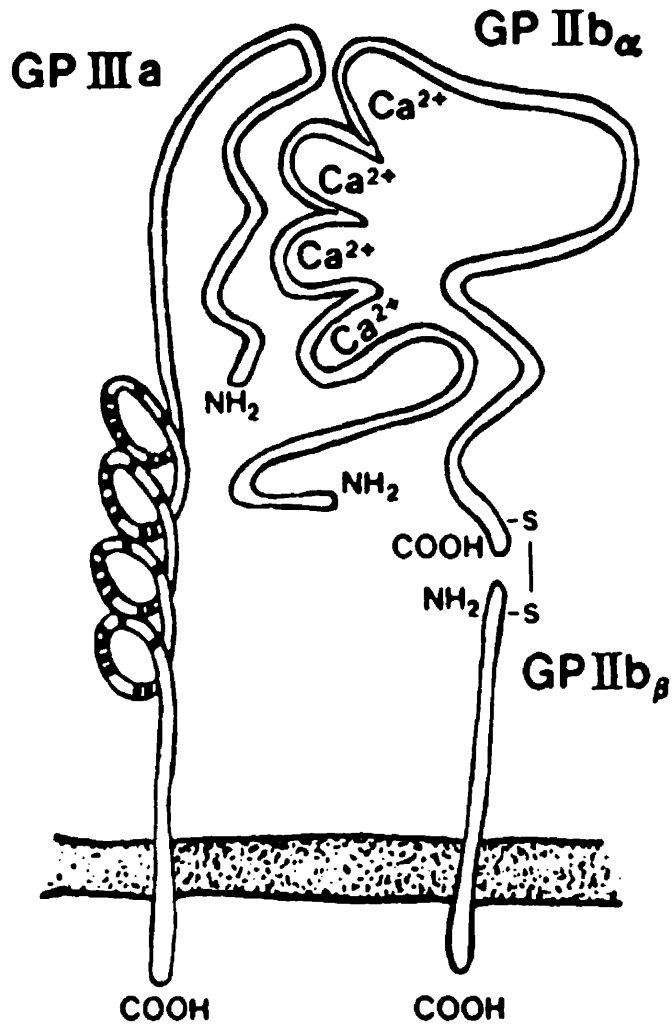
The genes encoding GPIIb and GPIIIa are linked together on the long arm of chromosome 17, at q21-22; the GPIIb gene spans 17.2 kb and contains 30 exons, while the GPIIIa gene is 46 kb long and contains 14 exons [Calvete 1995]. Both proteins are synthesized as single-chain precursors, which associate in the endoplasmic reticulum where they undergo N-linked glycosylation. Carbohydrate processing and addition of O-linked chains occurs in the Golgi, where pre-GPIIb is cleaved into two chains linked by a disulfide bond: an 856 a.a., 114 kDa heavy chain (GPIIb_h or GPIIbH) and a 149 a.a., 23 kDa light chain (GPIIb_l or GPIIbL) [Newman 1991; Calvete 1994]. GPIIb_h is entirely extracellular, while GPIIb_l has extracellular, transmembrane, and cytoplasmic domains (a.a. 1-103, 104-129, and 130-149, respectively). The mature form of GPIIIa remains as a single chain and has 762 a.a.; it is primarily extracellular (a.a. 1-689) but like GPIIb_l has a transmembrane domain (a.a. 690-715) and a short cytoplasmic C-terminal tail (a.a. 716-762).

Several major features of GPIIb and GPIIIa have been identified [Calvete 1994]. GPIIb_h contains seven intramolecular disulfide bridges, four N-linked glycosylation sites and one O-linked site, while GPIIb_l has only one disulfide bridge and a single N-linked glycosylation site. GPIIIa encompasses twenty-eight disulfide bridges, including two large loops at Cys⁵-Cys⁴³⁵ and Cys⁴⁰⁶-Cys⁶⁵⁵; six N-linked glycosylation sites; four cysteine-rich tandem repeats and another Cys-rich region at the amino terminus; and a cytoplasmic tyrosine phosphorylation (P-Tyr) site, identified by homology to P-Tyr sites in the insulin and EGF receptors [Phillips et al. 1988]. The intact complex serves as the

principal high affinity calcium-binding site on the surface of resting platelets, and also provides three or four medium-affinity and several low-affinity Ca^{2+} -binding sites (five on GPIIb and two on GPIIIa) [Brass & Shattil 1984; Rivas & González-Rodríguez 1991]; it has been shown to partially regulate Ca^{2+} flux across the membrane of unactivated platelets [Brass 1985]. Four putative calcium-binding domains in GPIIb_a have been localized based on homology to the EF hands of other Ca^{2+} -binding proteins (a.a. 243-254, 297-308, 365-376, and 426-437), while one such site has been identified in GPIIIa, at a.a. 118-131. Sections of both subunits are involved in the heterodimer interface: sequences in the first GPIIIa loop (a.a. 217-235, 262-298, 324-366, and 403-421); portions of the C-terminal half of GPIIb_a (a.a. 486-553, 696-734, and 780-817); and a region in the middle of GPIIb_b (a.a. 30-75). Electron microscopy studies have confirmed that hydrophobic sequences of GPIIb_b and GPIIIa found near the C-terminus are associated with the plasma membrane. A schematic representation of the GPIIb-IIIa complex is depicted in Figure V.

Within four to six hours of protein synthesis the mature GPIIb-IIIa complex is transported to the plasma membrane, where it becomes evenly distributed over the entire surface, loosely associated with the cytoskeleton and other membrane proteins [Calvete 1995]. By using monoclonal antibodies (mAb's) like AP-2 which recognize the intact complex on resting platelets, or other mAb's which specifically bind to one of the two glycoprotein subunits, it has been shown that there are approximately 50 000 such complexes within the membrane [Pidard et al. 1983; Phillips et al. 1988]. As this number increases two- to three-fold after platelet stimulation by strong agonists such as thrombin, resting platelets must have a large intracellular pool of GPIIb-IIIa [Niiya et al. 1987]. Internal stores of this receptor have been localized to invaginations of the plasma membrane known as the **surface-connected canalicular system (SCCS)** and to the membrane of cytoplasmic α -granules; in the latter some GPIIb-IIIa is occupied by Fg [Nurden 1996]. Thrombin stimulation leads to exposure of the SCCS and α -granule fusion with the plasma membrane, upregulating the surface expression of GPIIb-IIIa and

Figure V: The GPIIb-IIIa complex (from Phillips et al. 1988, Fig. 3)



other glycoproteins [Gerrard 1988]. Newly exposed GPIIb-IIIa complexes not already bound to Fg are fully functional as receptors for various adhesive ligands.

Glanzmann's thrombasthenia and GPIIb-IIIa polymorphisms

Glanzmann's thrombasthenia (GT) is a congenital bleeding disorder characterized by a prolonged bleeding time, impaired platelet aggregation, and abnormal clot retraction, despite normal platelet counts [Phillips & Agin 1977]. GT results from the failure of Fg to bind to activated platelets, and is due to decreased amounts of and/or molecular abnormalities in the GPIIb-IIIa complex [Bennett & Vilaire 1979; George & Nurden 1994]. GT patients were initially divided into two groups: **type I** individuals had less than 5% of GPIIb-IIIa, no Fg binding to ADP-stimulated platelets, and a complete absence of clot retraction and α -granule Fg, while **type II** patients had up to 25% of normal GPIIb-IIIa, low levels of Fg binding, 30-50% of α -granule Fg, and some clot retraction [Fournier et al. 1989]. Other individuals with GT have been described who have near-normal levels of GPIIb-IIIa yet their platelets are unable to bind Fg once activated; this is known as **variant GT**. In many of these people GPIIb and GPIIIa rapidly dissociate in the absence of calcium, something which may be due to point mutations near the Ca^{2+} -binding regions of GPIIb (Gly²⁴²-Asp; Arg³²⁷-His; and Gly⁴¹⁸-Asp) [Calvete 1995]. Other genetic defects identified in GPIIb include a 13-base deletion in exon 4 and a 4 kb deletion involving exons 2 to 9, while some defects in GPIIIa are the point mutations Asp¹¹⁹-Tyr, Arg²¹⁴-Gln, Cys³⁷⁴-Tyr, and Ser⁷⁵²-Pro, an 11-base deletion in exon 12, and a 7 kb insertion [Newman 1991].

Variations in GPIIb and GPIIIa gene splicing are also known which do not lead to GT; both genes are polymorphic and thus have more than one allelic form [Newman 1991]. Five alloantigens have been described for GPIIIa - **HPA-1 (PI^A or Zw)**, **HPA-4 (Pen or Yuk)**, **HPA-6 (Ca or Tu)**, **HPA-7 (Mo)**, and **HPA-8 (Sr)** - which are due to the substitutions Leu³³-Pro, Arg¹⁴³-Gln, Arg⁴⁸⁹-Gln, Pro⁴⁰⁷-Ala, and Arg⁶³⁶-Cys, respectively [Newman 1994]. GPIIb has only one alloantigen, **HPA-3 (Bak or Lek)**, caused by the mutation Ile⁸⁴³-Ser. These polymorphisms, along with those found on GPIa

and GPIb, lead to the immunologic syndromes **post-transfusion purpura (PTP)** and **neonatal alloimmune thrombocytopenic purpura (NATP)**. PTP is quite rare, with less than two hundred cases reported worldwide, while NATP is more common and may occur in one of every 2000 births.

Platelet activation and aggregation

A large number of platelet agonists are known, the most important of which is the serine protease **α -thrombin** [Bennett 1992]. Glycoprotein Ib is the high-affinity thrombin receptor on platelets, but only a small fraction of GPIb molecules bind thrombin [Nurden 1994]. The most abundant thrombin platelet receptor, having medium-affinity, is a member of the seven transmembrane domain (7-TM) protein family [Hawiger et al. 1994]. After cleavage by thrombin this modified receptor induces activation of **G-proteins** - a family of cytoplasmic, heterotrimeric GTP-binding proteins - which regulate the enzymes **adenylate cyclase**, **phospholipase A₂ (PLA₂)**, and **phospholipase C (PLC)**. Stimulation of the latter leads to hydrolysis of the membrane phospholipid PIP₂, generating the second messengers **inositol triphosphate (IP₃)** and **diacylglycerol (DAG)**. IP₃ mobilizes calcium from intracellular storage sites such as the dense tubular system, which in conjunction with the opening of membrane Ca²⁺ channels brings about a dramatic rise in the internal concentration of this ion. Calcium plays an important role in platelet activation responses, as do a multitude of proteins phosphorylated by DAG-activated **protein kinase C (PKC)**. In addition, some DAG is converted into **arachidonic acid (AA)**, which is also generated by the action of PLA₂ on membrane lipids. AA is then transformed into prostaglandins and thromboxanes: a number of these - such as **thromboxane A₂ (TXA₂)** - are potent platelet agonists, while other AA metabolites like **prostacyclin** are platelet inhibitors.

Thrombin is one of the most powerful platelet activators: in addition to liberation of AA it induces shape change, aggregation, and release of all three types of platelet granules (lysosomal, dense, and α -) [Holmsen 1994]. Other strong platelet agonists which bring about all six of these responses - known as the **basic platelet reaction** - are the

ECM protein **collagen**, the proteases **trypsin** and **cathepsin G**, and the calcium ionophore **A23187** [Si-Tahar et al. 1997]. As an intermediate platelet agonist, **TXA₂** has many of the same effects as thrombin but cannot induce the release of lysosomal granules. Weak platelet agonists include **ADP**, **PAF**, **vasopressin**, **serotonin**, and **epinephrine**; the first four of these molecules are able to trigger shape change and aggregation, but no granule secretion except in high concentrations. Supraphysiologic levels of epinephrine are required to induce platelet aggregation, so it likely does not stimulate platelets directly but instead potentiates the effects of other activators [Bennett 1992]. Like thrombin, some of the above platelet agonists (**TXA₂**, **PAF**, **serotonin**, and **epinephrine**) bind to G-protein-coupled 7-TM receptors and recruit many of the same intracellular mediators. Interaction of **ADP** with its receptor - a member of the **P₂** class of purinergic receptors known as **aggrecin** - also leads to an increased concentration of intracellular calcium, but does not appear to involve phospholipase C or PKC [Colman et al. 1994; Hawiger et al. 1994].

Weak activators like **ADP** can produce three distinct phases of platelet aggregation [Pedvis et al. 1988]. Low agonist concentrations (0.1-0.5 μM **ADP**) bring on shape change, pseudopod formation, and **primary, reversible microaggregation (PA)**: this is mediated by the binding of **Fg** or other adhesive proteins to activated **GPIIb-IIIa**, followed by the subsequent crosslinking of adjacent platelets into small aggregates containing less than ten cells [Leung & Nachman 1986; Colman et al. 1994]. **PA** cannot be detected by aggregometry (light transmission studies), but can be measured experimentally by microscopic or electronic particle quantitation of the decrease in the number of singlet platelets [Frojmovic et al. 1989]. Intermediate agonist levels (0.5-1.5 μM **ADP**) will induce the formation of larger **macroaggregates**, which are visualized as a reversible increase in light transmission, known as **TA-1**. Strong activators as well as large amounts of weak agonist (2-5 μM **ADP**) provoke the secretion of α - and dense granules - known as **release I** - and **AA** liberation [Zucker & Nachmias 1985]. **TXA₂** generation and **ADP** release recruit more platelets to the growing aggregate, while secreted proteins such as **TSP-1** help to mediate the **secondary, irreversible phase** of aggregation (**TA-2**). **TSP-1** interacts with fibrinogen in addition to its platelet receptor(s),

stabilizing the binding of Fg to GPIIb-IIIa and reinforcing the interactions between platelets [Gerrard 1988]. High concentrations of strong agonist will also induce the secretion of lysosomal granules (**release II**).

Activation of GPIIb-IIIa and ligand binding

In its native state on resting platelets GPIIb-IIIa is unable to bind significant amounts of ligand [Plow & Ginsberg 1989]. However, intracellular signals produced as a result of platelet stimulation lead to conformational changes in the extracellular portion of the receptor which allow it to interact with adhesive proteins, a process known as **inside-out signalling** [Schwartz et al. 1995]. Membrane-proximal cytoplasmic domains in both subunits of GPIIb-IIIa seem to be critical for this type of signal transduction. The relevant sequences for GPIIb and GPIIIa are Gly-Phe-Phe-Lys-Arg (**GFFKR**) and Leu⁷¹⁷-Asp⁷²³ respectively; these motifs are highly conserved throughout the integrin superfamily [Dedhar & Hannigan 1996]. The inactive conformation of the receptor found on resting platelets appears to be stabilized by the formation of a salt bridge between the terminal Asp and Arg residues from these sequences, while amino acid substitutions in either region increase ligand-binding affinity, presumably due to disruption of the bridge [Hughes et al. 1996]. Another important cytoplasmic sequence in GPIIIa and other β -subunits is Asn-Pro-X-Tyr (**NPXY**), which is required for GPIIb-IIIa activation and which has been implicated in the internalization of LDL receptors [Chen et al. 1990]. Finally, a point mutation a few residues downstream of the NPXY sequence, Ser⁷⁵²-Pro, leads to a variant of Glanzmann's thrombasthenia with defective activation of GPIIb-IIIa [Calvete 1995].

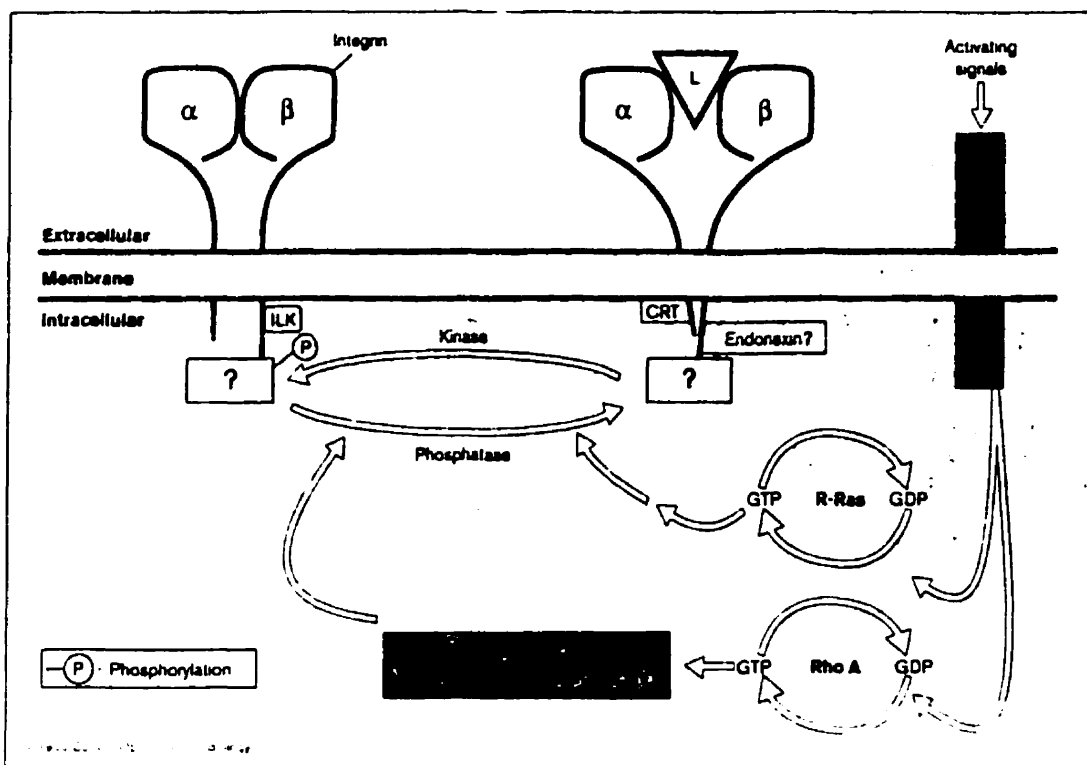
It is unclear which intracellular mediators interact with GPIIb-IIIa to prime it for ligand binding. There are at least three candidates: the calcium-binding protein **calreticulin (CRT)**, which binds to the **GFFKR** motif of several integrin α -subunits, disrupting the salt bridge and thereby stabilizing GPIIb-IIIa in an active conformation; β_3 **endonexin**, which binds specifically to GPIIIa in the region of the Ser⁷⁵²-Pro mutation described above; and the serine/threonine kinase **integrin-linked kinase (ILK)**, which

interacts with β_1 , β_2 , and β_3 integrins [Dedhar & Hannigan 1996]. Other likely regulatory proteins include members of the **Rho family of small GTPases** such as Rho A and R-Ras, which interact with protein kinases and phosphatases as well as with the actin cytoskeleton. Figure VI illustrates the relationship between many of the above molecules in the control of inside-out signalling, mediated by GPIIb-IIIa and other integrins.

GPIIb-IIIa recognizes a variety of ligands, most of which contain the tripeptide sequence Arg-Gly-Asp (RGD) [Gille & Swerlick 1996]. Normally GPIIb-IIIa only becomes competent to bind ligand after platelet stimulation by an agonist, but the receptor can also be activated directly: by proteolytic enzymes like **plasmin**, **α -chymotrypsin** and **neutrophil elastase**; by the complement membrane attack complex; and as will be explained below, by various peptides and mAb's [Niewiarowski et al. 1983; Colman et al. 1994; Hawiger et al. 1994]. Irrespective of the manner of GPIIb-IIIa activation, this process is associated with distinct conformational changes in the receptor, including the exposure of neoepitopes recognized by various mAb's [Plow & Ginsberg 1989]. One of these, **PAC-1**, interacts with the receptor at or near the ligand binding site, blocking both Fg binding and platelet aggregation [Shattil et al. 1985]. In addition, microenvironmental changes in the vicinity of the receptor that permit access of large adhesive proteins to the binding pocket also appear to regulate ligand binding, as small peptides containing the RGD sequence (**RGD-peptides**) can interact with the GPIIb-IIIa ligand binding site on both resting and activated platelets [Pytela et al. 1986]. RGD-peptides will therefore block the interaction of activated GPIIb-IIIa with its ligands and inhibit platelet aggregation. However, these peptides can themselves act as agonists and activate GPIIb-IIIa via changes in quaternary structure, priming the receptor for subsequent ligand binding and platelet aggregation [Parise et al. 1987; Du et al. 1991]. The interaction of these peptides with $\alpha_v\beta_3$ and GPIc-IIa - the other two platelet integrins which recognize the RGD sequence - may also affect platelet function and ligand binding.

The binding of adhesive proteins and of RGD-peptides to GPIIb-IIIa requires calcium or magnesium concentrations in the range of 1 mM [Bennett & Vilaire 1979; Steiner et al. 1989]. This prerequisite is distinct from the micromolar Ca^{2+} levels which

Figure VI: Integrin-mediated inside-out signalling (from Dedhar & Hannigan 1996, Fig. 2)



are necessary to maintain the intact heterodimer [Plow & Ginsberg 1989]. Interestingly, high concentrations of Mg^{2+} or Mn^{2+} have been shown to decrease ligand binding to and aggregation of activated platelets: reduced Ca^{2+} binding, as a result of competition for binding sites, may lead to changes in the conformation of GPIIb-IIIa [Gailit & Ruoslahti 1988; Gawaz et al. 1994]. There appear to be at least two medium-affinity divalent cation binding sites on GPIIb-IIIa that must be occupied for ligand binding to occur: one is at GPIIIa a.a. 118-131, while the other is likely within GPIIb residues 294-314 [D'Souza et al. 1994]. Both of these regions have been implicated in interactions with ligand; in the case of GPIIIa, binding of adhesive protein leads to the formation of a ternary complex between the ligand, cation, and receptor, followed by the displacement of divalent cations. Binding of Ca^{2+} to one or more low-affinity sites on GPIIIa regulates the dissociation rate of RGD ligands and induces cellular deadhesion [Hu et al. 1996].

The GPIIb-IIIa ligand binding pocket is comprised of non-contiguous sequences from both integrin subunits [Nurden 1994]. One important site on GPIIIa for interactions with ligand is a.a. 118-131: a peptide corresponding to this sequence was shown to bind to the tetrapeptide RGDF, while an antibody to this portion of β_3 blocked ligand binding to intact GPIIb-IIIa [D'Souza et al. 1994]. Within this sequence, Asp¹¹⁹, Ser¹²¹, and Ser¹²³ appear to be especially crucial, as substitution of any of these residues by an alanine abrogated Fg and PAC-1 binding to the activated receptor [Bajt & Loftus 1994]. These three residues are expected to participate in a binding site for divalent cations and adhesive ligands - known as MIDAS - which is highly conserved among integrin β -subunits [Schwartz et al. 1995]. This site is dysfunctional in the Cam variant of Glanzmann's thrombasthenia, where Asp¹¹⁹ is mutated to a tyrosine, causing defective ligand binding and abnormal interaction with Ca^{2+} and Mg^{2+} [Loftus et al. 1990]. A second domain on GPIIIa which interacts with RGD-containing proteins consists of residues 211-222, as a synthetic peptide corresponding to this sequence blocks the binding of Fg, Fn, vWF, and Vn to GPIIb-IIIa [Charo et al. 1991]. Certain essential amino acids in this sequence have been identified: two known mutations in Arg²¹⁴ lead to variant forms of GT, while substitution of Asp²¹⁷ or Glu²²⁰ by an alanine abolish PAC-1 binding

[Calvete et al. 1995; Tozer et al. 1996]. Peptides corresponding to GPIIIa residues 214-218 and 217-231 have also been shown to inhibit Fg binding to GPIIb-IIIa.

With regards to GPIIb, the Fg γ chain dodecapeptide H12 has been crosslinked to GPIIb_α residues 294-314, which encompass the second putative Ca²⁺-binding domain [D'Souza et al. 1990]. Peptides from this region of GPIIb_α inhibit the binding of adhesive ligands to the intact receptor, as well as clot retraction and platelet aggregation; they also bind directly to Fg and Vn [D'Souza et al. 1991; Taylor & Gartner 1992]. This site does not appear to interact with RGD sequences, unlike another Fg-binding region of GPIIb_α, a.a. 184-193: mutations of Gly¹⁸⁴, Tyr¹⁸⁹, Tyr¹⁹⁰, Phe¹⁹¹, and Gly¹⁹³ within this sequence blocked GPIIb-IIIa binding to Fg, PAC-1 and two other ligand-mimetic mAb's [Kamata et al. 1996]. Additional putative ligand-binding sites on GPIIb_α include residues 42-73, 696-724, and 752-768 - which have been crosslinked to RGD- and/or γ chain-peptides - along with a.a. 656-667, a sequence shown to interact with Fg.

Ligand binding leads to further conformational changes in GPIIb-IIIa, exposing neoepitopes known as **ligand-induced binding sites (LIBS)**. These sites can be detected with various mAb's; they likely regulate receptor function by promoting the binding of additional ligand and by taking part in signal transduction across the plasma membrane [Frelinger et al. 1988]. One of the best known anti-LIBS antibodies is **PMI-1**, which will interact with an epitope at the C-terminal end of the GPIIb heavy chain (a.a. 842-857) if GPIIb-IIIa is occupied, but cannot bind to resting platelets, on which the LIBS site is hidden [Calvete 1995]. LIBS have also been identified by mAb's in several regions of GPIIIa: **AP5** recognizes a divalent cation-sensitive epitope at the N-terminus (a.a. 1-6) [Honda et al. 1995]; **AP6** interacts with part of the ligand binding pocket (a.a. 211-222) if it is occupied by Fg, but not by RGD- or γ chain-peptides [Nurden et al. 1996]; **D3GP3** binds between residues 422-490; and several antibodies, including **anti-LIBS2 (Ab 62)**, recognize a site adjacent to the transmembrane domain (between residues 602-690). Certain anti-LIBS Ab's can activate GPIIb-IIIa directly, since the binding of D3GP3 to resting platelets leads to Fg binding and platelet aggregation, while anti-LIBS2 induces these effects as well as granule secretion [Kouns et al. 1990; Frelinger et al. 1991]. Other

antibodies directed against LIBS suppress platelet functions: **anti-LIBS1⁵** blocks aggregation, secretion, and clot retraction, while PMI-1 decreases adhesion to and spreading on collagen [Shadle et al. 1984; Frelinger et al. 1990]. These inhibitory effects are not due to abolition of ligand binding to GPIIb-IIIa, as several anti-LIBS Ab's in fact promote the interaction of Fg with its receptor, but are likely caused by antibody interference with post-occupancy events.

GPIIb-IIIa ligands

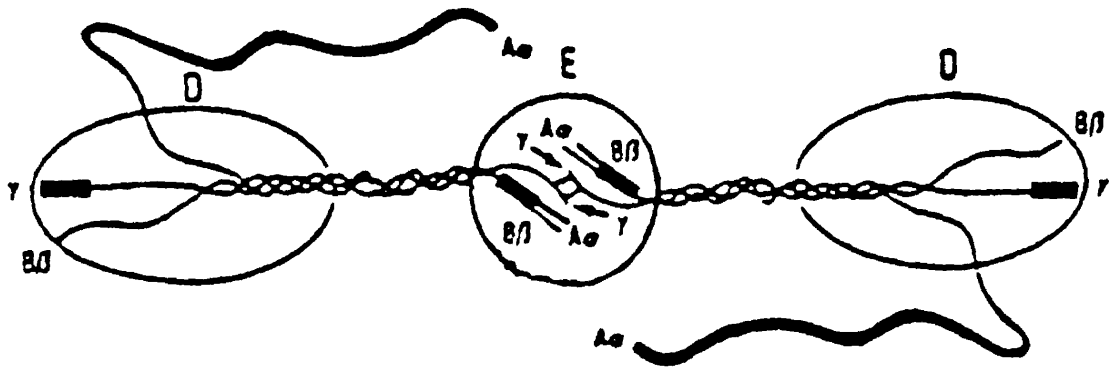
a) Fibrinogen (Fg)

Fibrinogen, the principal adhesive ligand for GPIIb-IIIa under normal physiological conditions, is a large glycoprotein with a molecular weight of approximately 340 kDa [Plow et al. 1984]. Plasma Fg - produced by hepatic parenchymal cells - is present in the circulation at a concentration of 3-4 mg/ml (~ 10 μ M); some of this Fg is endocytosed by megakaryocytes and platelets, where it is stored in cytoplasmic α -granules [Harrison et al. 1989; Doolittle et al. 1996]. Fg has an extended triglobular structure linked by α -helices called coiled-coils, and is composed of three pairs of polypeptide chains interconnected by disulfide bonds - **A α** , **B β** , and **γ** - which in platelets have 610, 461, and 411 amino acids, respectively [Hantgan et al. 1994]. However, alternative mRNA splicing can lead to modified γ chains; the most common of these, found in about 10% of circulating Fg, is γ' , where the last four amino acids (408-411) have been replaced by a 20-residue sequence [Hettasch et al. 1992]. In all forms of Fg, the N-termini of the six polypeptide chains are located in the central zone, called the **E domain**. **B β** and γ chain C-termini are found at the peripheral ends of the molecule, called **D domains**, while the **A α** chains are longer and wind back towards the centre. A representation of the Fg homodimer is shown in Figure VII.

The H12 dodecapeptide located at the C-terminal end of the γ chain (a.a. 400-411), having the amino acid sequence His-His-Leu-Gly-Gly-Ala-Lys-Gln-Ala-Gly-Asp-

⁵ this antibody recognizes an unspecified site on GPIIIa

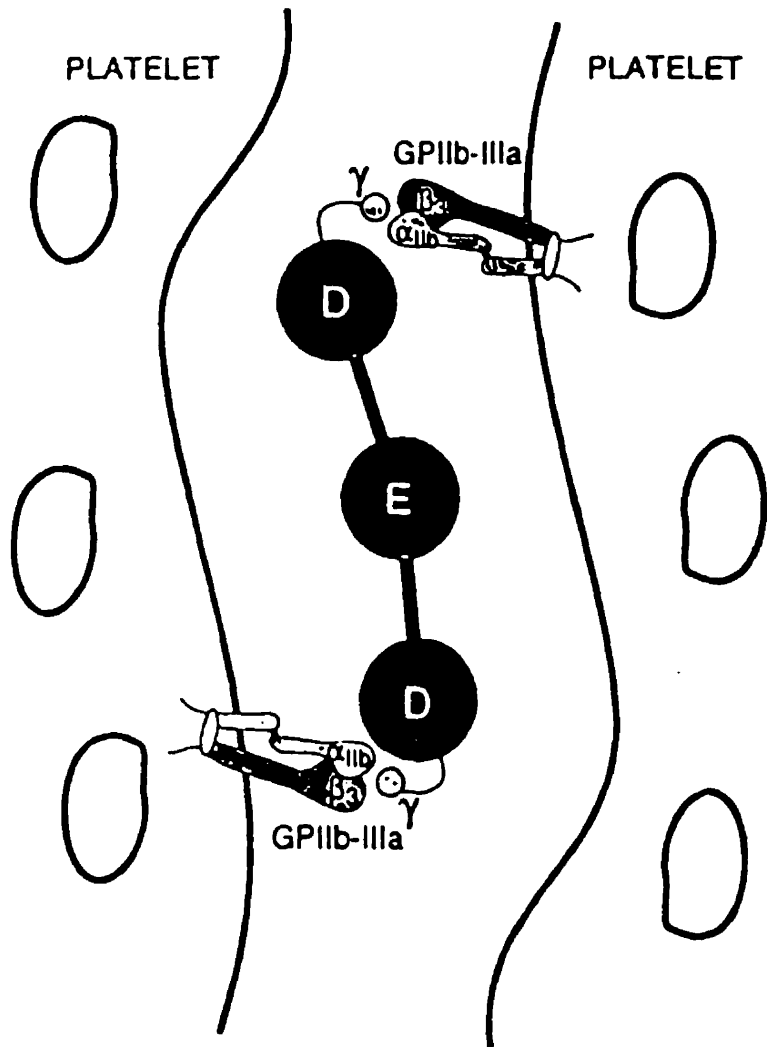
Figure VII: Fibrinogen (from Plow et al. 1984, Fig. 2A)



Val (HHLGGAKQAGDV), is required for the initial binding of Fg to GPIIb-IIIa [Savage et al. 1995]. Platelet aggregation and binding of Fg to its receptor were inhibited by a synthetic peptide corresponding to these residues; like the RGD-peptides, this sequence was able to activate GPIIb-IIIa [Parise et al. 1987]. Furthermore, reduced binding to GPIIb-IIIa and defective platelet aggregation were seen with the γ' variant or with γ 407, which lacks the final four amino acids in the H12 sequence (AGDV) [Hettasch et al. 1992; Farrell & Thiagarajan 1994]. Two other putative receptor binding sites in Fg are the A α chain tetrapeptides **Arg-Gly-Asp-Phe** (a.a. 95-98) and **Arg-Gly-Asp-Ser** (a.a. 572-575). However, these RGD-containing sequences do not seem to play a major role in interactions with GPIIb-IIIa, as mAb's to these regions only partially inhibited platelet adhesion to immobilized Fg, while mutation of either aspartic acid residue to a glutamate had no effect on platelet aggregation [Cheresh et al. 1989]. Electron microscopy has confirmed that the C-terminal end of the γ chain, but not the A α tetrapeptides, associates with GPIIb-IIIa. Figure VIII illustrates the crosslinking of adjacent platelets via interactions of Fg γ chain termini with GPIIb-IIIa.

Fg and GPIIb-IIIa associate in a 1:1 ratio [Nurden 1994]. Initial binding takes place within seconds and can be reversed by chelation of divalent cations or by excess unbound Fg, equilibrium binding is reached after 5-15 minutes, and by one hour the interaction becomes irreversible [Harrison et al. 1989; Peerschke 1992]. By 24 hours of binding to platelets some Fg is internalized and stored in the SCCS or in cytoplasmic α -granules. The maximum number of Fg molecules binding to each platelet appears to be somewhat variable, ranging from 5 000 to 50 000 [Niewiarowski et al. 1983]. Scatchard plot analysis has shown the dissociation constant (K_d) for the Fg-GPIIb-IIIa interaction to be from 80-360 nM: Fg likely binds to a single class of receptors on platelets, although several groups have demonstrated the presence of both high and low affinity Fg receptors. The interaction of Fg with GPIIb-IIIa requires divalent cations and was found to be maximal in the presence of 0.5 mM Ca^{2+} or 2.5 mM Mg^{2+} , while it is also affected by temperature and agonist strength [Bennett & Vilaire 1979]. Saturation of GPIIb-IIIa occurs at Fg concentrations of around 500 nM [Marguerie et al. 1979].

Figure VIII: Platelet crosslinking by Fg (from Hawiger 1995a, Fig. 1)



γ His-His-Leu-Gly-Gly-Ala-Lys-Gln-Ala-Gly-Asp-Val

Binding to GPIIb-IIIa exposes previously hidden epitopes on Fg, known as **receptor-induced binding sites (RIBS)**, which can be detected with various mAb's. One of these RIBS, recognized by **155B16**, is at the RGDF sequence (A α 95-98); the inaccessibility of this site on soluble Fg further suggests that these residues do not participate in initial binding to GPIIb-IIIa [Ugarova et al. 1993]. Other RIBS on Fg include γ chain a.a. 112-119 and 373-385, recognized by **9F9** and **anti-Fg-RIBS-I**, respectively [Zamarron et al. 1991]. These newly exposed sites may also be able to bind to GPIIb-IIIa, enhancing the affinity of the receptor-ligand interaction [Calvete 1995].

GPIIb-IIIa can interact with Fg immobilized on polymer beads or on the subendothelium; on the latter Fg becomes bound to ECM proteins like TSP-1⁶, Fn, and **entactin**⁷ [Wu & Chung 1991; Gartner et al. 1993; Hantgan et al. 1994]. Unlike soluble fibrinogen, surface-bound Fg binds to GPIIb-IIIa on both activated and unactivated platelets, inducing spreading and irreversible adhesion; upon binding to Fg, resting platelets also become activated and aggregate [Savage & Ruggeri 1991; Savage et al. 1992]. Maximal adherence of unstimulated platelets requires the entire Fg molecule and is much weaker than for activated platelets, which attach equally well to intact fibrinogen or to Fg fragments containing the H12 or RGDS sequences. However, under conditions of flow only the complete Fg dimer can support the adhesion of activated platelets [Savage et al. 1995].

Fg can bind to other integrins aside from GPIIb-IIIa: the VLA receptor $\alpha_v\beta_1$; the cytoadhesins $\alpha_v\beta_3$ and LRI; and the Leu-CAM subfamily members MAC-1 and p150,95 [Gille & Swerlick 1996]. The interaction of Fg with $\alpha_v\beta_1$ and $\alpha_v\beta_3$ occurs exclusively via the RGDF and/or RGDS sites, unlike its association with GPIIb-IIIa and the LRI, which may additionally be mediated by the γ chain C-terminal ADGV residues [Gresham et al. 1992]. MAC-1 can likewise bind to this region of the γ chain as well as to γ a.a. 190-202,

⁶ via A α residues 113-126 and B β 243-252 [Hantgan et al. 1994]

⁷ This adhesive protein binds via an RGD sequence to the LRI on PMN and macrophages, where it stimulates phagocytosis and chemotaxis; it also binds to other matrix proteins like Ln, Fn, and Col [Wu & Chung 1991].

while A α 17-19 (**Gly-Pro-Arg**) was shown to bind to p150,95 [Wright et al. 1988; Loike et al. 1991; Altieri et al. 1993]. The interaction of GPIIb-IIIa-bound Fg with the above leukocyte integrins (LRI, MAC-1, and p150,95), like that of platelet P-selectin and ICAM-2 with their leukocyte counter-receptors, helps to mediate the adhesion of monocytes and neutrophils to activated platelets [Diacovo et al. 1994; Nurden 1994]. Association of soluble Fg with these leukocyte integrins induces PMN activation, leading to oxidative burst and phagocytosis [Ruf & Patscheke 1995]. In addition, soluble Fg enhances leukocyte adhesion to and migration through the endothelium by acting as a bridging molecule between the two cell types; it interacts with endothelial cell ICAM-1 via the γ chain residues 117-133 [Languino et al. 1995]. Finally, the Fg γ C-terminus (a.a. 397-411) can also bind to receptors on staphylococci and streptococci to induce clumping; these receptors, however, do not appear to be related to the integrin superfamily [Hawiger 1995b].

One other important role of Fg is to serve as a precursor for **fibrin (Fb)**, the main component of the hemostatic plug. In the last step of the coagulation cascade Fg is converted into Fb by thrombin: this enzyme cleaves small peptides - called **fibrinopeptides A and B** - from the N-terminal regions of the Fg A α and B β chains [Doolittle et al. 1996]. The release of these peptides exposes new N-terminal sequences such as A α Gly-Pro-Arg^d which interact with certain domains on other Fg molecules; this initiates the polymerization process, leading to the formation of protofibrils that are 15-20 units long. **Factor XIII**, which is activated by thrombin, then introduces covalent crosslinks between the individual Fb molecules. In this way a fibrin network develops at the periphery of platelet aggregates, trapping nearby red and white blood cells to form a stable hemostatic plug [Hirsh & Brain 1979]. After 24-48 hours most of the platelets have been lysed by macrophages and neutrophils, resulting in a plug composed primarily of Fb polymers. A few days later, once wound healing has begun, fibrin degradation

^d mentioned above as the Fg binding site for the leukocyte integrin p150,95

(fibrinolysis) will proceed via proteases such as **plasmin**, which is generated from its inactive precursor **plasminogen** by enzymes like **tissue plasminogen activator (t-PA)**.

b) von Willebrand Factor (vWF)

The importance of von Willebrand Factor in platelet adhesion and aggregation was first recognized in patients with **von Willebrand Disease (vWD)**, the most common congenital bleeding disorder, which is due to various abnormalities in vWF [Montgomery & Collier 1994]. This adhesive glycoprotein has since been found to play a major role in thrombus formation under the conditions of high shear stress which are encountered in small vessels and occluded arteries [Peterson et al. 1987]. Wall shear stress (τ), measured in dynes/cm², refers to the force per unit area applied by flowing blood to the vessel surface [Kroll et al. 1996]. τ is related to the wall shear rate (G) - expressed in reciprocal seconds (s⁻¹) - by the equation $\tau = \eta \times G$, where η is the fluid viscosity. As the viscosity of whole blood is 0.038 poise, physiological shear stresses can easily be converted to shear rates and vice versa. Some typical values for the wall shear rate and stress of various blood vessels are as follows: 20-200 s⁻¹ (1-8 dynes/cm²) for veins; 300-800 s⁻¹ (11-30 dynes/cm²) for large arteries; 500-1600 s⁻¹ (19-61 dynes/cm²) for arterioles; 800-10 000 s⁻¹ (30-380 dynes/cm²) for stenotic vessels; and up to 16 000 s⁻¹ (600 dynes/cm²) in some areas of the microcirculation [Yung and Frojmovic 1982]. Very high shear forces lead to morphological, biochemical, and functional changes in platelets, such as aggregation and granule secretion, and also affect endothelial cells and the ECM [Brown et al. 1975].

vWF synthesis occurs primarily in the Weibel-Palade bodies of endothelial cells, and to a lesser extent in MK α -granules [Meyer & Girma 1993]. Mature vWF is comprised of a series of multimers having a variable number of 260 kDa (2050 a.a.) monomers, each of which contains four types of repeated domains, called **A**, **B**, **C**, and **D**. The N-terminal **D3** region has binding sites for **heparin** and for one of the coagulation factors, **Factor VIII**, which circulates in plasma in a 1:1 complex with vWF. Just downstream from **D3** is the **A1** loop, which also has a heparin binding site, as well as

sequences for interaction with **collagen**, platelet **GPIb**, **sulfatides** (sulfated glycolipids), and the snake venom protein **botroctin**. A little further downstream is the homologous A3 loop, which has a second binding site for collagen. Close to the C-terminal end - in the C1 domain - is the tripeptide Arg¹⁷⁴⁴-Gly-Asp, which is involved in binding to GPIIb-IIIa, $\alpha_v\beta_3$, and the LRI [Gille & Swerlick 1996].

vWF circulates in plasma at a concentration of 7-10 $\mu\text{g/ml}$ and is an important component of the extracellular matrix [Bennett 1992]. Damage to the vessel wall exposes the underlying ECM, inducing binding of plasma vWF to subendothelial adhesive proteins such as collagen. This will lead to a conformational change in vWF which allows it to interact with GPIb; similar changes in vWF quaternary structure are also provoked by binding to botroctin or the antibiotic **ristocetin**, and by high shear stress [Meyer & Girma 1993]. Interaction of vWF with GPIb initiates platelet adhesion to the ECM and causes the opening of a transmembrane calcium channel; the resulting increase in intracellular Ca^{2+} will activate GPIIb-IIIa via conformational changes [Ikeda et al. 1993]. Normally Fg is the principal GPIIb-IIIa ligand, as it has a much higher plasma concentration than vWF, but the latter becomes particularly important at high shear rates: binding of Fg to GPIIb-IIIa drops off with increasing shear and is negligible above 900 s^{-1} , while vWF binds maximally at this G and can mediate irreversible platelet adhesion to subendothelium - via interactions with GPIIb-IIIa - at G's of up to 6000 s^{-1} [Savage et al. 1996]. vWF is likewise essential for platelet aggregation at shear rates above 2000 s^{-1} , whereas at 300 s^{-1} aggregation is mediated primarily by Fg [Peterson et al. 1987; Ikeda et al. 1991]. However, both GPIb and GPIIb-IIIa are required for the adherence of unactivated platelets to immobilized vWF, while only GPIIb-IIIa is necessary for binding to Fg [Savage et al. 1992].

c) Thrombospondin-1 (TSP-1)

The thrombospondins are a family of extracellular calcium binding proteins, of which there are five known members: **thrombospondin-1, -2, -3, -4**, and **cartilage oligomeric matrix protein (COMP)** [Lawler 1995]. TSP-1, the best characterized of the

five, is the most abundant constituent of platelet α -granules and is also synthesized by EC, SMC, and fibroblasts [Sixma 1994; Rabhi-Sabile et al. 1996]. It is only present in plasma at very low concentrations (less than 250 ng/ml), but higher levels of TSP-1 are found in the ECM as well as on the surface of activated platelets. TSP-1 is a homotrimeric 450 kDa glycoprotein, which like vWF contains four kinds of domains: a procollagen-like region, four complement-like (**type 1**) repeats, two EGF-like (**type 2**) sequences, and twelve Ca^{2+} -binding domains (**type 3** repeats). There are at least four known sites of cell attachment to TSP-1: a heparin-binding domain at the N-terminus which interacts with cell surface proteoglycans and sulfatides; sequences in the first two complement-like regions which also bind to proteoglycans and sulfatides as well as CD36 (platelet GPIV) and another membrane receptor of M_r 50 kDa; an Arg-Gly-Asp sequence in the last Ca^{2+} -binding domain which recognizes the two platelet β_3 integrins (GPIIb-IIIa and $\alpha_v\beta_3$); and a C-terminal region which binds to integrin-associated protein (CD47), as well as unidentified receptors of M_r 80 and 105 kDa [Gao et al. 1996]. TSP-1 also interacts with the adhesive proteins Fg, Fb, Fn, Col, Ln, and vWF; with components of the fibrinolytic system such as plasminogen and its activators; with the cytokine **transforming growth factor- β** (TGF- β); and with platelet GPIa-IIa [Agbanyo et al. 1993; Legrand et al. 1994; Hess et al. 1995].

TSP-1 is quite sensitive to calcium concentrations, and undergoes a conformational change near the C-terminus if Ca^{2+} levels are low [Sixma 1994]. In the absence of calcium, surface-coated TSP-1 will not support platelet adhesion and in fact inhibits binding to immobilized Fg or Fn, while if Ca^{2+} and Mg^{2+} are present platelets can adhere to TSP-1 at shear rates as high as 1800 s^{-1} [Agbanyo et al. 1993]. Stimulation of platelets by thrombin or collagen leads to α -granule release and surface expression of TSP-1 - bound to platelet receptors such as CD47, GPIV, GPIIb-IIIa, GPIa-IIa, and/or $\alpha_v\beta_3$ - which interacts with GPIIb-IIIa-bound Fg to crosslink and stabilize newly formed platelet aggregates [Leung & Nachman 1986]. In the absence of Fg, TSP-1 was also found to induce the aggregation of resting platelets via a mechanism involving GPIV [Tuszynski et al. 1988]. Antibodies against various regions of TSP-1 inhibited Fg binding

to GPIIb-IIIa as well as platelet aggregation, while peptides corresponding to TSP-1 sequences interfered with α - and dense granule secretion, likely by affecting platelet signalling [Legrand et al. 1992; Rabhi-Sabile et al. 1996]. In addition, TSP-1 has been implicated in the regulation of biological processes like fibrinolysis, angiogenesis, development, and cell proliferation and migration [Lawler 1995].

d) Fibronectin (Fn)

Fibronectin, another adhesive glycoprotein, is an integral component of the ECM and is additionally found in plasma, platelet α -granules, and other cells [Sixma 1994]. It plays an essential role in cell adhesion to the subendothelium, and is also involved in migration, differentiation, phagocytosis, tissue remodelling, and wound healing [Kefalides 1994]. Plasma Fn (300 μ g/ml) comes from the liver and is composed of two 250 kDa chains which both contain twelve **type I**, two **type II**, and fifteen **type III** repeats; the two chains differ only in the length of the so-called **III-connecting segment (IIICS)**, which has a maximum of 120 amino acids and is found between repeats III-14 and III-15 [Dixit et al. 1985]. Matrix Fn is synthesized by EC, SMC, and fibroblasts, and has one or two extra **type III** repeats compared to the plasma protein (**EIIIA** and **EIIIB**), both of which are also found in platelets [Schick et al. 1996]. Various functional sites in Fn have been characterized: two binding domains for **fibrin** and two others for **heparin**, with one of each located near the N- and C-termini; a **collagen** binding domain comprised of four type I and the two type II repeats; the principal **cell attachment domain**, which binds via the RGDS sequence in III-10 to several integrins ($\alpha_3\beta_1$, $\alpha_5\beta_1$, $\alpha_8\beta_1$, $\alpha_v\beta_1$, $\alpha_v\beta_3$, $\alpha_v\beta_6$, GPIIb-IIIa, and the LRI) [Schnapp et al. 1995; Gille & Swerlick 1996]; further sites of attachment to GPIIb-IIIa in III-8 and -9, as well as in the C-terminal heparin-binding domain [Mohri et al. 1996]; a cell attachment domain in IIICS which interacts with $\alpha_4\beta_1$ and $\alpha_4\beta_7$; and binding sites for two other integrins ($\alpha_2\beta_1$ and MAC-1), TSP-1, entactin, activated Factor XIII (Factor XIIIa), and actin [Wu & Chung 1991].

Activated platelets adhere to and spread on immobilized Fn at shear rates up to 300 s^{-1} ; these events are dependent on GPIIb-IIIa, as well as GPIc-IIa and GPIb-vWF

[Beumer et al. 1994; Kroll et al. 1996]. However, the Fn-GPIIb-IIIa interaction does not appear to be important for platelet adhesion to the ECM under flow conditions, and resting platelets only attach to surface-bound Fn via GPIc-IIa [Sixma 1994]. Fn appears to be involved in platelet aggregation, as a mAb which binds to a region of Fn containing the cell attachment domain inhibited the aggregation of thrombin-stimulated platelets, while the size of platelet thrombi was decreased in Fn-depleted plasma [Dixit et al. 1985]. This contribution of Fn to aggregate formation is likely due to interactions with Fg and/or TSP-1, but high concentrations of Fn can block aggregation by preventing Fg or vWF from binding to GPIIb-IIIa. Fn also plays a role in wound healing by becoming crosslinked to fibrin by Factor XIIIa, helping to recruit fibroblasts and other cells into the clot [Kefalides 1994].

e) Vitronectin (Vn)

Vitronectin - also known as **S-protein** - helps to regulate a number of hemostatic events in vivo, such as cell adhesion and migration, angiogenesis, phagocytosis, and wound healing [Preissner & Jenne 1991; Hess et al. 1995]. This 78 kDa glycoprotein is synthesized mainly in the liver and is present in plasma at a concentration of 250-450 µg/ml, but has been detected in platelets and monocytes/macrophages as well. As is the case for Fg, Vn is not a constituent of the subendothelium, although it can associate with several components of the ECM via heparin- and collagen-binding motifs. Heparin, complement proteins C5b-7, or complexes of thrombin with **serine protease inhibitors (SERPIN's)** such as antithrombin (AT) III induce a conformational change in Vn, exposing binding sites for these molecules and for the opioid peptide β-endorphin. Additional functional domains have been located in Vn: two binding sites for other SERPIN's like **plasminogen activator inhibitor-1 (PAI-1)**; an RGD sequence for interaction with various integrins ($\alpha_8\beta_1$, $\alpha_v\beta_1$, $\alpha_v\beta_3$, $\alpha_v\beta_5$, $\alpha_v\beta_8$, GPIIb-IIIa, and the LRI); and binding sites for plasminogen, Factor XIIIa, and the cytokines TGF-β and **platelet-derived growth factor (PDGF)** [Schnapp et al. 1995; Gille & Swerlick 1996].

Vn is not known to play a role in platelet aggregation, although high concentrations will inhibit Fg and vWF binding to GPIIb-IIIa. Activated platelets adhere to and spread on immobilized Vn via GPIIb-IIIa, unlike resting platelets which cannot attach to this surface [Savage & Ruggeri 1991]. Furthermore, the interaction of Vn with $\alpha_v\beta_3$ and GPIIb-IIIa may be necessary for platelet formation, as this protein was found to co-localize with the two integrins at sites of pro-platelet generation from megakaryocytes [Hess et al. 1995]. Vn promotes thrombus formation by scavenging heparin - thus slowing down the inhibition of thrombin by AT III or other SERPIN's - and by retaining and stabilizing PAI-1 in the ECM where it can suppress fibrinolysis [Preissner & Jenne 1991]. However, formation of a Vn-PAI-1 complex also appears to lead to thrombin inactivation.

f) Collagen type I (Col I)

Nineteen different collagens have been characterized, of which there are two main classes: **fibrillar** (types I, II, III, V, and XI) and **non-fibrillar** [Kehrel 1995]. The latter contains two subgroups - **fibril-associated collagens with interrupted triple helices** (types IX, XII, XIV, and XVI) and **sheet-forming collagens** (types IV, VIII, and X) - as well as two nonaligned members, types VI and VII. All collagens consist of three chains in a triple helical conformation and many also contain noncollagenous domains. The collagens are major constituents of the subendothelium and play an essential role in cell adhesion; nine types of collagen (I, III-VI, VIII, and XII-XIV) have been found in the vessel wall, of which Col I and III are the most prominent [Saelman et al. 1994; Kroll et al. 1996]. All the fibrillar collagens - particularly Col I and III - are strong platelet agonists and can induce aggregation and granule release, while Col IV and VI also promote aggregate formation. The main platelet collagen receptor is thought to be GPIa-IIa, which binds to at least eight of the collagens (I-VIII), but other likely platelet binding sites include GPIb-bound vWF, GPIIb-IIIa, GPIV, GPVI, and an 85 kDa protein [Sixma 1994].

Collagen type I is the most abundant form of collagen in the body [Kehrel 1995]. SMC synthesize subendothelial Col I, which is closely linked to other matrix adhesive proteins and is elevated in atherosclerotic vessels [Coller et al. 1989; Sixma 1994]. Under static conditions platelet adhesion to Col I is promoted by Mg^{2+} and inhibited by Ca^{2+} , while adhesion under flow depends on the presence of Fn and/or vWF, particularly at high shear rates. Although Col I primarily interacts with GPIa-IIa, it can also bind to GPIIb-IIIa (and other integrins) via an RGD sequence not recognized by $\alpha_2\beta_1$ [Yamada & Kleinman 1992; Gille & Swerlick 1996]. Platelet adhesion to Col I was found to be partially inhibited by mAb's to GPIIb (**PMI-1**) or the intact GPIIb-IIIa complex (**10E5**) [Shadle et al. 1984].

GPIIb-IIIa antagonists

Fg binding to GPIIb-IIIa and platelet aggregation are blocked not only by various adhesive ligands, RGD- and Fg γ chain-peptides, and anti-GPIIb-IIIa mAb's, but by many other compounds as well. Chief among these are the **disintegrins**, a group of more than forty low molecular weight proteins isolated from the venom of vipers and rattlesnakes [Niewiarowski et al. 1994]. These compounds are at least 3000 times more potent than RGDS in suppressing aggregation, but are similar to the RGD-peptides in that they have little effect on platelet shape change or granule release. Almost all of the disintegrins contain an RGD sequence, but additional sites could be involved in binding to GPIIb-IIIa and other integrins. Like the RGD-peptides, many disintegrins bind with equal affinity to resting or activated platelets and can induce conformational changes in the Fg receptor. GPIIb-IIIa antagonists have also been isolated from the venom of leeches and ticks.

Post-occupancy events

Binding of GPIIb-IIIa to adhesive ligand immobilized on the ECM or attached to another platelet initiates a complex intracellular signalling cascade [Fox 1993; Schwartz et al. 1995]. This cascade - known as **outside-in signalling** - promotes platelet aggregation by inducing clustering of GPIIb-IIIa within the membrane, receptor

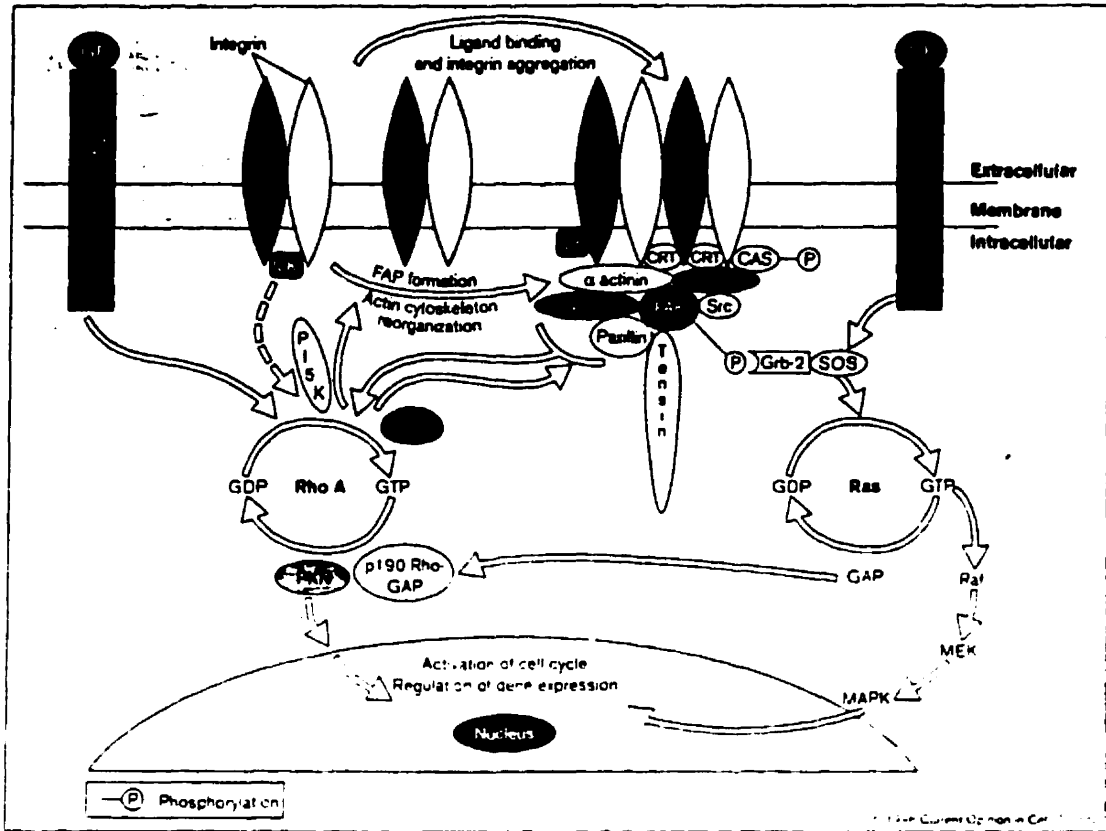
association with other membrane glycoproteins, and attachment to a reorganized actin cytoskeleton; these processes are regulated in part by the GTPase **Rho A** and the tyrosine kinase **pp125^{FAK}** (**FAK**) [Peerschke 1992; Dedhar & Hannigan 1996]. Rearrangement of the cytoskeleton has a number of consequences, including stabilization of the **Fg-GPIIb-IIIa** interaction, platelet spreading, and movement of the occupied receptor towards the centre of the platelet, which causes clot retraction. **GPIIb-IIIa**-mediated outside-in signalling is also thought to mediate events like calcium influx across the membrane, **Na⁺/H⁺** exchange, and a rise in intracellular pH.

Clustered **GPIIb-IIIa** forms structures called focal adhesion plaques (**FAP**), in which the receptor is linked to cytoskeletal proteins such as **α -actinin**, **talin**, **vinculin**, **paxillin**, and **tensin**, as well as signalling molecules like **calreticulin (CRT)**, **cadherin-associated substrate (CAS)**, and the tyrosine kinases **FAK** and **pp60^{Src}** (**Src**) [Dedhar & Hannigan 1996]. Phosphorylation of **FAK** - perhaps induced by **Rho A**-associated kinases like **PI3K** and **ROCK** - will cause it to associate with **Grb-2**, which is itself linked to the guanidine exchange factor **SOS**. **SOS** then turns on the GTPase **Ras**, leading to activation of the protein kinases **Raf**, **MEK**, and **MAPK**. The latter, as well as other kinases such as **Rho A**-associated **PKN**, translocate to the nucleus where they activate cell cycle regulatory molecules and transcription factors involved in cell proliferation and differentiation. Ligand binding and integrin clustering are also known to phosphorylate a variety of other cytoplasmic proteins and activate enzymes such as the tyrosine kinase **pp72^{Syk}** (**Syk**) and the **Ca²⁺**-dependent protease **calpain**, whose roles in the above sequence are still unclear [Calvete 1995; Schwartz et al. 1995]. Figure IX illustrates the relationship between some of the above molecules.

Platelet lipids

Lipids comprise approximately 50% of the platelet plasma membrane by weight, with protein and carbohydrate accounting for 35-40% and 8-10%, respectively [Phillips 1982]. There are three types of platelet lipids: **phospholipids** (~ 77% of the lipid mass), which have a glycerol backbone attached to a polar phosphate-containing head group and

Figure IX: Integrin-mediated outside-in signalling (from Dedhar & Hannigan 1996, Fig. 3)



two fatty acid chains; neutral lipids like **cholesterol** (~ 21% of the lipid mass), which has the four-ring structure characteristic of steroids; and **glycolipids** (~ 3% of the lipid mass), which contain one fatty acid chain, a sphingolipid, and a polar head group linked to one or more sugar residues [Marcus 1982]. The phospholipids can be distinguished on the basis of their head group. There are five major platelet phospholipids: **phosphatidylcholine (PC)** or **lecithin**, representing 38% of total platelet phospholipid; **phosphatidylethanolamine (PE)**, 27%; **sphingomyelin (SM)**, 17%; **phosphatidylserine (PS)**, 10%; and **phosphatidylinositol (PI)**, 5%. As can be seen in Figure X, PC, SM, and PE are all neutral at physiological pH, while PS and PI are negatively charged. Generic structures of phospholipids, cholesterol, and glycolipids are also depicted in Figure X.

Phospholipids and cholesterol help to maintain the integrity of platelet (and other cell) membranes, which adopt a bilayer conformation: the hydrophobic fatty acid chains and steroid rings associate in the middle of the bilayer, while the polar head groups face towards the cell interior and exterior [Phillips 1982]. There is an asymmetric distribution of phospholipids in the membrane due to the action of an aminophospholipid translocase [Nurden 1994]. SM is found mainly on the platelet surface, PS and PI are primarily inside the cell, and PC and PE are present on both leaflets, although the majority of the latter is also intracellular. However, platelet stimulation leads to translocase inactivation and mobilization of other enzymes acting on membrane phospholipids - including **PC-specific phospholipases C and D**, **PI-specific PLC**, and **PLA₂** - which generate the aforementioned IP₃, DAG, and AA as well as **phosphatidic acid (PA)** and **lyso-PA** [Smyth et al. 1992]. Membrane lipid reorganization is accompanied by the release of microparticles with procoagulant activity, which results in the exposure of PS and additional PE on the platelet surface [Schick 1994]. These phospholipids provide an optimal environment for the generation of two products of the coagulation cascade - **Factor Xa** and **thrombin** - via interactions with **Factors VIIIa** and **Va** respectively, catalyzing the formation of fibrin [Walsh 1994].

Platelet lipids have been implicated in the regulation of cellular processes such as maturation and adhesion [Schick 1994]. They are intimately associated with membrane proteins: lipid groups like **palmitic acid** and **glycosylphosphatidylinositol (GPI)** help to anchor cytoskeletal components and glycoproteins - including p24, GPIIb β , and GPIX - to the plasma membrane. GPIIb and/or GPIIIa appear to be palmitoylated post-translationally as well, something which increases upon platelet activation; this type of acylation may therefore be important for receptor function, perhaps by influencing protein folding or orientation [Cierniewski et al. 1989]. Ligand binding to GPIIb-IIIa is clearly affected by lipids, as addition of PA to the purified receptor increased the proportion of complexes competent to bind Fg, while lyso-PA was a strong inducer of interactions with this adhesive protein [Smyth et al. 1992]. Certain lipids have been shown to regulate the ligand binding specificity of and induce conformational changes in $\alpha_v\beta_3$: when this receptor was inserted into PC vesicles it only interacted with Vn, but in the presence of PC and PE it attached to vWF and Fn as well, and bound these ligands with higher affinity when surrounded by a mixture of PC/PE/PS/PI/Cholesterol [Conforti et al. 1990]. Integrin function in leukocytes also appears to be regulated by lipid, as a moiety called **integrin modulating factor-1 (IMF-1)** generated in activated neutrophils was found to enhance the ligand-binding properties of MAC-1 and LFA-1 [Hermanowski-Vosatka et al. 1992].

BACKGROUND PART 2

Liposomes

Artificial lipid vesicles (**liposomes**) can be classified into two broad groups: **multilamellar vesicles (MLV's)**, which consist of several concentric lipid bilayer membranes separated by aqueous compartments, and **unilamellar vesicles (UV's)**, which have only a single bilayer surrounding the inner hydrophilic environment [Szoka & Papahadjopoulos 1980]. UV's are further subdivided into **small UV's (SUV's)** - with diameters less than 0.05 μm - and **large UV's (LUV's)**, with diameters above this value; like LUV's, MLV's are quite heterogeneous in size and have diameters ranging from 0.05-10 μm [Hope et al. 1986]. As LUV's have high trapped volumes they are useful in vivo for the delivery of water-soluble drugs and other therapeutic agents, which can be encapsulated into the internal compartment during vesicle preparation; LUV's are also widely used in vitro as model membrane systems to study the roles of specific proteins. MLV's have little aqueous space and are thus much more suitable for the administration of hydrophobic compounds, which can be embedded in the lipid bilayers.

Parameters such as liposome size and lamellarity can be regulated by various preparation techniques, while the lipid composition will affect surface charge and bilayer fluidity [Szoka & Papahadjopoulos 1980]. Like native cell membranes, liposome bilayers are normally impermeable to ions and charged polar molecules. However, at a certain temperature - known as the **phase transition temperature (T_c)** - the bilayer becomes much more permeable after undergoing a transition from a gel to a fluid state. Below T_c - in the gel phase - phospholipid fatty acid chains have a rigid conformation, while in the fluid or liquid-crystalline phase - above T_c - each chain is much more free to rotate around its axis and diffuse laterally within the membrane. T_c is influenced by the phospholipid content: saturated fatty acids, especially those with long carbon chains, promote the gel phase due to strong hydrophobic interactions; unsaturated fatty acids have the opposite effect, favouring the liquid-crystalline state; and the nature of the polar head group is also important, as T_c is significantly higher for PE than for PC [Bonté & Juliano 1986].

Cholesterol lessens the impact of phase transition on bilayer permeability due to interactions of the steroid rings with phospholipid fatty acid chains: below T_c the membrane is more fluid than normal, while above T_c permeability is lower than it would be in the absence of cholesterol. When phospholipids having different T_c 's are mixed, each one undergoes a separate gel-fluid transition, known as **phase separation**; this is likewise seen when mixtures of neutral lipids such as PC and anionic lipids like PS are exposed to calcium, which results in the formation of gel-state PS-Ca²⁺ complexes along with fluid PC domains.

Preparation of liposomes

Liposomes can be made from a wide variety of lipids, with phospholipids (and cholesterol) being the most frequently used [Szoka & Papahadjopoulos 1980]. As a number of preparation techniques are known, each of which has particular advantages and disadvantages, the method of choice will depend primarily on the desired liposome properties. A few of the most common procedures are outlined below.

Direct hydration involves solubilization of lipid in an organic solvent, which is removed to produce a dry lipid film, followed by hydration with aqueous buffer and gentle agitation of the mixture [Hope et al. 1986]. This procedure is often used to prepare MLV's because it is fast and relatively easy; the trapped volume and trapping efficiency are low, however, and there may be an unequal distribution of solute from one bilayer to the next. The MLV's produced can subsequently be converted into LUV's by multiple **freeze-thaw cycles** and/or by **extrusion** through polycarbonate filters under high pressure, or transformed into SUV's by **sonication**.

In **reverse phase evaporation (REV)**, LUV's are generated from an emulsion of solubilized lipid and aqueous buffer upon removal of the organic solvent by vacuum [Szoka & Papahadjopoulos 1980]. This technique is quite popular because many different combinations of lipid can be used, and because the enclosed volume and trapping efficiency are high. The latter two characteristics are also true of **ethanol injection** and **ether infusion**; like REV these procedures may not be useful for encapsulation or

incorporation of protein due to the denaturing effect of the organic solvent [Rigaud et al. 1995]. During REV some MLV's are also formed along with the LUV's, although this process can be followed by extrusion to produce vesicles of a more uniform size.

Detergent removal is widely used for the insertion of membrane proteins into liposomes [Rigaud et al. 1995]. Dry lipid is solubilized in a mixture of buffer and detergent to form mixed micelles; after removal of detergent by **dialysis, gel chromatography, hydrophobic adsorption, or dilution**, the micelles coalesce into LUV's. A variation on this procedure involves the use of preformed liposomes rather than simple lipids, with enough detergent added to destabilize - but not completely solubilize - the vesicles. Regardless of the technique used, detergent removal generally takes several hours, forming proteoliposomes with a high trapped volume and a low capture efficiency. These vesicles may still contain residual detergent in the lipid bilayer [Hope et al. 1986].

Reconstitution of membrane proteins into liposomes

Proteins can be isolated from biological membranes by one of three main procedures: addition of detergent, with which proteins form mixed micelles; dissolution in organic solvent; or mechanical fragmentation [Rigaud et al. 1995]. Once isolated and purified, proteins are inserted into liposomes - resulting in **proteoliposomes** - by a number of methods, including several mentioned above: direct hydration, REV, sonication, freeze-thawing, and detergent removal. Another approach to the reconstitution of purified protein is direct incorporation into preformed liposomes; for this technique to be successful, the phospholipid vesicles must contain 'defects' in the bilayer due to the presence of 'contaminants' such as cholesterol, short-chain phosphatidylcholines, detergents, fatty acids, or other proteins [Scotto et al. 1987]. This strategy was employed in the simultaneous transfer of numerous platelet membrane proteins directly to liposomes, something which also occurred using a combination of REV, sonication, and extrusion [Rybak & Renzulli 1993].

Detergent removal is the most frequently used procedure for the preparation of proteoliposomes [Rigaud et al. 1995]. This technique requires a knowledge of the

particular detergent's **critical micelle concentration (cmc)**, the concentration at which detergent monomers self-assemble into micellar aggregates. Detergents with high cmc's such as **deoxycholate** and **octyl glucoside (OG)** generally form small micelles and can easily be removed from solution by any of the methods described above. On the other hand, low cmc detergents like **Triton X-100 (TX-100)** associate in large micelles and are only efficiently eliminated by hydrophobic adsorption. Structures of these detergents are shown in Figure XI.

Solubilization of preformed liposomes by detergent occurs according to a three-stage model regulated by the total detergent concentration ($[D]_t$), illustrated in Figure XII [Paternostre et al. 1988; Rigaud et al. 1995]. In **stage I** added detergent is partitioned between the aqueous medium and the lipid bilayer, something which continues until $[D]_t$ is approximately equal to the cmc. During **stage II** - where $[D]_t$ is higher - there is a gradual solubilization of lipid, leading to the co-existence of lipid-detergent mixed micelles and lipid bilayers saturated with detergent. By **stage III**, where the detergent concentration is at its highest level, phospholipids have been completely solubilized into mixed micelles. The most important factor governing the solubilization process is the molar ratio of detergent to lipid in the aggregates, R_{eff} ; this can be calculated by the equation $R_{eff} = ([D]_t - [D]_{cmc})/[L]$, where $[D]_{cmc}$ is the detergent's cmc and $[L]$ is the total lipid concentration. Values of R_{eff} at the onset and completion of solubilization - known as R_{onset} and R_{sol} - have been determined for a number of detergents. Changes in the turbidity of the lipid-detergent suspension will also reflect the degree of solubilization, as seen in Figure XII: in stage I the optical density (OD) remains constant, in stage II it decreases sharply with addition of detergent, and in stage III it levels off. The $[D]_t$ associated with optimal reconstitution of detergent-solubilized protein depends on the detergent: with OG, protein incorporation is maximal around the cmc; for TX-100, insertion is best in stage II; and using cholate, proteoliposome formation is most efficient in stage III. Other important considerations in detergent-mediated protein reconstitution include the rate of detergent removal and the tendency of the protein to self-aggregate.

Figure XI: Common detergents (from Rigaud et al. 1995, Fig. 2)

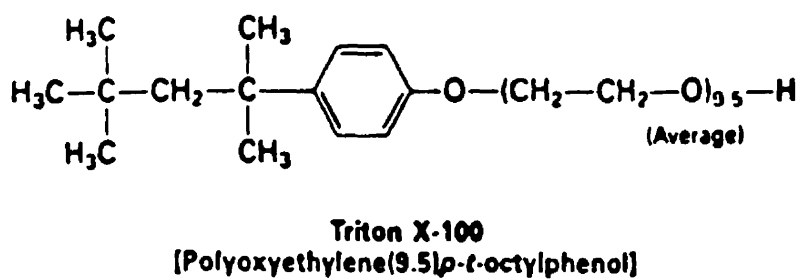
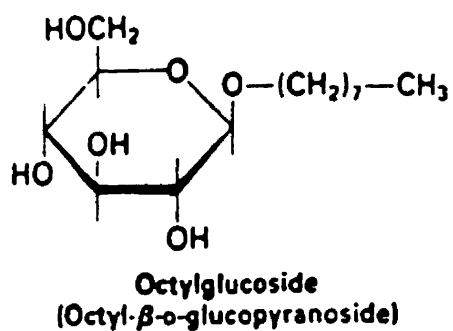
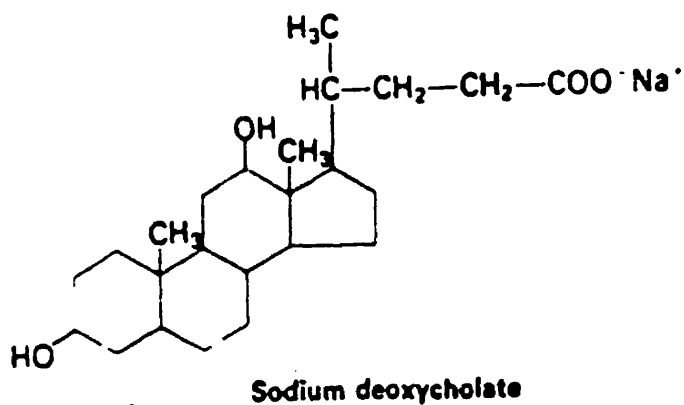
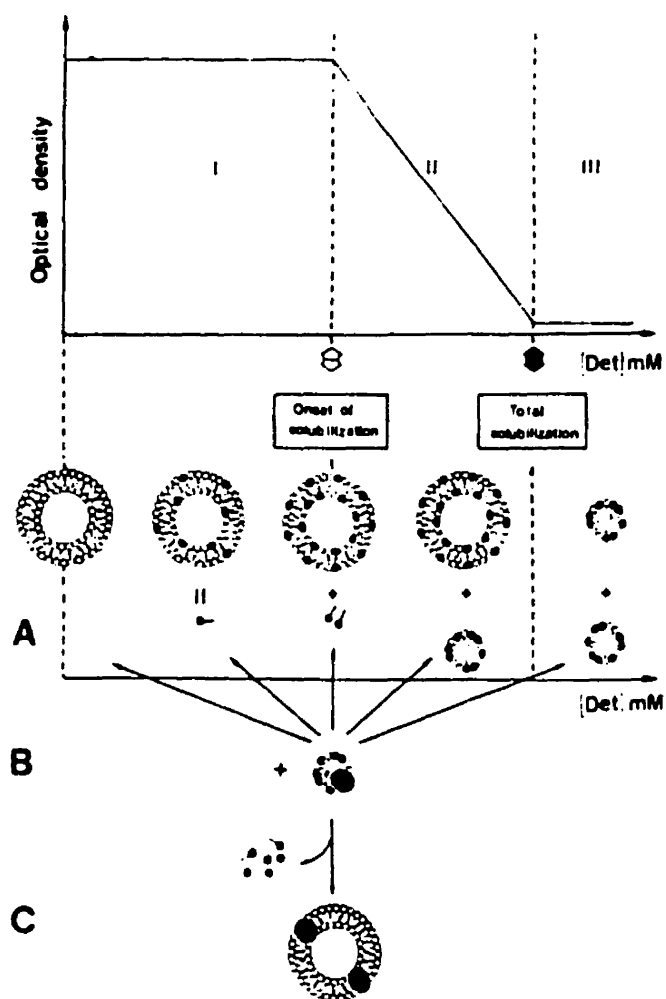


Figure XII: Membrane protein reconstitution (from Rigaud et al. 1995, Fig. 6)



Step A: liposome solubilization

Step B: addition of protein

Step C: removal of detergent

Liposome-liposome interactions

Contact between cell membranes is influenced by various non-specific interactions [Parsegian et al. 1979]. The most important of these is the repulsion due to the removal of water from the surface as cells approach one another, known as the **hydration force**. This acts as a kinetic barrier to the interaction of cells of diameter 20 nm or greater, causing neutral PC bilayers to be separated by 25-30 Å [Parsegian & Rand 1983]. **Electrostatic repulsion** between charged bilayers is much weaker than the hydration force but further increases cell separation to 60 Å or more. Long-range **Van der Waals attraction** helps to partially overcome these repulsive forces but is not strong enough to promote durable cell contact. In the absence of specific interactions involving adhesive ligands and their membrane receptors, bilayer deformation is required for cell adhesion. This is governed by the elastic and viscous properties of the membrane as well as by the vesicle surface area to volume ratio [Evans & Parsegian 1983].

Biological membranes and/or liposomes in contact with one another may participate in a phenomenon known as **lipid transfer**, where there is an exchange of lipid molecules between cell membranes; this must be preceded by **aggregation**, destabilization, and **fusion** [Walter & Siegel 1993]. Aggregation can be thought of as taking place in two stages, involving the attraction of rigid spheres followed by sphere deformation [Evans & Parsegian 1983]. The initial rate of liposome aggregation is proportional to the square of the initial cell concentration N_0 , while the rate of fusion depends on the number of dimer aggregates. Liposome aggregation and fusion are slowed by the presence of charged phospholipids, which increase the stability of the vesicles [Grit & Crommelin 1993]. However, bilayers containing anionic species such as PS have a tendency to aggregate and fuse when exposed to divalent cations, which serve as electrostatic linkages between PS phosphate groups, forming anhydrous complexes. The effect of cholesterol depends on the phospholipid composition and the molar steroid:PC ratio, but in general appears to enhance Ca^{2+} - or Mg^{2+} -induced liposome-liposome interactions [Stamatatos & Silvius 1987]; similar effects are seen when the bilayers are

destabilized by lysophospholipids or fatty acids. Other factors which affect liposome aggregation and fusion in vitro are the temperature, pH, and ionic strength of the medium.

Injection of liposomes into the bloodstream dramatically increases their aggregability due to the adsorption of plasma proteins such as fibrinogen [Semple et al. 1996]. Characteristics like size, shape, charge, hydrophobicity, and conformation will influence protein binding to the liposomes, which may occur by electrostatic attraction and/or hydrophobic interactions [Bergers et al. 1993]. Liposomes containing packing defects, such as gel-state long-chain phosphatidylcholine vesicles, exhibit preferential interaction with proteins [Blume & Cevc 1993]. Protein adsorption and liposome aggregation can be markedly decreased by incorporation of up to 50 mol% cholesterol into the bilayer - which reduces membrane permeability - or by covalent attachment of molecules such as **polyethylene glycol (PEG)**, which acts as a surface barrier. This type of modification significantly prolongs liposome circulation time in vivo.

Liposome adhesion to surfaces

A liposome adheres to a surface by minimizing its overall free energy ΔG [Xia & van de Ven 1992]. This value is characterized by several types of free energy: ΔG_w , the free energy of liposome-surface interactions, which is dependent on the contact area and the surface energy; ΔG_k , the free energy of liposome deformation, which is dependent on the rigidity of the lipid bilayer; ΔG_{pv} , the free energy due to changes in liposome volume or in the difference between the internal and external pressure; and ΔG_γ , the free energy resulting from the surface tension of the lipid bilayer, which is due to changes in liposome surface area. For a constant volume and pressure difference, and a given bilayer area, the ΔG in adhering to a surface is determined by the gain in energy due to liposome deformation and the loss in energy due to an increased contact area. Liposomes with a diameter of less than 80 nm have a very high bending energy and thus will not undergo adhesion, but above this critical value adhesion increases with vesicle size. Adherence of liposomes is also promoted by an acidic pH, elevated calcium and salt concentrations, and for dynamic studies, a high flow rate (up to a maximal level).

MATERIALS

Chemicals and products were purchased from the following companies or institutions:

Abbott Laboratories, Montreal, Quebec: sterile sodium chloride solution

J.T. Baker Chemical Co., Phillipsburg, New Jersey: boric acid (H_3BO_3); calcium chloride (CaCl_2); potassium chloride (KCl); sodium carbonate (Na_2CO_3)

BDH Inc., Toronto, Ontario: diethyl ether ($\text{C}_4\text{H}_{10}\text{O}$); disodium hydrogen orthophosphate (Na_2HPO_4); sodium bicarbonate (NaHCO_3); sodium chloride (NaCl); sodium dihydrogen orthophosphate ($\text{NaH}_2\text{PO}_4 \cdot \text{H}_2\text{O}$); sodium hydroxide (NaOH)

Bio-Rad Laboratories, Hercules, California: Bio Beads SM-2 adsorbent

Calbiochem Corp., La Jolla, California: fluorescein isothiocyanate (FITC)-celite; the hexapeptide H-Gly-Arg-Gly-Asp-Ser-Pro-OH (GRGDSP)

DRK-Blutspendedienst, Baden-Württemberg, Germany: human serum albumin (HSA)

Enzyme Research Laboratories Inc., South Bend, Indiana: purified human fibrinogen

Fisher Scientific Co., Fair Lawn, New Jersey: disodium ethylenediamine tetraacetate ($\text{Na}_2\text{C}_{10}\text{H}_{14}\text{O}_8\text{N}_2 \cdot 2\text{H}_2\text{O}$); hydrochloric acid (HCl); magnesium chloride hydrate ($\text{MgCl}_2 \cdot 6\text{H}_2\text{O}$); silicon oil; sulfuric acid (H_2SO_4)

Flow Cytometry Standards Corp., Research Triangle Park, North Carolina: FACScan calibration beads

ICN Biomedicals Inc., Aurora, Ohio: ammonium molybdate tetrahydrate ($(\text{NH}_4)_6\text{Mo}_7\text{O}_{24} \cdot 4\text{H}_2\text{O}$); Fiske & SubbaRow Reducer

Pharmacia Biotech AB, Uppsala, Sweden: Sephadex G-25 coarse

Polysciences Inc., Warrington, Pennsylvania: carboxylated latex beads of diameter 0.50, 0.78, 2.47, 3.80, and 4.33 μm ; gluteraldehyde

Sigma Chemical Co., St. Louis, Missouri: bovine brain L- α -phosphatidyl-L-serine (PS); bovine serum albumin (BSA) Fraction V; cholesterol (Chol); egg yolk L- α -phosphatidylcholine (PC); hydrogen peroxide (H_2O_2); N-[2-hydroxyethyl]piperazine-N'-[2-ethanesulfonic acid (HEPES); n-octyl- β -D-glucopyranoside (octyl glucoside or OG)

University of Pennsylvania, Philadelphia, Pennsylvania: *FITC-PAC-1*, a fluorescently labelled IgM mAb against activated GPIIb-IIIa

The following individuals or companies generously provided antibodies or other compounds:

Genentech, San Francisco, California: *AP-2*, an IgG mAb against resting GPIIb-IIIa

Dr. G. Matsueda, Princeton University, Princeton, New Jersey: *4A5*, an IgG mAb against the Fg γ chain C-terminus

Dr. R. McEver, Oklahoma Medical Research Foundation, Oklahoma City, Oklahoma: *S12*, an IgG mAb against P-selectin

Dr. E. F. Plow, Cleveland Clinic Foundation, Cleveland, Ohio: *anti-Fg-RIBS-1*, an IgG mAb specific for GPIIb-IIIa-bound Fg

Dr. T. Weller, F. Hoffmann-LaRoche Ltd., Basel, Switzerland: *Ro 44-9883*, a non-peptide analogue of GRGDSP

EXPERIMENTAL METHODS

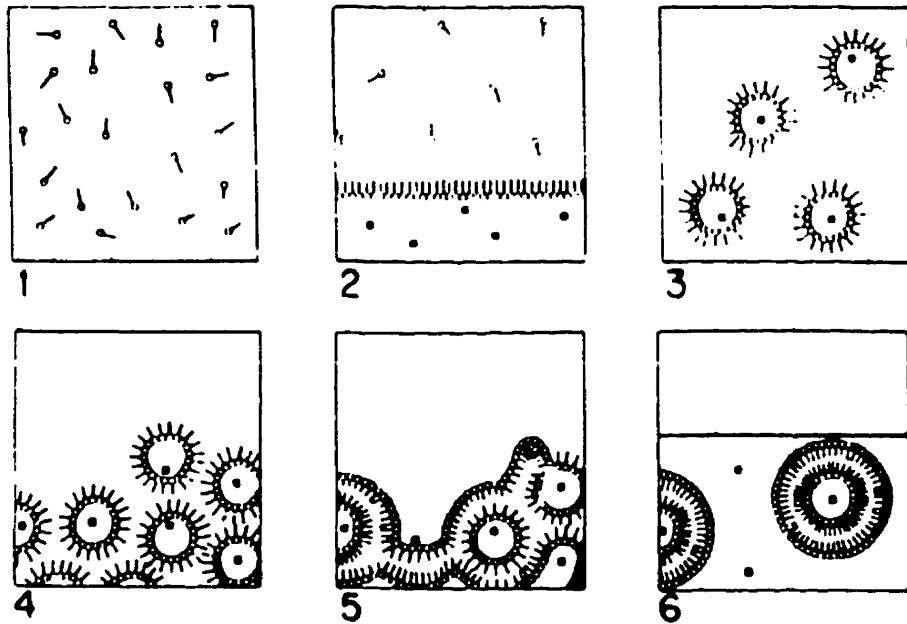
Preparation of liposomes

Liposomes were prepared from a mixture of 15 mg PC, 3.75 mg PS, and 6.25 mg Chol (60:15:25 w/w/w or 48.7:11.4:40.0 mol/mol/mol) by reverse-phase evaporation (REV) [Szoka & Papahadjopoulos 1978; Rybak et al. 1988]. The lipids were placed in a round-bottom flask and any organic solvents were removed by evaporating under pressure using a water aspirator for 5-10 minutes, after which the lipids were dissolved in 2 ml diethyl ether. 0.5 ml H/S buffer (10 mM HEPES, 150 mM NaCl, pH 7.4) was added and the resulting two-phase system was sonicated for 2 minutes in a bath-type sonicator (Laboratory Supplies Co., Hicksville, NY). The ether was then removed by rotary evaporation for 5-10 minutes using the water aspirator. 1 ml H/S buffer was added and the suspension was evaporated for an additional 20-30 minutes to eliminate any traces of ether. The vesicles were then transferred to a 1.5 ml Eppendorf tube and were centrifuged at 10 000 g for 15 minutes. The pellet was resuspended in 1 ml H/S buffer and the tube was recentrifuged as above. After resuspension in 1 ml H/S buffer, the liposomes were stored at 4 °C and remained stable for several weeks; these were known as **control-liposomes**. A depiction of the REV procedure is outlined in Figure XIII.

Quantitative analysis of liposome lipid

Phospholipid phosphorus was determined by the method of Bartlett [Bartlett 1959]. 50 μ l of the liposome suspension was placed in a large glass test tube (25 x 200 mm) to which were added 1 ml ddH₂O and 0.5 ml 10 N H₂SO₄. The mixture was heated at 180-200 °C in a silicon oil bath for 30 minutes, at which point two drops of 30% H₂O₂ were added and the solution reheated at 180-200 °C for another 30 minutes; this process allows the complete decomposition of phospholipid. Then 0.2 ml 5% ammonium molybdate tetrahydrate, 0.2 ml 7.9% Fiske & SubbaRow Reducer, and 4.4 ml ddH₂O were added to the solution, which was reheated in boiling water for 10 minutes, forming a blue product. The optical density of this unknown product is read at 830 nm using a

Figure XIII: Preparation of liposomes by reverse phase evaporation (from Szoka & Papahadjopoulos 1978, Fig. 4)



Step 1: solubilize phospholipids and cholesterol in organic solvent

Step 2: add aqueous buffer to generate a two-phase system

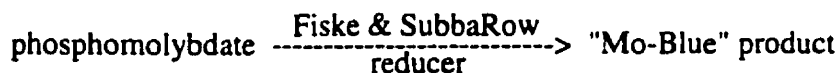
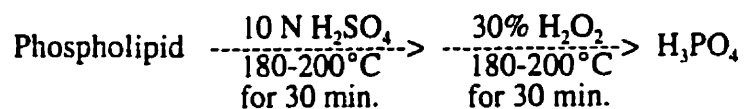
Step 3: sonicate mixture to form an emulsion of lipid micelles

Step 4: remove organic solvent under vacuum

Steps 5 & 6: collapse gel by adding buffer and evaporating all solvent, resulting in the formation of large unilamellar vesicles

UV/visible spectrophotometer (Pharmacia Biotech Ltd., Cambridge, England).

Phosphorus content was determined by comparing the OD value to a calibration curve obtained using known amounts of $\text{NaH}_2\text{PO}_4 \cdot \text{H}_2\text{O}$ and the same procedure as described above. The total lipid concentration was then calculated based on the initial ratio of phospholipid to cholesterol in the liposomes; results are expressed as mean \pm standard error (SE) of the values for all preparations. The chemical reaction for Bartlett's assay is as follows:



Characterization of liposomes and platelets

Various characteristics of control-liposomes were compared to those of activated, fixed human platelets (AFP) prepared by Qingde Liu⁹ [Xia & Frojmovic 1994]. Light-scattering properties, cell concentration and fluorescence were determined by diluting the suspension in H/S buffer and reading for 20 seconds on a FACScan flow cytometer (Becton-Dickinson Canada, Mississauga, ON). The concentrations of different liposome preparations were compared by normalizing each to 5 mM lipid and setting the forward scatter (FSC) threshold to 120; results are expressed as mean \pm SE. Cell size was estimated by comparison of the FSC profile with that of latex beads of various diameters, as well as by looking at the cells with a Coulter Multisizer II particle analyzer (Coulter Electronics Ltd., Luton, England). The extent of liposome aggregation was determined by

⁹ AFP were prepared by incubating resting platelets with a prostacyclin derivative to inhibit platelet activation and with GRGDSP to induce conformational changes in GPIIb-IIIa, followed by fixation with paraformaldehyde [Xia and Frojmovic 1994].

placing the cells on a glass slide and examining them using a light microscope (Carl Zeiss, Germany). Two sets of at least 200 cells on each slide were classified as singlets, doublets, triplets, quartets, quintets, or larger aggregates using a differential counter (Fisher Scientific, Fair Lawn, NJ). Results are expressed as mean \pm standard deviation (SD).

Solubilization of liposomes by octyl glucoside

Liposomes were incubated with a broad range of concentrations of the non-ionic detergent n-octyl- β -D-glucopyranoside (**octyl glucoside** or **OG**), in order to determine the ideal OG concentration for incorporation of GPIIb-IIIa (see below). Liposome solubilization was examined by two different methods.

a) Flow cytometry

Disappearance of liposomes with increasing [OG] could be analyzed by flow cytometry. 18 μ l of the liposome suspension (\sim 15 000/ μ l) was incubated with 2 μ l OG in 0.6 ml Eppendorf tubes; final lipid and OG concentrations were 5 mM and 0-40 mM, respectively. After a 2.5 to 15 minute incubation, the liposome/OG mixture was diluted 1:149 in H/S buffer and read for 20 seconds on the FACScan. Changes in liposome number were calculated as a percentage of the liposome number in the absence of detergent, for the population as a whole as well as for two subpopulations. Results are expressed as mean \pm SE of the values from three separate experiments.

b) Spectrophotometry

Decreases in liposome turbidity could be assayed by spectrophotometry. Three different lipid concentrations were studied: 1.25, 2.5, and 5 mM. In each case, 500 μ l of the liposome suspension was put in a quartz cuvette and the optical density (OD) at 500 nm was measured [Paternostre et al. 1988]. The OG concentration was gradually increased from 2.5 to 40 mM; after each addition of OG the sample was stirred for 2 minutes followed by measurement of the OD₅₀₀.

Preparation of GPIIb-IIIa-liposomes

Elizabeth Brown had previously purified GPIIb-IIIa from the membrane fraction of human platelets by lentil lectin affinity chromatography followed by gel filtration chromatography [Ramsamooj et al. 1990]. Fractions eluted from the second column - with an HSC buffer (10 mM HEPES, 130 mM NaCl, 3 mM CaCl₂, pH 7.4) containing 30 mM OG - were stored at -80°C. The purified receptor was reconstituted into preformed liposomes by destabilization with OG followed by detergent removal via hydrophobic adsorption. Aside from the ideal OG concentration a number of other variables were also tested, including the lipid:protein and Bio-Bead:detergent ratios, the length of the detergent removal stage, and the temperature at which this took place. The following outlines the most successful protocol.

After thawing, GPIIb-IIIa was preactivated by a 1 hour incubation with 1 mM of the hexapeptide **GRGDSP¹⁰**, which induces a conformational change in the receptor [Du et al. 1991]. Liposomes were resuspended in HSC buffer and then destabilized by incubation with OG for 10 minutes; final lipid and OG concentrations were 5 mM and 15-30 mM, respectively. Activated GPIIb-IIIa was then added (lipid:protein 10:1 w/w or ~ 4300:1 mol/mol) and the mixture was stirred for 1 hour. Bio-Beads SM-2¹¹ were then added to remove the detergent by hydrophobic adsorption (4.5 mg wet beads/ μ mol OG) [Philippot et al. 1983]; this was accomplished by stirring the solution at 4°C for 6 hours. The proteoliposomes (**GPIIb-IIIa-liposomes**) were then washed with HSC buffer to remove the GRGDSP and Bio-Beads. **OG-treated-liposomes** were prepared by a similar procedure but were not exposed to GPIIb-IIIa.

¹⁰ to make a stock solution of 30 mM, 10 mg of the peptide was reconstituted in 567 μ l of Tyrode's I buffer (140 mM NaCl, 3 mM KCl, 12 mM NaHCO₃, 0.4 mM NaH₂PO₄·H₂O, pH 7.4) and 4 μ l of 10 N NaOH

¹¹ degassed by rotary evaporation (under vacuum) and stored in HSC buffer

Fluorescent labelling of Fg and mAb's

Fluorescein isothiocyanate (FITC)-Fg was prepared as previously described [Xia et al. 1996]. Approximately 5 mg of 11 mg/ml human Fg was diluted in PBS buffer in a 1.5 ml Eppendorf tube (150 mM NaCl, 2 mM NaH₂PO₄·H₂O, 8 mM Na₂HPO₄, pH 7.4). Several μ l of 5% Na₂CO₃ were added to bring the pH of the solution to 8.5. After dimming the lights, FITC-celite was suspended in PBS and added to the Fg solution; final Fg and FITC-celite concentrations were 2 mg/ml and 1 mg/ml, respectively. The tube was then vortexed, covered with aluminum foil, and put on an end-to-end mixer for 1 hour. Following this the tube was centrifuged for 5 minutes at 10 000 g to pellet the celite. To separate FITC-Fg from free FITC, the supernatant was loaded onto a Sephadex G-25 filtration column - pre-washed with 1% BSA and extensively rinsed with PBS - and eluted with PBS. The fluorescence (OD₄₉₅) and protein levels (OD₂₈₀) of each fraction were determined using a spectrophotometer; after pooling all fractions having an OD₄₉₅/OD₂₈₀ (F:P) ratio of 1.0-1.5, these two absorbance values were measured again. The FITC-Fg was then aliquoted into 0.6 ml Eppendorf tubes and stored at -80°C until further use.

Calculation of the molar F:P and the Fg concentration for the pooled fractions are as previously described [Xia et al. 1996]. The latter was determined using the equation $[Fg] = (OD_{280} - \beta \times OD_{495})/\epsilon_{280}$, where β is the correction factor for the contribution of FITC at 495 nm (equal to 0.286) and ϵ_{280} is the extinction coefficient for Fg at 280 nm, equal to 1.60. This value - in mg/ml - is then divided by the molecular weight of Fg (340 000 g/mol) to determine the molar Fg concentration. The molar concentration of FITC associated with Fg is calculated by $[FITC] = OD_{495}/\epsilon_{495}$, where ϵ_{495} is the extinction coefficient for FITC at 495 nm, equal to 5.56×10^4 . Knowledge of this value enables calculation of the molar F:P ratio, which is given by $[FITC]/[Fg]$. Results are expressed as mean \pm SE of the F:P ratio and [Fg] calculated for a number of FITC-Fg preparations made in our laboratory.

Aside from PAC-1 which was purchased pre-labelled, all other mAb's were conjugated with FITC in our laboratory according to an established protocol [Shattil et al.

1987]. Antibody concentrations and F:P ratios were calculated in a similar manner as described for Fg.

Calibration of FACScan fluorescence

The number of fluorescent FITC-Fg or -mAb molecules bound to each liposome or platelet (see below) could be estimated using latex beads coupled to a pre-determined number of fluorescein molecules, known as the mean equivalent soluble fluorescence (MESF). By plotting this value against the mean fluorescence intensity (FI), a linear calibration was obtained for the photomultiplier tube setting of 630 used in all experiments. Division of the calculated Fg or mAb MESF by the F:P ratio for these compounds enabled estimation of the number of molecules bound. For liposomes results are expressed as mean \pm SE for several different preparations and for platelets as mean \pm SE of multiple assays using the same preparation.

Test for the presence of GPIIb-IIIa in the liposomes

The anti-GPIIb-IIIa mAb AP-2 - labelled with FITC - was used to detect whether the proteoliposomes contained the intact GPIIb-IIIa complex. 1 μ l of the liposome suspension (\sim 15 000/ μ l) was incubated with 2.63 μ l FITC-AP-2¹² in the dark for 60 minutes; the total volume was 15 μ l (final AP-2 concentration of 0.044 mg/ml or 275 nM). After 1:9 dilution with HSC buffer, the sample was read on the FACScan for 20 seconds to determine FI due to binding of AP-2. To quantitate non-specific binding, the IgG mAb S12 against platelet P-selectin - also conjugated with FITC - was incubated with the liposomes instead of AP-2 but at the same concentration. For comparison purposes, similar concentrations of control- and OG-treated-liposomes, as well as AFP, were tested for AP-2 and S12 binding.

¹² thawed and then centrifuged at 10 000 g for 5 minutes immediately before use; this was likewise done for Fg and all other antibodies used

FITC-Fg binding to liposomes or platelets

The GPIIb-IIIa-liposomes were initially tested for their ability to bind Fg. 1 μ l of the liposome suspension (~ 15 000/ μ l) was incubated in the dark with FITC-Fg in THAMC buffer (Tyrode's I buffer, 5 mM HEPES, 1 mg/ml BSA, 1 mM $\text{MgCl}_2 \cdot 6\text{H}_2\text{O}$, 1 mM CaCl_2 , pH 7.4) for 30-60 minutes; the total volume was 15 μ l (final Fg concentration of 10-500 nM). After 1:9 dilution with HSC buffer, the sample was read on the FACScan for 20 seconds to determine FI due to binding of Fg. To quantitate non-specific binding, 1 mM GRGDSP or 1 μ M of its non-peptide analogue **Ro 44-9883 (Ro)**¹³ was added to the liposome suspension just prior to addition of Fg. Specific binding was calculated as FI (Fg alone) - FI (Fg + GRGDSP/Ro). For comparison purposes, similar concentrations of control- and OG-treated-liposomes, as well as AFP, were tested for Fg binding in the presence and absence of GRGDSP/Ro. In addition, 100 μ g/ml of the anti-GPIIb-IIIa mAb **FITC-PAC-1** was incubated for 30 minutes with the liposomes or AFP in place of FITC-Fg, again in the presence or absence of GRGDSP. All of the above binding assays were performed in duplicate and the results averaged.

To investigate the saturability of the interaction of Fg with GPIIb-IIIa-liposomes, 1 μ l of the liposome suspension (~ 15 000/ μ l) was incubated with FITC-Fg in the dark for 60 minutes; the total volume was 15 μ l (final Fg concentration of 5-1000 nM). After 1:9 dilution with HSC buffer, the samples were read on the FACScan for 20 seconds to determine FI due to binding of Fg. To quantitate non-specific binding, 1 mM GRGDSP was added to the liposome suspension just prior to addition of Fg. For comparison purposes, the saturability of Fg binding to similar concentrations of AFP was evaluated in the presence and absence of GRGDSP; all of the above binding assays were performed in duplicate and the results averaged. A plot of bound Fg (**B**) versus the ratio of bound to free Fg (**B/F**) enabled calculation of the dissociation constant (**K_d**) and the maximum number of molecules bound (**B_{max}**) by the Scatchard method [Scatchard 1949]. Results are expressed as mean \pm SE of the values for a number of liposome preparations.

¹³ to make a stock solution of 4.51 mM, 5 mg of the peptidomimetic was dissolved in 2 ml of Tyrode's I buffer (pH 7.4)

To investigate the time-dependence of Fg binding to GPIIb-IIIa-liposomes, 5 μ l of the liposome suspension ($\sim 15\,000/\mu$ l) was incubated with FITC-Fg in THAMC buffer for 0-60 minutes; the total volume was 1 ml (final Fg concentration of 100 nM). At various timepoints the sample was read on the FACScan for 50 seconds to determine FI due to binding of Fg. To quantitate non-specific binding, 1 mM GRGDSP was added to the liposome suspension just prior to addition of Fg. For comparison purposes, the time-dependence of Fg binding to similar concentrations of control-liposomes and AFP was evaluated in the presence and absence of GRGDSP. All of the above binding assays were performed in duplicate and the results averaged.

To investigate the calcium-dependence of Fg binding to GPIIb-IIIa-liposomes, 1 μ l of the liposome suspension ($\sim 15\,000/\mu$ l) was incubated in the dark with FITC-Fg in THAMC buffer for 30 minutes in the presence or absence of the chelating agent EDTA; the total volume was 150 μ l (final Fg and EDTA concentrations of 100 nM and 5 mM, respectively). The samples were then read on the FACScan for 50 seconds to determine FI due to binding of Fg. For comparison purposes, the calcium-dependence of Fg binding to similar concentrations of control-liposomes and AFP was evaluated in the presence and absence of EDTA. All of the above binding assays were performed in duplicate and the results averaged.

Stir-induced aggregation studies

GPIIb-IIIa-liposomes were examined for their ability to undergo stir-induced aggregation mediated by Fg. 120-150 μ l of the liposome suspension (15 000-20 000/ μ l) was put in a disposable glass cuvette (6.9 x 45 mm) containing a metal stir bar, to which was added unlabelled Fg (final concentration of 100 or 500 nM). The cuvette was stirred at 250 or 1000 rpm in an aggregometer for 0-60 minutes; at certain timepoints duplicate 5 μ l subsamples were withdrawn and fixed in 20 μ l of 0.8% gluteraldehyde, while for a few timepoints 10 μ l subsamples were also withdrawn but not fixed. Two 10 μ l aliquots from each fixed sample were then diluted 1:14 with HSC buffer and read on the FACScan for 20 seconds to determine the number of particles. The percent aggregation (PA) could be

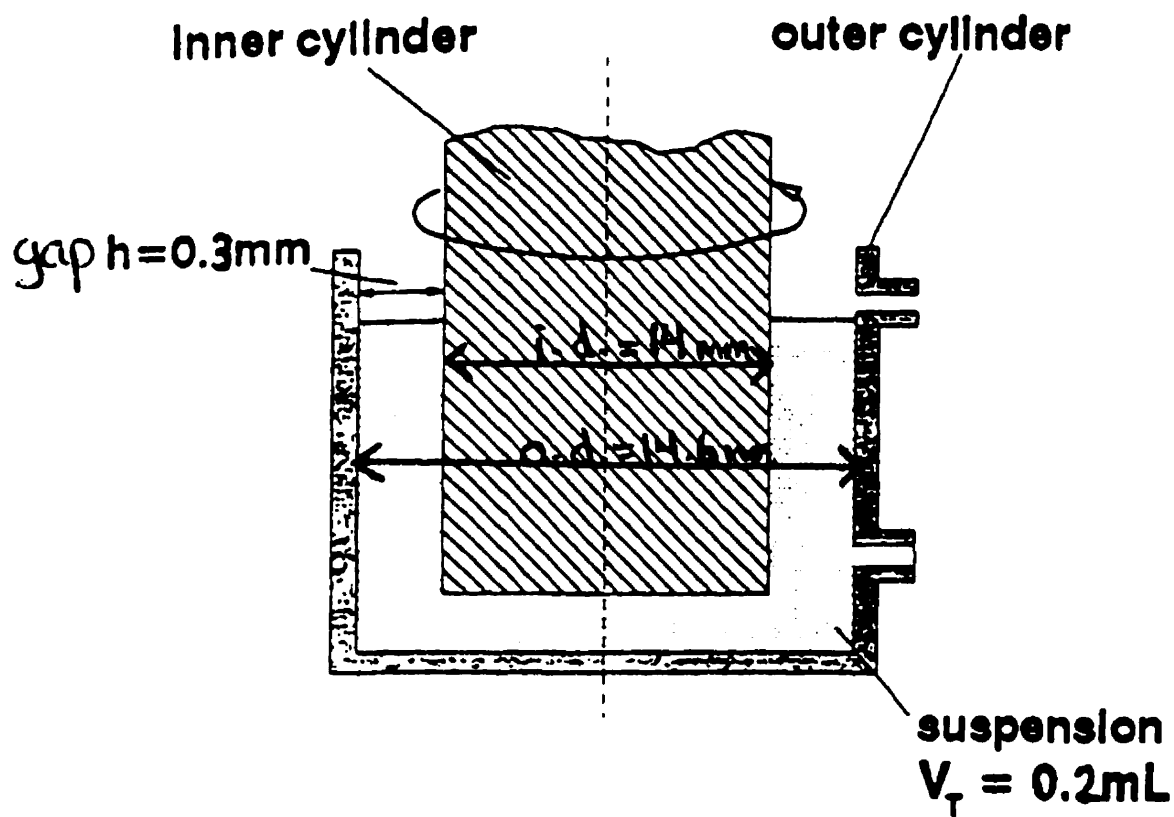
calculated from the equation $PA = (1 - N_t/N_0) \times 100\%$, where N_t is the number of particles at time t and N_0 is the number of particles at time = 0 [Frojmovic et al. 1989]. The unfixed samples were placed on glass slides and examined for aggregation using a light microscope as described for the control-liposomes. In order to assess whether changes in particle number were specifically due to interactions between Fg and GPIIb-IIIa, liposome suspensions were stirred in the absence of Fg as well as in the presence of $1 \mu\text{M}$ Ro (added to the cuvette just prior to addition of Fg). For comparison purposes, similar concentrations of control-liposomes or AFP were evaluated for their ability to undergo stir-induced aggregation in the presence of $Fg \pm Ro$, as well as in the absence of Fg.

Shear-induced aggregation studies

GPIIb-IIIa-liposomes were then examined for their ability to undergo shear-induced aggregation mediated by Fg. The micro-couette used to generate shear flow was similar to one described previously by our laboratory [Xia & Frojmovic 1994]: it was composed of two concentric plexiglass cylinders of diameters 14.6 mm (outer diameter) and 14 mm (inner diameter), with a gap h between the two of 0.3 mm. Uniform shear rates of $1\text{-}2000 \text{ s}^{-1}$ can be produced between the two cylinders by rotation of the inner cylinder at a particular velocity, while the outer cylinder remains stationary. Suspensions of up to $400 \mu\text{l}$ are added through the bottom outlet, while $10\text{-}20 \mu\text{l}$ subsamples are collected through the upper outlet after plugging the bottom one. The shear rate can be calculated by the equation $G = \omega \times r/h$, where ω is the angular velocity and r is the radius of the inner cylinder. Knowledge of the shear rate can then allow an estimation of the initial rate of particle aggregation, which is proportional to G , N_0 , the cube of the particle radius a , and the capture efficiency α^{14} . A diagram of the micro-couette apparatus is shown in Figure XIV.

¹⁴ This is the fraction of shear-induced collisions between two particles that result in doublet formation [Xia & Frojmovic 1994].

Figure XIV: Co-axial cylinder micro-couette (modified from Xia & Frojmovic 1994, Fig. 1)



200-250 μl of the GPIIb-IIIa-liposome suspension (10 000-15 000/ μl) was put in a 0.6 ml Eppendorf tube, to which was added unlabelled Fg (final concentration of 500 nM). After a 2 minute incubation, the suspension was put into the micro-couette and sheared at 50 s^{-1} for 0-10 minutes. At various timepoints the couette was stopped: duplicate 10 μl subsamples were withdrawn and fixed in 40 μl of 0.8% gluteraldehyde. For a few timepoints 10 μl subsamples were also withdrawn but not fixed. Two 15 μl aliquots from each fixed sample were then diluted 1:9 with HSC buffer and read on the FACScan for 20 seconds to determine the number of particles; PA could be calculated as above. The distribution of cells in the unfixed samples was examined under the microscope as above. In order to assess whether changes in particle number were specifically due to interactions between Fg and GPIIb-IIIa, liposome suspensions were sheared in the absence of Fg as well as in the presence of 1 μM Ro (added to the suspension just prior to addition of Fg). For comparison purposes, similar concentrations of control-liposomes were evaluated for their ability to undergo shear-induced aggregation in the presence or absence of Fg.

Binding of liposomes or platelets to Fg immobilized on latex beads

In order to investigate the binding of GPIIb-IIIa-liposomes to immobilized Fg, latex beads were labelled with FITC-Fg (**Fg-beads**). 200 μl of a 2.5% suspension of 4.3 μm diameter beads was incubated in 1 ml borate buffer (0.1 M boric acid, pH 8.5) for 3 minutes, centrifuged at 10 000 g for 1 minute, and then resuspended in 1 ml fresh buffer. After repeating this process, FITC-Fg was added and incubated with the beads for 20 minutes; the final Fg concentration was 450 nM. Human serum albumin (final concentration of 15 mg/ml) was then incubated with the beads for 20 minutes to try to reduce future non-specific binding, followed by centrifugation of the beads as above and resuspension in 1 ml fresh buffer. The same concentration of HSA was again incubated with the beads for another 20 minutes, followed by centrifugation as above and resuspension in 1 ml distilled water. Albumin-labelled beads (**Alb-beads**) were prepared

by a similar procedure but were not exposed to Fg. The concentration and fluorescence of both sets of beads were then quantitated by dilution in HSC buffer and FACScan analysis.

For binding studies involving GPIIb-IIIa-liposomes, Fg- or control Alb-beads were added to a disposable glass cuvette containing the liposome suspension as well as a stir bar (final liposome and bead concentrations of 20 000/ μ l and 10 000/ μ l, respectively). The cuvette was stirred at 1000 rpm in an aggregometer for 0-10 minutes; at certain timepoints duplicate 5 μ l subsamples were withdrawn and fixed in 20 μ l of 0.8% gluteraldehyde. Two 10 μ l aliquots from each fixed sample were then diluted 1:14 with HSC buffer and read on the FACScan for 20 seconds to determine the number of both liposomes and beads, which could be seen as two distinct populations on the FACScan dot-plot; PA for each group could be calculated as above. Liposome suspensions were also stirred in the presence of 1 μ M Ro (added to the cuvette just prior to addition of the Fg-beads). For comparison purposes, similar concentrations of OG-treated-liposomes or AFP were evaluated for their ability to undergo stir-induced co-aggregation with Fg-beads \pm Ro, as well as with Alb-beads.

Binding of mAb's to GPIIb-IIIa-bound Fg

The anti-Fg mAb's 4A5 and anti-Fg-RIBS-I - conjugated with FITC - were used to determine whether the Fg bound to GPIIb-IIIa-liposomes was 'normal'. 1 μ l of the liposome suspension (~ 15 000/ μ l) was incubated with unlabelled Fg in THAMC buffer for 30 minutes; the total volume was 15 μ l (final Fg concentration of 25 nM). The suspension was diluted 1:4 with HSC buffer, followed by the addition of FITC-4A5 or FITC-anti-Fg-RIBS-I (final concentration was 25 nM for the former and 10 nM for the latter). After incubation for 5-10 minutes, the samples were diluted 1:1 with HSC buffer and read on the FACScan for 20 seconds to determine FI due to binding of 4A5 or anti-Fg-RIBS-I. To quantitate non-specific binding, 1 μ M Ro was added to the liposome suspension just prior to addition of Fg. For comparison purposes, binding of both of these mAb's to similar concentrations of OG-treated-liposomes or AFP previously incubated

with 25 nM Fg was evaluated in the presence and absence of Ro. All of the above binding assays were performed in duplicate and the results averaged.

The time-dependence of 4A5 binding to Fg immobilized on GPIIb-IIIa-liposomes was then examined. As above, 1 μ l of the liposome suspension (~ 15 000/ μ l) was incubated with unlabelled Fg in THAMC buffer for 30 minutes; the total volume was 25 μ l (final Fg concentration of 25 nM). The suspension was diluted 1:7 with HSC buffer, followed by incubation with FITC-4A5 for 0-5 minutes (final concentration of 25 nM). At various timepoints the sample was read on the FACScan for 10 seconds to determine FI due to binding of 4A5. For comparison purposes, the time-dependence of 4A5 binding to similar concentrations of OG-treated-liposomes or AFP previously incubated with 25 nM Fg was also evaluated.

RESULTS AND DISCUSSION

Characterization of control-liposomes

Liposomes were prepared by the REV technique so as to generate mainly large unilamellar vesicles (LUV's) of a size distribution similar to human platelets, which have diameters of 2-3 μm [Frojmovic & Milton 1982]. The lipid composition was chosen in order to approximate the phospholipid:cholesterol and phosphatidylcholine: phosphatidylserine ratios found in the platelet membrane [Marcus 1982] - outlined in Table I - and had previously been used in other liposome studies done in our laboratory. It is worth noting that the proportion of PC to PS exposed on the surface of the resting platelet is substantially higher than the indicated values, as phospholipases can digest 45% of the membrane PC but only 9% of membrane PS [Schick 1994]. However, platelet activation leads to externalization of PS and PE, bringing the PC:PS ratio much closer to the value of Table I; the proportion of PC to PS in liposomes is therefore comparable to that of the activated platelet surface. As the liposomes were prepared at room temperature, and the phase transition temperatures of both phospholipids are much lower¹⁵, the vesicles were clearly in the fluid phase with no membrane phase separation.

The liposomes were found to have a lipid concentration of 6.2 ± 2.9 mM (n=3) as determined by Bartlett's assay. Flow cytometric analysis using an FSC threshold of 120 estimated that a 5 mM liposome suspension corresponded to a cell concentration of $7.4 \pm 2.4 \times 10^5/\mu\text{l}$ (n=3). Figure 1a illustrates the liposome FACScan light-scattering profile. This dot-plot could easily be distinguished from that of activated, fixed platelets (AFP), shown in Figure 1b. Figure 2a is a forward scatter histogram of control-liposomes and AFP. As previously determined for fixed platelets, the mean FSC is a good indicator of geometric size [Frojmovic & Wong 1991]. From Figure 2a it is clear that many liposomes were similar in size to platelets, although the former had a greater variation in terms of

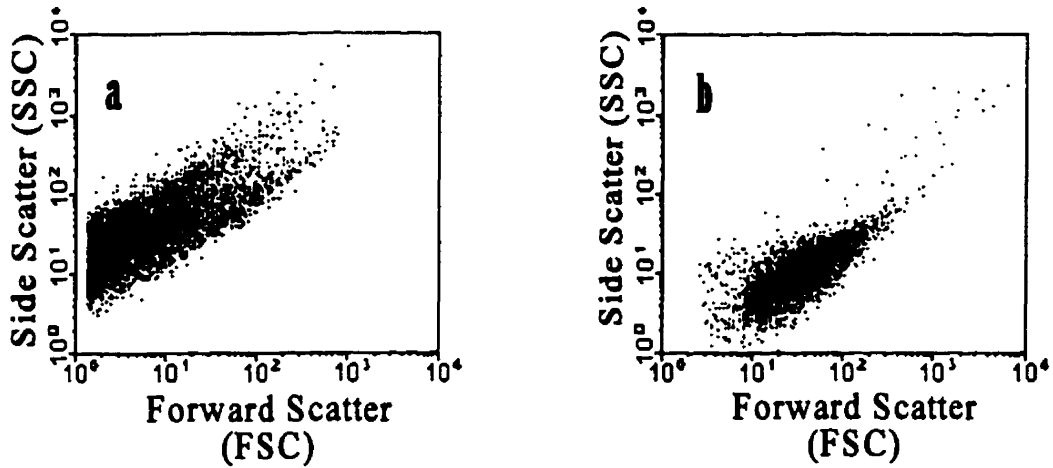
¹⁵ egg PC has a T_c of -15 to -7°C and brain PS has a T_c of $6-8^\circ\text{C}$ [Szoka & Papahadjopoulos 1978]

diameter, which ranged from less than 0.5 μm to at least 4 μm . Electronic particle analysis determined the mean liposome diameter to be approximately 1.4 μm , while that of platelets was about 2.5 μm ; the former is likely an overestimation of the actual value because the analyzer was unable to detect particles with diameters smaller than 1.0 μm . As depicted in Figure 2b, liposomes also demonstrated a similar side scatter distribution as platelets. In the absence of FITC-labelled compounds, liposomes and platelets exhibited minimal fluorescence, with FI values for both cell types of 1.0-2.0 (arbitrary units); a fluorescence histogram for the former is shown in Figure 2c. Examination of liposomes using a light microscope determined that there was minimal aggregation, with $85.0 \pm 0.7\%$ of particles as singlets, $12.5 \pm 0.2\%$ as doublets, $1.6 \pm 0.4\%$ as triplets, and 0.9% as quadruplets. The multiplets may correspond to some of the largest particles detected by flow cytometry.

Table I: Phospholipid:cholesterol and phosphatidylcholine:phosphatidylserine ratios in platelet membranes and REV liposomes (platelet values from Marcus 1982)

	Platelet	Liposome
<i>Phospholipid (% by weight)</i>	77	75
<i>Cholesterol (% by weight)</i>	21	25
<i>Phospholipid:Chol (w/w)</i>	3.7	3.0
<i>PC (% by weight)</i>	29	60
<i>PS (% by weight)</i>	8	15
<i>PC:PS (w/w)</i>	3.8	4.0

Figure 1: FACScan scatter profiles of (a) control-liposomes and (b) fixed platelets



Liposomes or activated, fixed platelets were diluted in buffer and read for 20 seconds on the FACScan.

Figure 2a: Liposome and platelet FSC histograms

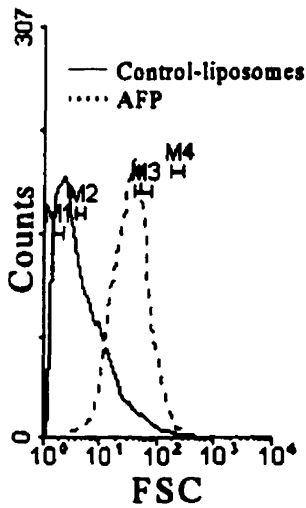


Figure 2b: Liposome and platelet SSC histograms

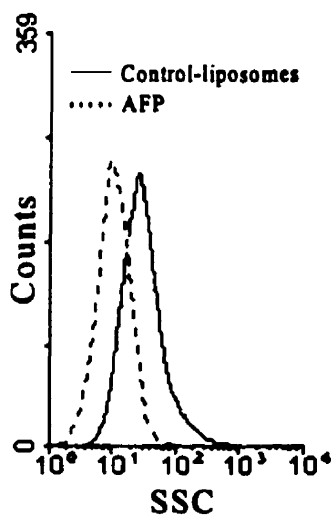
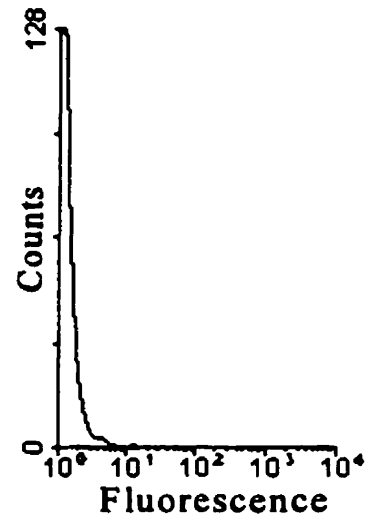


Figure 2c: Control-liposome fluorescence histogram



Liposomes or activated, fixed platelets were diluted in buffer and read for 20 seconds on the FACScan. For Fig. 2a, M1, M2, M3, and M4 represent the FSC of latex beads of diameter 0.50 μm , 0.78 μm , 2.47 μm , and 3.80 μm , respectively.

Liposome solubilization by octyl glucoside

a) Flow cytometry

Figure 3 shows the FACScan profiles of the same 5 mM liposome suspension seen in Figure 1a after incubation with different concentrations of octyl glucoside at room temperature for 5 minutes. These dot-plots clearly provide evidence of two distinct liposome populations - poorly differentiated in Figure 1a - with preferential solubilization of the lower group **R2**. This group accounts for $64.4 \pm 2.3\%$ ($n=3$) of the liposomes and is expected to consist of LUV's, while the liposomes in the upper group **R1** have a more complex structure - reflected by the higher side scatter values - and thus are likely MLV's.

As can be seen in Figure 4, the number of R1 liposomes decreases markedly with minimal addition of detergent but changes little as the [OG] is increased further. The number of R2 liposomes, on the other hand, drops only slightly until the [OG] is just below the critical micelle concentration - approximately 17 mM [Rigaud et al. 1995] - at which point the vesicles are quickly solubilized with additional detergent. As this group makes up the bulk of the liposomes, such a trend is also seen when looking at the population as a whole. Similar graphs were obtained irrespective of the length of time the liposomes were incubated with OG (2.5-15 minutes), implying that equilibrium is reached very rapidly.

b) Spectrophotometry

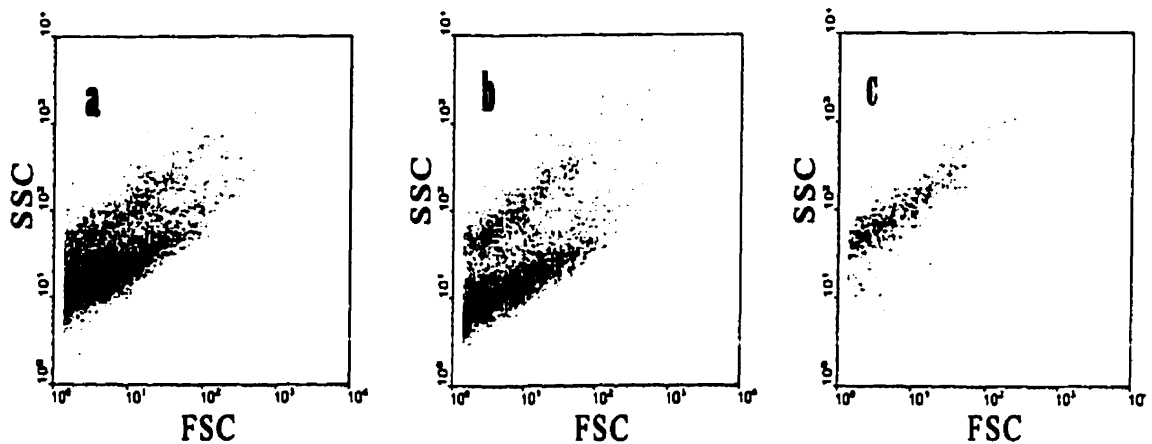
Figure 5 illustrates the effect of successive additions of octyl glucoside on liposome turbidity for three different lipid concentrations. As expected from the three-stage model, turbidity remains constant until a critical detergent concentration is reached, at which point the optical density falls off and then eventually stabilizes. There is therefore somewhat of a discrepancy between this method and the previously described flow cytometric analysis, which detected disappearance of liposomes with minimal addition of detergent. Furthermore, the [OG] required for solubilization of 50% of a 5 mM liposome suspension (EC_{50}) is much lower as determined by flow

cytometry (~ 18 mM) than by spectrophotometry (~ 30 mM). Differences between the two methods may be due in part to the inability of the FACScan to detect particles having diameters of less than 0.2 μm , a problem which does not exist for turbidity measurements.

As determined by spectrophotometry, the octyl glucoside concentrations at which solubilization begins for 2.5 mM and 5 mM lipid are in good agreement with calculations of the $[D]_i$ associated with R_{sat} ¹⁶, while amounts of OG required for complete liposome solubilization are somewhat higher than R_{sol} ¹⁶ $[D]_i$ levels; theoretical and experimental values for these parameters are listed in Table II. The experimental OD measurements are fairly close to those of Paternostre et al., who likewise examined the changes in REV liposome turbidity seen upon addition of OG [Paternostre et al. 1988]. Like the results presented in Table II, this group found that solubilization commenced very close to the predicted $[OG]$ and finished at a higher detergent concentration than expected. However, they also showed that for lipid concentrations of 2.5 mM and above, addition of OG induced a rapid increase in turbidity - after an initial decline - followed by a sharp drop to low levels.

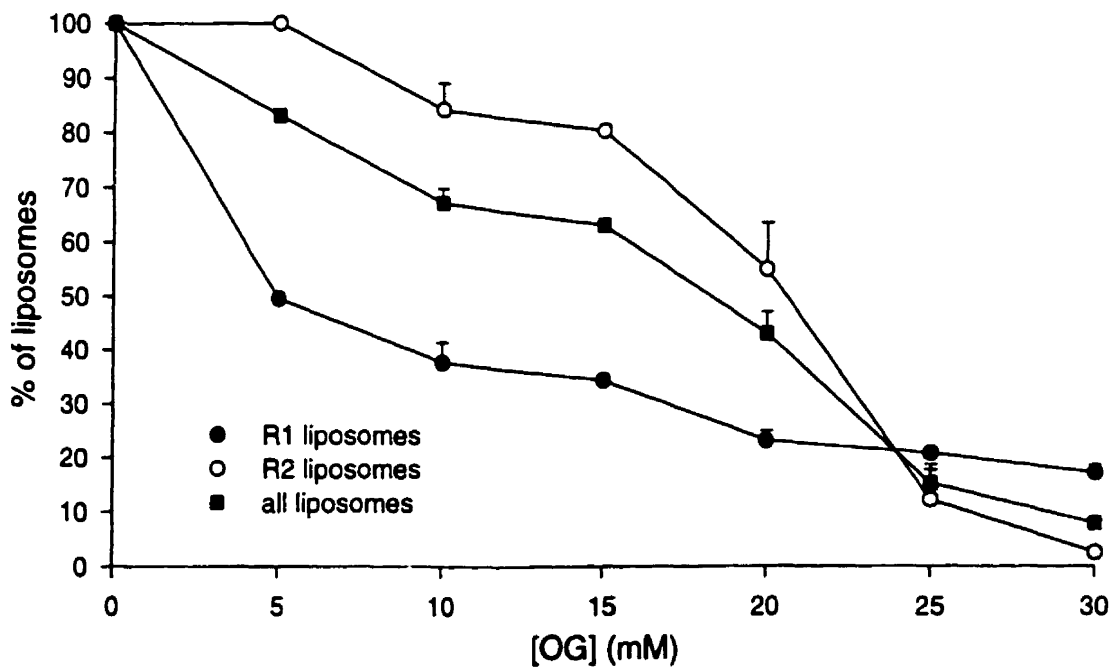
¹⁶ R_{sat} and R_{sol} are the effective detergent-to-lipid molar ratios in detergent-saturated liposomes and mixed micelles respectively [Rigaud et al. 1995].

Figure 3: FACScan scatter profile of 5 mM liposomes in the presence of (a) 10 mM, (b) 20 mM, or (c) 30 mM octyl glucoside



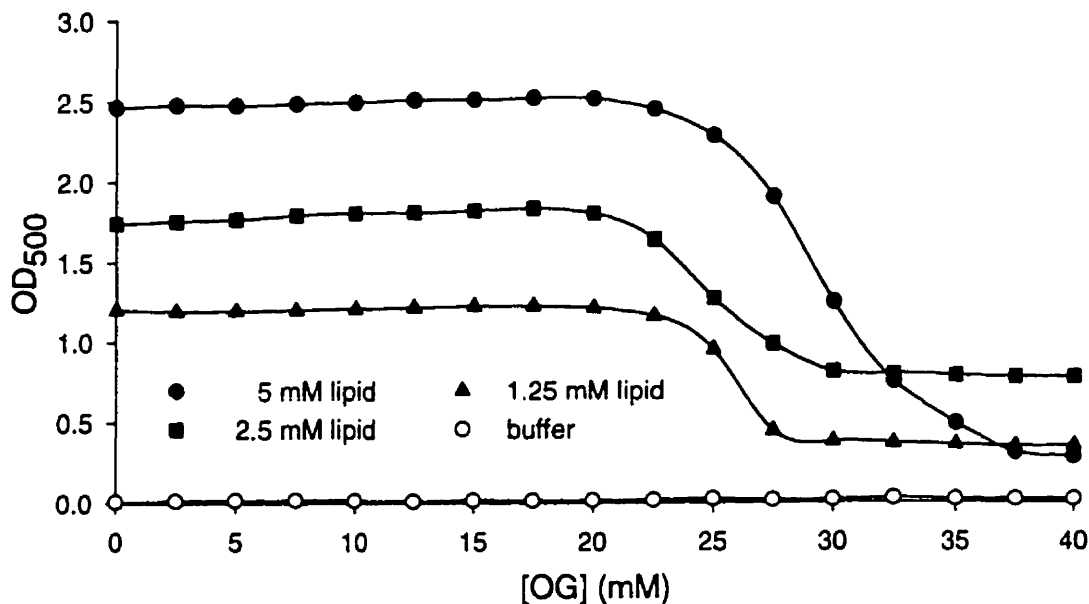
A 5 mM liposome suspension was incubated with various concentrations of octyl glucoside (OG) for 5 minutes at room temperature. Suspensions were then diluted in buffer and read for 20 seconds on the FACScan.

Figure 4: Effect of octyl glucoside concentration on number of liposomes



A 5 mM liposome suspension was incubated with various concentrations of octyl glucoside (OG) for 5 minutes at room temperature. Suspensions were then diluted in buffer and read for 20 seconds on the FACScan to determine the cell count. Results represent the mean of three separate experiments \pm standard error (SE).

Figure 5: Effect of octyl glucoside concentration on liposome turbidity



Octyl glucoside (OG) was added in 2.5 mM increments to a 1.25, 2.5, or 5 mM liposome suspension. After each addition of OG the suspension was stirred for 2 minutes, followed by measurement of the optical density at 500 nm using a spectrophotometer.

Table II: Theoretical and experimental values of R_{sat} and R_{sol} for three lipid concentrations in the presence of octyl glucoside

[Lipid] (mM)	Theoretical concentrations ¹⁷		Experimental concentrations ¹⁸	
	R_{sat} (mM)	R_{sol} (mM)	R_{sat} (mM)	R_{sol} (mM)
1.25	18.6	20.3	22.5	27.5
2.5	20.3	23.5	20	30
5	23.5	30	22.5	37.5

¹⁷ Calculated using the equation $R_{eff} = ([D]_t - [D]_{cmc})/[L]$, where R_{eff} represents either R_{sat} or R_{sol} , $[D]_t$ is the total detergent concentration, $[D]_{cmc}$ is the detergent's cmc and $[L]$ is the total lipid concentration [Rigaud et al. 1995]. For OG, R_{sat} and R_{sol} are approximately 1.3 and 2.6 respectively.

¹⁸ determined from Figure 4

Characterization of FITC-Fg

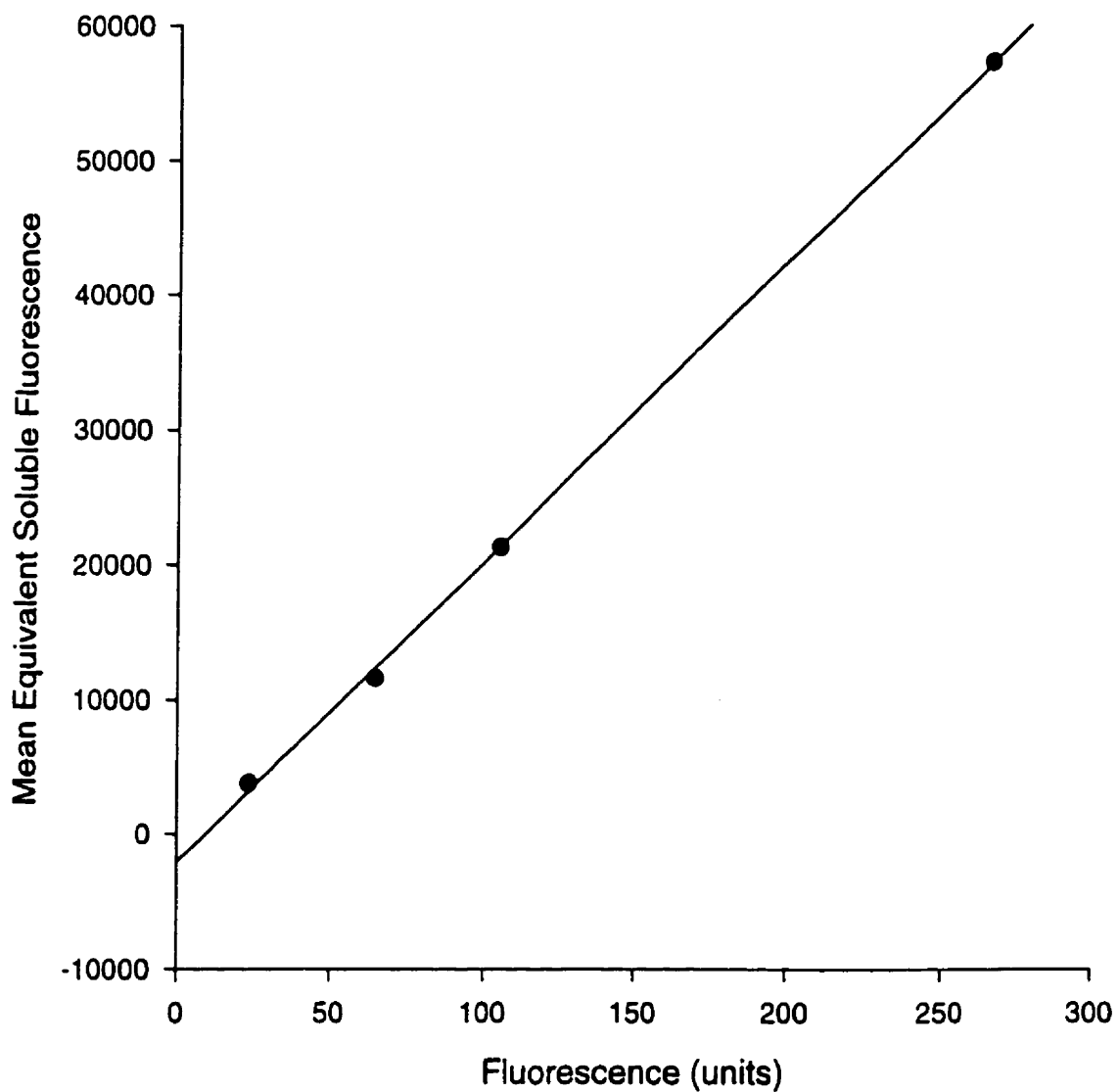
The Fg concentration and molar F:P ratio of FITC-Fg were quite consistent over a number of preparations, with average values of $5.6 \pm 0.4 \mu\text{M}$ (n=5) and 4.0 ± 0.4 (n=5) respectively. The stock solution was then diluted for binding studies.

Calibration of FACScan fluorescence

A plot of the mean fluorescence intensity (FI) versus mean equivalent soluble fluorescence (MESF) for the calibration beads is shown in Figure 6. For this graph the slope was **223.2** and the y-intercept was **-2071.1**. The equation relating MESF and FI is therefore:

$$\text{MESF} = 223.2 \times \text{FI} - 2071.1 \quad (\text{Eq. 1})$$

Figure 6: FACScan fluorescence calibration curve



Latex beads coupled to a known number of fluorescein molecules were diluted in buffer and read for 20 seconds on the FACScan to determine fluorescence.

Preparation and characterization of GPIIb-IIIa-liposomes

The insertion of GPIIb-IIIa into LUV's during their formation by REV had previously been attempted in our laboratory using the method of Rybak et al., who generated GPIIb-IIIa-containing phosphatidylcholine vesicles with a mean diameter of about 5 μm [Rybak et al. 1988]. The liposomes made in our lab were of a similar size range, but in contrast to the results of Rybak's group no functional proteoliposomes were detected as measured by the binding of several fluorescent antibodies to the GPIIb-IIIa complex. Rybak was also able to successfully incorporate the Fg receptor into lipid vesicles by direct hydration/freezing-thawing [Rybak 1986], while other investigators have accomplished this by detergent dialysis [Baldassare et al. 1985; Phillips et al. 1992], but the proteoliposomes generated by these techniques would be much too small (diameters of 200 nm or less) to be useful for FACScan or light microscopy studies. In order to maintain the size distribution of the control-liposomes, it was decided to reconstitute GPIIb-IIIa into preformed liposomes by destabilization with octyl glucoside followed by detergent removal via hydrophobic adsorption. This approach was advantageous for other reasons as well: the tendency for OG-generated proteoliposomes to have a high asymmetry with regards to protein orientation; the relative ease with which OG can be eliminated from solution compared to other detergents; and the overall simplicity of the procedure [Rigaud et al. 1995].

Because of the discrepancy between the flow cytometric and spectrophotometric methods with regards to OG-mediated solubilization of the 5 mM liposome suspension, several detergent concentrations between 15 and 30 mM were initially tested to determine the optimal OG level for preparation of GPIIb-IIIa-liposomes. As shown in Figures 7a and 7b, the FSC and SSC histograms for these liposomes were similar to those for the control group, indicating that the proteoliposomes also had a broad size distribution and diameters of the same order of magnitude as fixed platelets (AFP). There was a significant loss of lipid during the protein incorporation procedure, as flow cytometric liposome counts were consistently less than 10% of control values. Protein insertion appeared optimal with an [OG] of 30 mM; this detergent concentration was

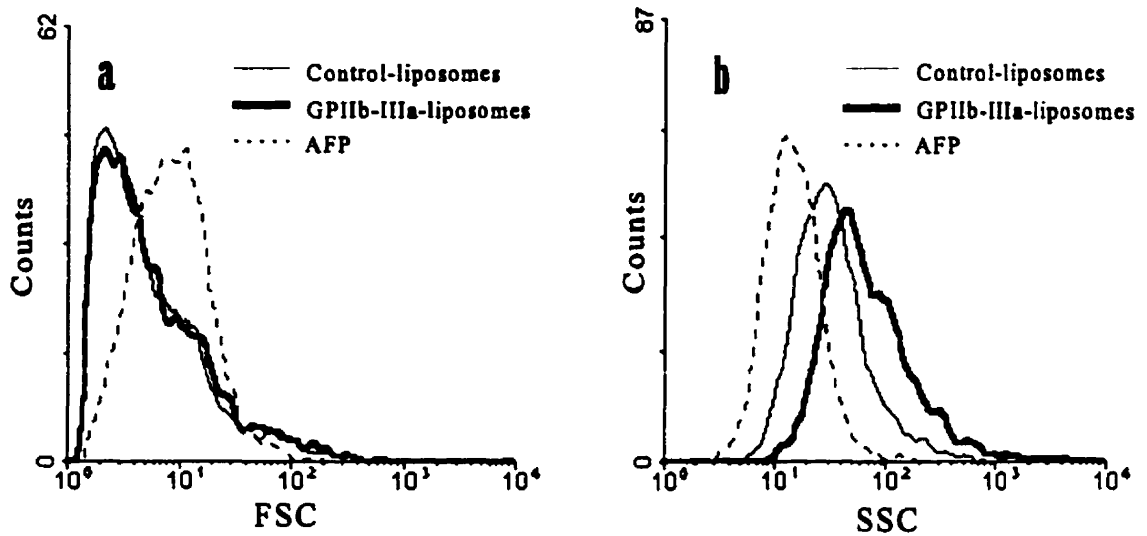
therefore used for all subsequent reconstitution experiments. The presence of GPIIb-IIIa was assessed by the binding of FITC-AP-2 - a fluorescently labelled IgG mAb against the resting complex [Pidard et al. 1983] - to the proteoliposomes. Figure 8 is a representative fluorescence histogram depicting the binding of AP-2 to liposomes and platelets, with FI values of 567, 7.3, and 754 for GPIIb-IIIa-liposomes, control-liposomes, and AFP respectively. As these proteoliposomes only exhibit one peak, the entire population appears to contain GPIIb-IIIa, with a similar distribution as for platelets. In 5 out of 14 preparations a second peak having low FI could also be seen, representing between 10.6% and 35.1% of all liposomes (mean of $21.2 \pm 4.0\%$); these vesicles therefore did not contain the intact receptor in the correct orientation. Control- and OG-treated-liposomes showed minimal specific AP-2 binding.

The total number of FITC-AP-2 molecules bound to the GPIIb-IIIa-liposomes could be determined by using Eq. 1 to calculate the MESF and then dividing by the F:P ratio, assuming a 1:1 stoichiometry. Non-specific binding was expressed in terms of molecules bound of the anti-P-selectin mAb FITC-S12 and was subtracted from the total to give a value for specific AP-2 binding. There was a significant amount of variability with regards to the number of Fg receptors inserted into liposomes from one preparation to the next, but on average $39\ 000 \pm 6\ 000$ molecules ($n=11$) were incorporated, with minimum and maximum values of 10 000 and 64 000 respectively. These numbers are in line with the approximately 50 000 GPIIb-IIIa molecules thought to exist on resting platelets [Pidard et al. 1983; Phillips et al. 1988] as well as the $30\ 000 \pm 3\ 000$ molecules calculated for one preparation of AFP ($n=6$). However, recent work involving 7E3 - another anti-GPIIb-IIIa IgG mAb - has shown that the intact IgG can bind to two GPIIb-IIIa molecules, whereas the monovalent F_{ab} only binds to one [Wagner et al. 1996]. The true number of GPIIb-IIIa complexes on platelets may therefore be twice as high as previously thought, and the liposomes may similarly have many more receptors than indicated above.

Figure 9 is a contour plot demonstrating that the FI due to binding of AP-2 increases with FSC for both GPIIb-IIIa-liposomes and AFP. The surface density

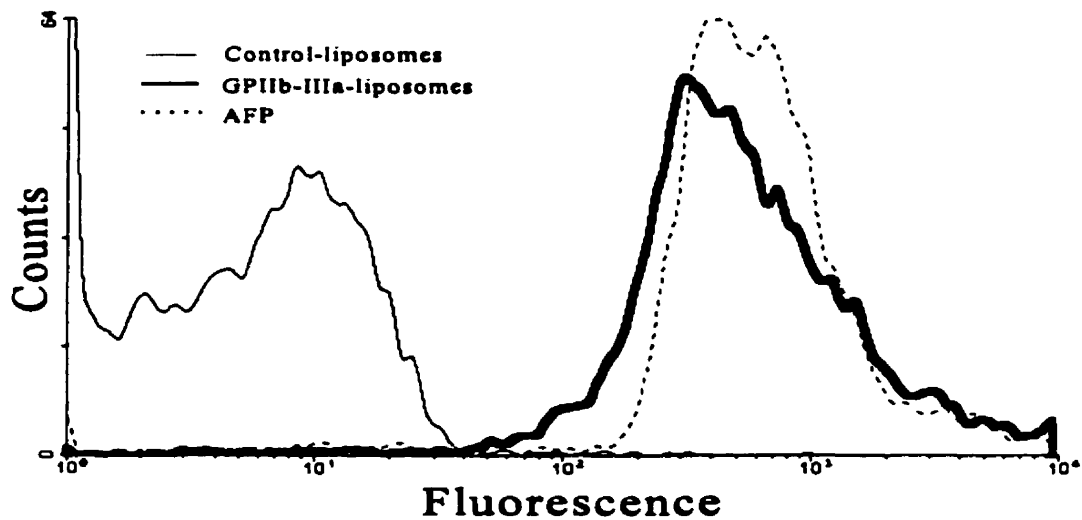
(number of GPIIb-IIIa complexes per unit surface area) thus remains approximately constant with increasing liposome or platelet size. Table III compares the GPIIb-IIIa surface density for resting platelets, AFP, and GPIIb-IIIa-liposomes. On average the latter thus had more than four times as many receptors per unit area as AFP, and about 2.5 times as many as resting platelets.

Figure 7: FSC (a) and SSC (b) histograms for GPIIb-IIIa-liposomes



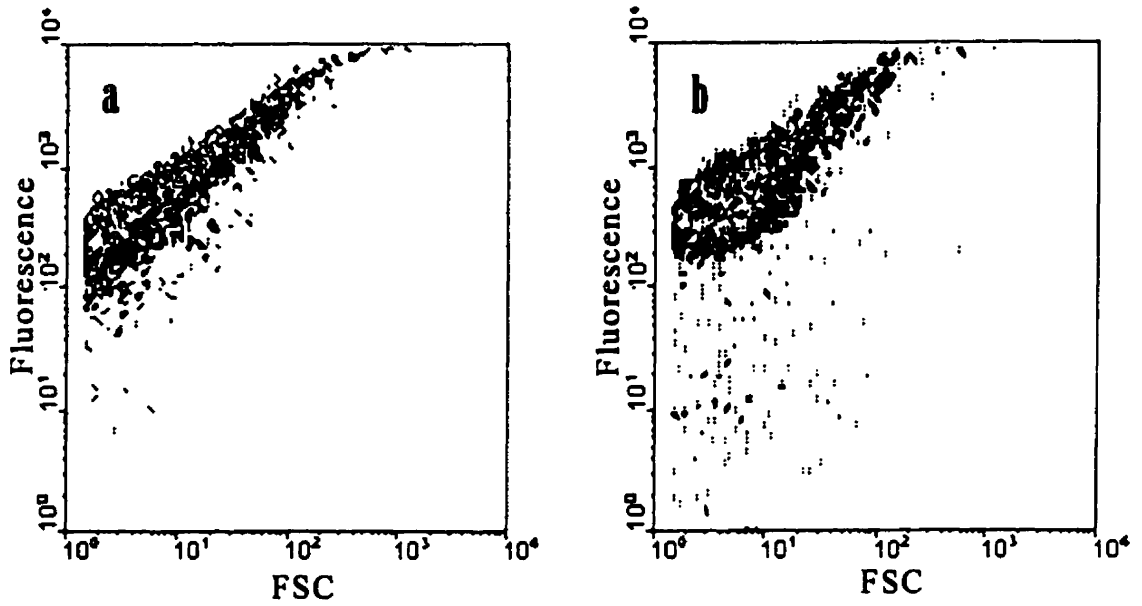
Liposomes or activated, fixed platelets ($\sim 1000/\mu\text{l}$) were diluted in buffer and read for 20 seconds on the FACScan.

Figure 8: Fluorescence histogram of FITC-AP-2 binding to liposomes and platelets



Liposomes or activated, fixed platelets ($\sim 1000/\mu\text{l}$) were incubated with 275 nM FITC-AP-2 for 60 minutes at room temperature. Suspensions were then diluted in buffer and read for 20 seconds on the FACScan to determine fluorescence.

Figure 9: Contour plot of FITC-AP-2 binding to (a) GPIIb-IIIa-liposomes and (b) platelets



Liposomes or activated, fixed platelets (~ 1000/ μ l) were incubated with FITC-AP-2 for 60 minutes at room temperature. Suspensions were then diluted in buffer and read for 20 seconds on the FACScan.

Table III: Estimated GPIIb-IIIa surface density on platelets and liposomes

Cell type	approx. # of GPIIb-IIIa	average surface area (μm^2) ¹⁹	GPIIb-IIIa density (#/ μm^2)
<i>resting platelet</i>	50 000	20	2500
<i>AFP</i>	30 000	20	1500
<i>GPIIb-IIIa-liposome</i>	39 000	6	6300

¹⁹ By treating platelets and liposomes as spheres, the surface area can be calculated using $\pi \times d^2$, where d is the diameter. The mean diameter was taken to be 2.5 μm for platelets and 1.4 μm for liposomes, as determined by electronic particle analysis.

Fg binding to GPIIb-IIIa-liposomes

GPIIb-IIIa-liposomes and AFP, but not control- or OG-treated-liposomes, exhibit specific binding to FITC-Fg as assessed by flow cytometry. This is illustrated by Figure 10a, which is a representative fluorescence histogram for the equilibrium binding of 500 nM Fg. Binding was considered to be specific if it was substantially inhibited by preincubation with 1 mM GRGDSP or 1 μ M Ro, both of which bind to GPIIb-IIIa and block receptor-ligand interactions. Figure 10b is a representative plot for the equilibrium binding of 500 nM Fg. Fluorescence in the presence of Ro was taken as non-specific binding and subtracted from the total to give the Fg-specific FI, which could then be converted into numbers of Fg molecules bound (**B**) as for AP-2.

Proteoliposomes demonstrating specific Fg binding will be referred to as **GPIIb-IIIa*-liposomes**. Specific binding was seen with various Fg concentrations and several liposome preparations, although there was some fluctuation in FI for a given [Fg] due to variations in the F:P ratio of the FITC-Fg used and in the number of receptors incorporated into a particular batch of liposomes. Some proteoliposome preparations showed no or minimal specific Fg binding despite high numbers of receptors, and will be referred to as 'resting' or **GPIIb-IIIa⁰-liposomes**. This may have been due to an ineffective 'preactivation' procedure - incubation of soluble GPIIb-IIIa with GRGDSP should normally induce irreversible conformational changes in the receptor which allow it to bind Fg - as the problem was sometimes resolved by proteoliposome incubation with the above RGD-peptide. Incorrect orientation of the reconstituted GPIIb-IIIa or inadequate washing of the liposomes to remove the peptide used for preactivation are other possible explanations for the lack of Fg binding.

Figure 11a is a representative curve of the saturability of the Fg-GPIIb-IIIa interaction for proteoliposomes and AFP under equilibrium conditions (see below). For the liposomes fluorescence rises rapidly with increasing [FITC-Fg] and then levels off around 200 nM, while the binding of Fg to platelets continues to increase up to a concentration of 500 nM. Conversion of FI values to number of Fg molecules bound and division by the maximal value ($F_{g,max}$) enables determination of receptor occupancy

for each concentration of ligand. As the receptor occupancy for 500 nM Fg is always 100%, as shown in Figure 11b, the B-value associated with this [Fg] can be considered to represent Fg_{max} ; such values for four different GPIIb-IIIa*-liposome preparations and for four separate assays done on the same AFP preparation are shown in Tables IV and V. The maximum number of Fg molecules bound by the proteoliposomes was always significantly lower than the number of GPIIb-IIIa complexes, as can be seen in Table IV. For fixed platelets, on the other hand, the ratio of Fg per GPIIb-IIIa was much closer to 1:1, as illustrated by Table V.

Differences between the two cell types in terms of relative Fg binding may be reconciled in part by considering the structure of the Fg molecule. As Fg has two γ chain C-termini which can bind to GPIIb-IIIa - as well as a number of A α RGD sites which may also interact with the receptor - it is likely that some Fg molecules will bind to two adjacent receptors on the same cell. Because the liposomes have a much higher GPIIb-IIIa surface density than AFP (shown in Table III), it is reasonable that for the former many more Fg molecules will participate in bivalent intraparticle crosslinking. This hypothesis is supported by considering the binding of Fg to activated unfixed platelets, which bind approximately 30 000 molecules of Fg but likely have at least 50 000 GPIIb-IIIa receptors [Peerschke 1995]. Their Fg/GPIIb-IIIa ratio (~ 0.6) is thus between that of the liposomes and AFP, while their GPIIb-IIIa surface density is likewise at an intermediate level (see Table III).

In addition to Fg_{max} , Figure 11a provides an estimate of the dissociation constant K_d , which is the ligand concentration required for binding to reach 50% of maximum: for three different GPIIb-IIIa*-liposome preparations, this was found to be 51 ± 13 nM. The K_d can also be determined by way of a Scatchard plot, shown for the GPIIb-IIIa*-liposomes of Figure 11a in Figure 11c, which illustrates the relationship between bound Fg (**B**) and the ratio of bound to free ligand (**B/F**) for each Fg concentration. If all binding sites have a similar affinity, one straight line would be expected to pass through most of the datapoints, with the x-intercept representing the maximum number of molecules bound (B_{max}). This should be close to the corresponding Fg_{max} value; for

example, preparation 3 from Table IV was calculated to have a B_{max} of 20 552.

However, the liposomes of Figure 11c - as well as other proteoliposome preparations - appear to have two classes of Fg binding sites. Other investigators working with GPIIb-IIIa-liposomes observed only a single type of binding site [Baldassare et al. 1985; Parise & Phillips 1985; Rybak 1986], while for platelets both one and two classes have been reported [Niewiarowski et al. 1983]. The inverse of the steeper slope in Figure 11c represents the K_d for the high-affinity binding sites, calculated to be 23 ± 1 nM, while the low-affinity K_d - from the other slope - is 142 ± 66 nM. The former is close to the K_d 's of 4.5 and 15 nM reported for the binding of Fg to GPIIb-IIIa-liposomes prepared by Baldassare et al. or Parise & Phillips, respectively, and is considerably lower than the K_d of 750 nM reported by Rybak. The above high-affinity K_d is also less than that calculated for the binding of Fg to GPIIb-IIIa reconstituted into planar lipid bilayers (50 nM) [Müller et al. 1993], as well as for the interaction of Fg with agonist-stimulated platelets (80-360 nM) and with AFP (70-255 nM) [Xia et al. 1996].

The next characteristic of the Fg-GPIIb-IIIa interaction examined was time-dependence, shown in Figure 12a for the binding of 100 nM FITC-Fg to GPIIb-IIIa*-liposomes or AFP. Values of V_{max} - the rate of increase in fluorescence due to binding of Fg - are 21.3 units min^{-1} for the liposomes and 38.8 units min^{-1} for the platelets, while the $t_{1/2}$ - the time required for binding to reach 50% of maximum - is about 4 minutes for platelets and 5 minutes for liposomes. These $t_{1/2}$ values are slightly higher than the 2 minutes reported for platelets maximally activated by ADP [Frojmovic et al. 1994]. For both AFP and GPIIb-IIIa*-liposomes equilibrium was reached by about 20 minutes, with maximal specific FI values (FI_{max}) of 232.7 for the former and 106.7 for the latter. Knowledge of V_{max} and FI_{max} allows determination of the rate of Fg binding: $k_2 = V_{max}/(FI_{max} \times m_0)$, where m_0 is the molar concentration of ligand at time $t=0$, in this case 10^{-7} M [Frojmovic et al. 1991b]. k_2 was calculated to be $1.2 \times 10^{-6} \text{ M}^{-1} \text{ min}^{-1}$ for the liposomes and $1.7 \times 10^{-6} \text{ M}^{-1} \text{ min}^{-1}$ for the platelets. These values are somewhat lower than the k_2 of $8 \times 10^{-6} \text{ M}^{-1} \text{ min}^{-1}$ reported for binding of the IgM mAb PAC-1 to ADP-stimulated platelets; this mAb interacts with the GPIIb-IIIa ligand-binding site on

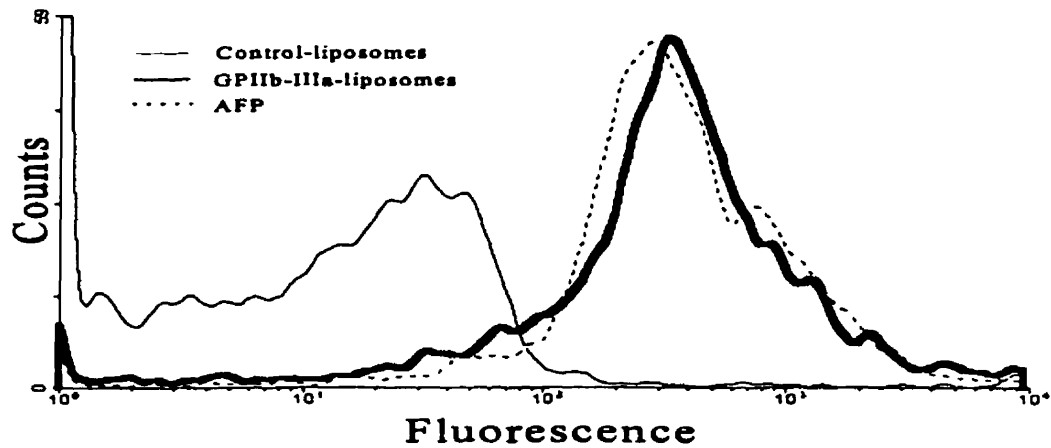
activated platelets [Shattil et al. 1985]. Other groups have likewise observed time-dependent binding of Fg to GPIIb-IIIa-liposomes [Parise & Phillips 1985; Rybak 1986].

Figure 12b looks at the effect of Fg concentration on the time course of binding to a different preparation of GPIIb-IIIa*-liposomes. For 100 nM Fg the $t_{1/2}$ was about 4 minutes and maximal binding occurred by 20 minutes. The Fl_{max} (205.9 units) was similar to that seen with the liposomes in Figure 13a, but the V_{max} and k_2 were almost three times as high (60.3 min^{-1} and $2.9 \times 10^{-6} \text{ M}^{-1} \text{ min}^{-1}$, respectively). With 500 nM Fg binding was very rapid, with a $t_{1/2}$ of around 30 seconds and maximal binding seen by 3 minutes; the Fl_{max} was 335.3 units. V_{max} (405.9 min^{-1}) was more than sixfold higher than for 100 nM Fg but the k_2 ($2.4 \times 10^{-6} \text{ M}^{-1} \text{ min}^{-1}$) was slightly lower. Conversion of the Fl value associated with a particular timepoint to number of Fg molecules bound and division by the maximal value for 500 nM Fg (Fg_{max}) enables determination of receptor occupancy as a function of time, shown in Figure 12c. As can be seen, occupancy for 500 nM Fg is close to 80% by 1 minute and almost 100% by 2 minutes, whereas for 100 nM Fg occupancy is less than 10% at 1' and reaches a maximum of 60% by 20'.

As illustrated by Figure 13, binding of FITC-Fg to GPIIb-IIIa*-liposomes and to AFP - but not to control-liposomes - is dependent on the presence of calcium, as chelation of this cation by EDTA largely abolished interactions with Fg. The Ca^{2+} -dependence of Fg binding to GPIIb-IIIa-liposomes has previously been demonstrated, while the requirement of divalent cations for this receptor-ligand interaction has long been established for platelets [Bennett & Vilaire 1979; Parise & Phillips 1985].

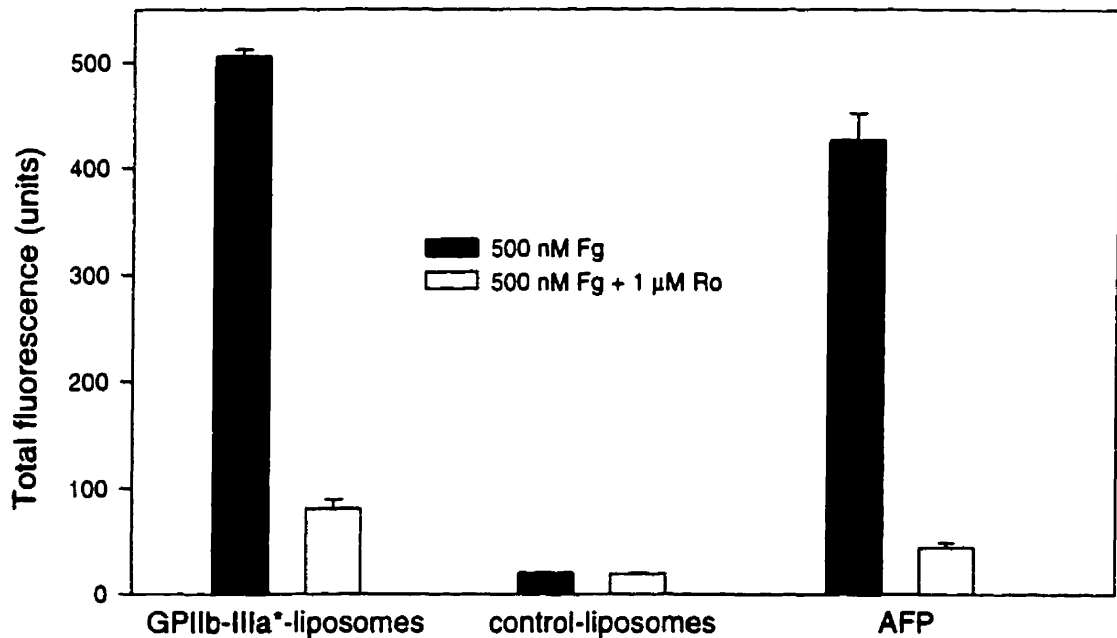
As shown in Figure 14, GPIIb-IIIa*-liposomes and AFP also exhibited GRGDSP-inhibitable binding to PAC-1. Since this mAb was used at a saturating concentration (100 $\mu\text{g/ml}$ or $\sim 100 \text{ nM}$), the maximum number of bound PAC-1 molecules can be calculated; it was found to be 3300 for the liposomes and 1700 for AFP. These values are significantly lower than the mean Fg_{max} for 500 nM Fg shown in Tables IV and V, as well as the 10 000-15 000 PAC-1 molecules shown to bind to ADP-activated platelets. This discrepancy may be due in part to inaccuracies in calculating the PAC-1 F:P ratio.

Figure 10a: Fluorescence histogram of FITC-Fg binding to liposomes and platelets



Liposomes or activated, fixed platelets (~ 1000/ μ l) were incubated with 500 nM FITC-Fg for 60 minutes at room temperature. Suspensions were then diluted in buffer and read for 20 seconds on the FACScan.

Figure 10b: Specificity of FITC-Fg binding to liposomes and platelets



Liposomes or activated, fixed platelets (~ 1000/ μ l) were incubated with 500 nM FITC-Fg \pm 1 μ M Ro for 60 minutes at room temperature. Suspensions were then diluted in buffer and read for 20 seconds on the FACScan to determine fluorescence. Results represent the mean of duplicate samples \pm standard deviation (SD).

Table IV: Fg_{max} and # of Fg/GPIIb-IIIa for four GPIIb-IIIa-liposome preparations

	1	2	3	4	Mean \pm SE
# of GPIIb-IIIa ²⁰	36 386	26 239	42 979	63 622	42 307 \pm 7895
Fg_{max} ²¹	11 526	5 460	21 836	29 338	17 040 \pm 5313
# of Fg per GPIIb-IIIa	0.317	0.208	0.508	0.461	0.374 \pm 0.07

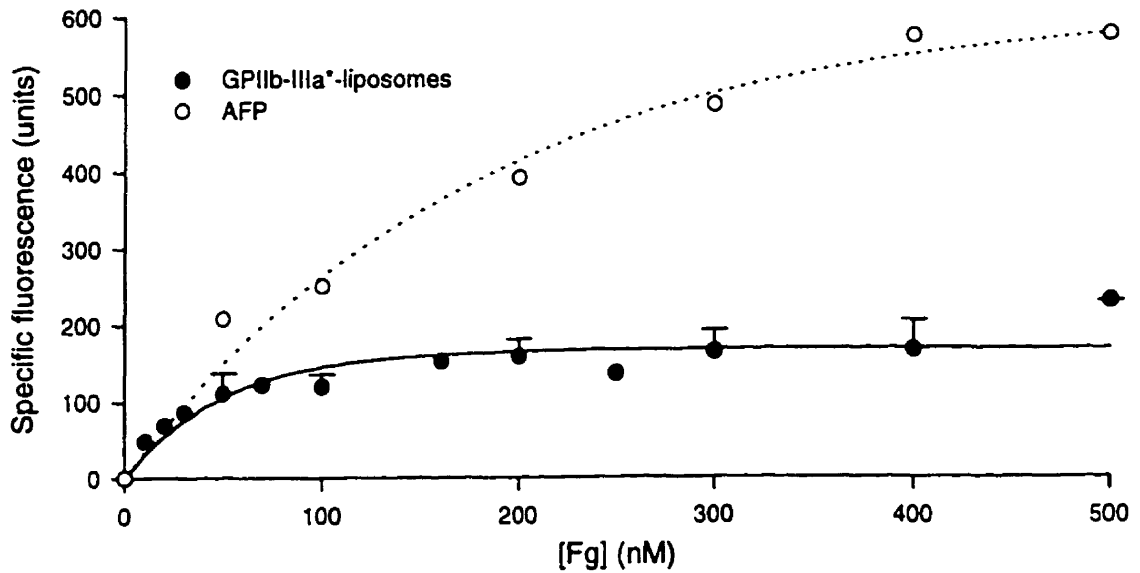
Table V: Fg_{max} and # of Fg/GPIIb-IIIa for four assays done on one AFP preparation

	1	2	3	4	Mean \pm SE
# of GPIIb-IIIa ²⁰	38 912	28 146	21 047	24 489	28 149 \pm 3869
Fg_{max} ²¹	25 987	22 568	19 571	21 898	22 506 \pm 1326
# of Fg per GPIIb-IIIa	0.668	0.802	0.930	0.894	0.824 \pm 0.06

²⁰ determined from the specific binding of 275 nM FITC-AP-2

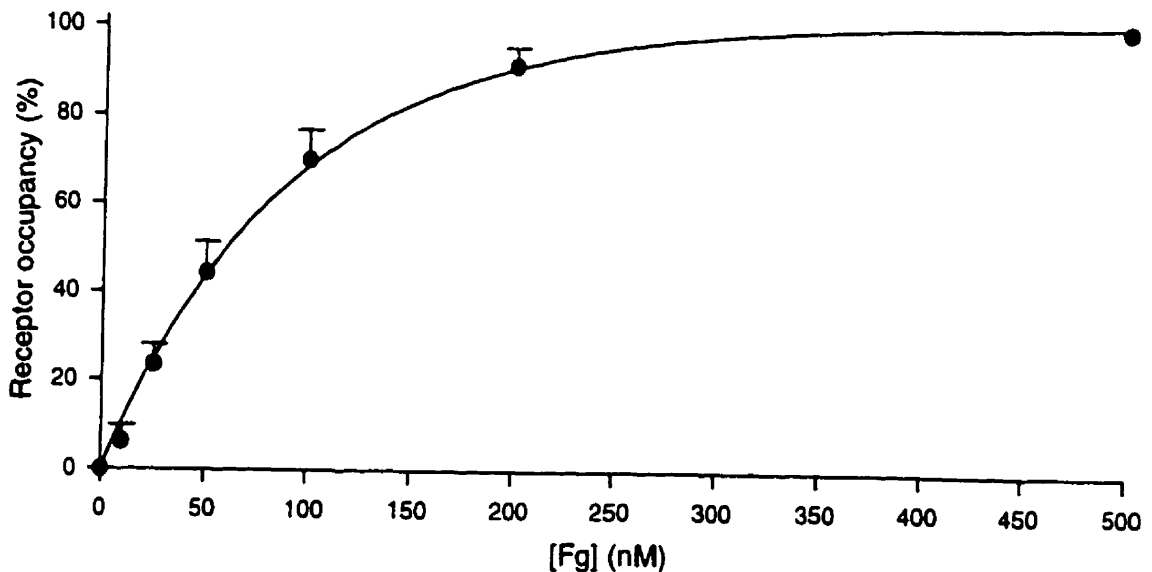
²¹ determined from the specific binding of 500 nM FITC-Fg

Figure 11a: Saturability of FITC-Fg binding to liposomes and platelets



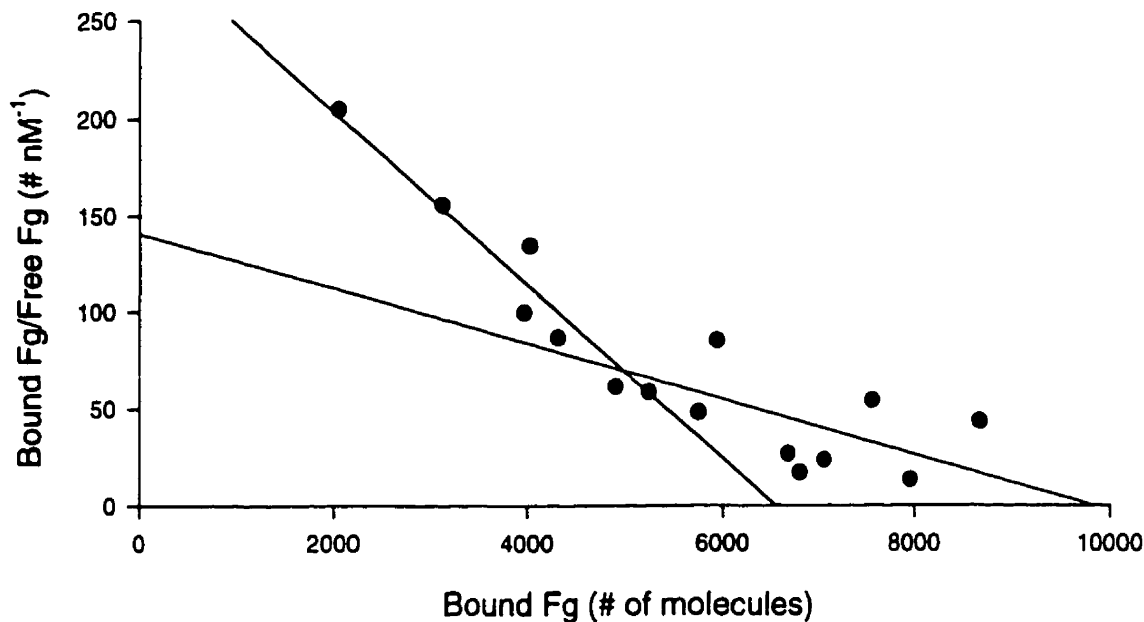
Liposomes or activated, fixed platelets ($\sim 1000/\mu\text{l}$) were incubated with 10-500 nM FITC-Fg \pm 1 mM GRGDSP for 60 minutes at room temperature. Suspensions were then diluted in buffer and read for 20 seconds on the FACScan to determine fluorescence. Each datapoint represents specific binding and is the mean of two separate experiments \pm SD.

Figure 11b: Concentration-dependence of GPIIb-IIIa*-liposome receptor occupancy by FITC-Fg



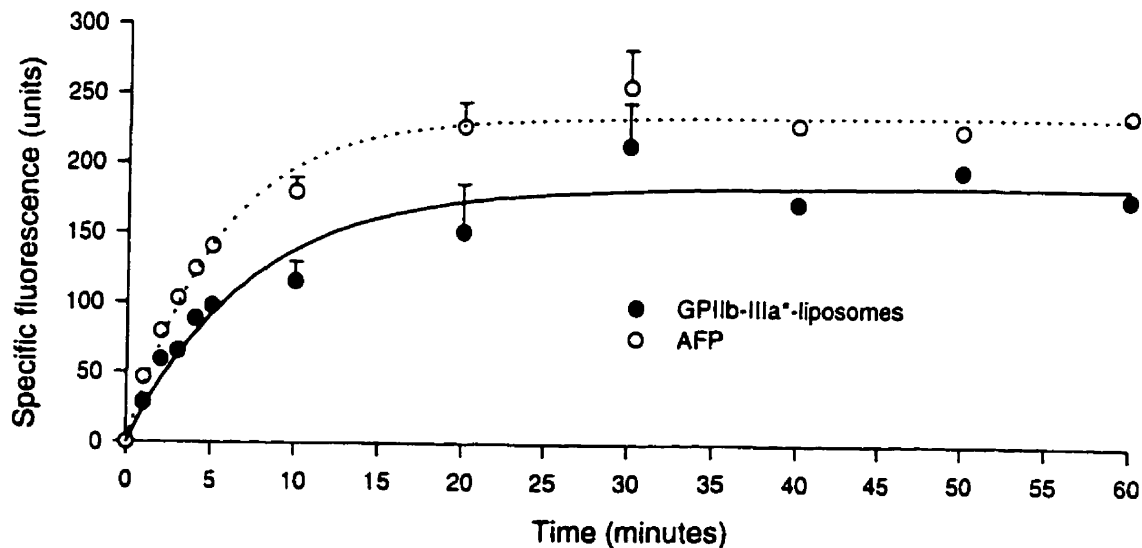
Receptor occupancy was determined by converting specific fluorescence values to # of Fg molecules bound (B), and then dividing by $F_{g_{max}}$. Results represent the mean of three separate experiments \pm SE.

Figure 11c: Scatchard plot of FITC-Fg binding to GPIIb-IIIa*-liposomes



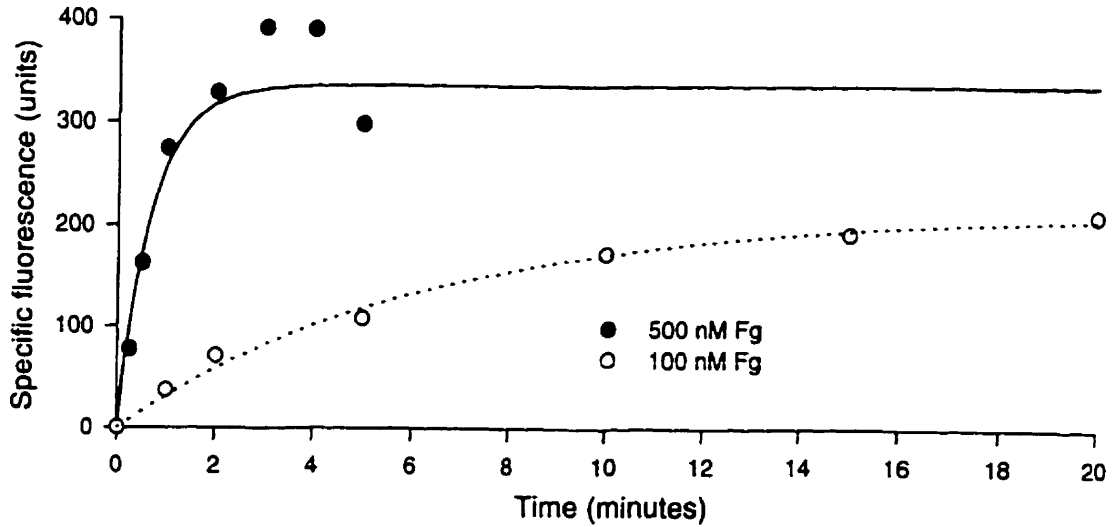
Datapoints were determined by converting FI values from Figure 11a to # of Fg molecules bound (B).

Figure 12a: Time-dependence of FITC-Fg binding to liposomes and platelets



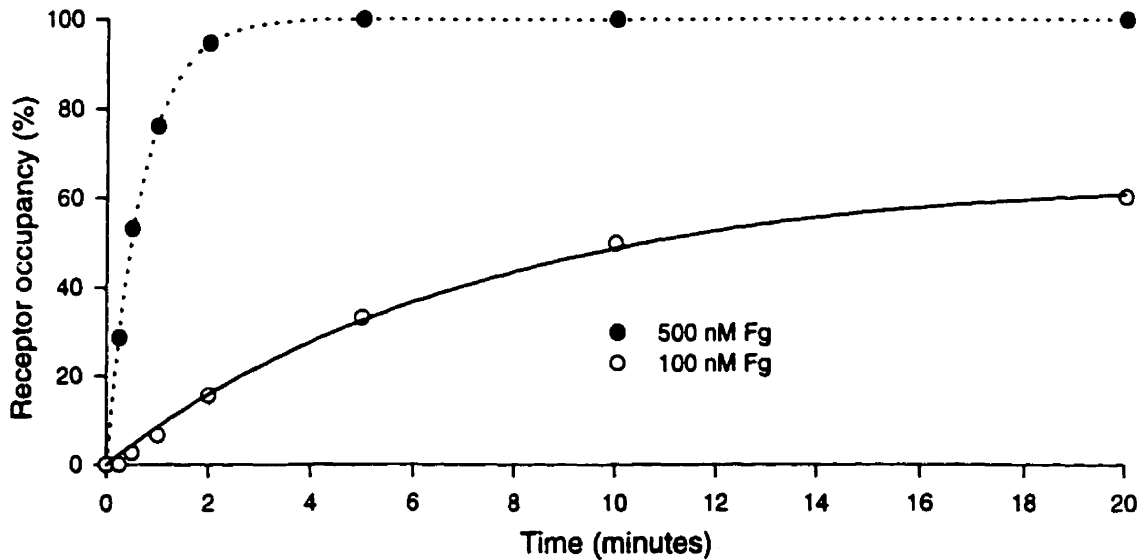
Liposomes or activated, fixed platelets (~ 1000/ μ l) were incubated with 100 nM FITC-Fg \pm 1 mM GRGDSP for 0-60 minutes at room temperature. Suspensions were read for 50 seconds on the FACScan to determine fluorescence. Each datapoint represents specific binding and is the mean of two separate experiments \pm SD.

Figure 12b: Time-dependence of FITC-Fg binding to GPIIb-IIIa*-liposomes for two different Fg concentrations



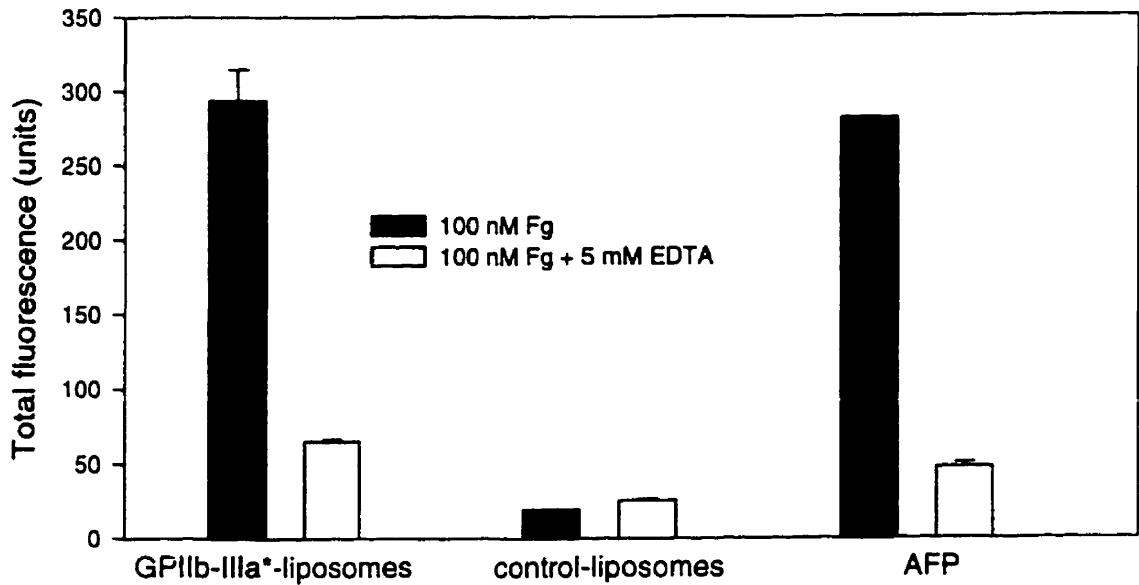
Liposomes (~ 1000/ μ l) were incubated with 100 or 500 nM FITC-Fg \pm 1 μ M Ro for 0-20 minutes at room temperature. Suspensions were read for 20 seconds on the FACScan to determine fluorescence. Each datapoint represents the specific binding determined from the mean values of total and non-specific fluorescence for duplicate samples.

Figure 12c: Time-dependence of GPIIb-IIIa*-liposome receptor occupancy by FITC-Fg



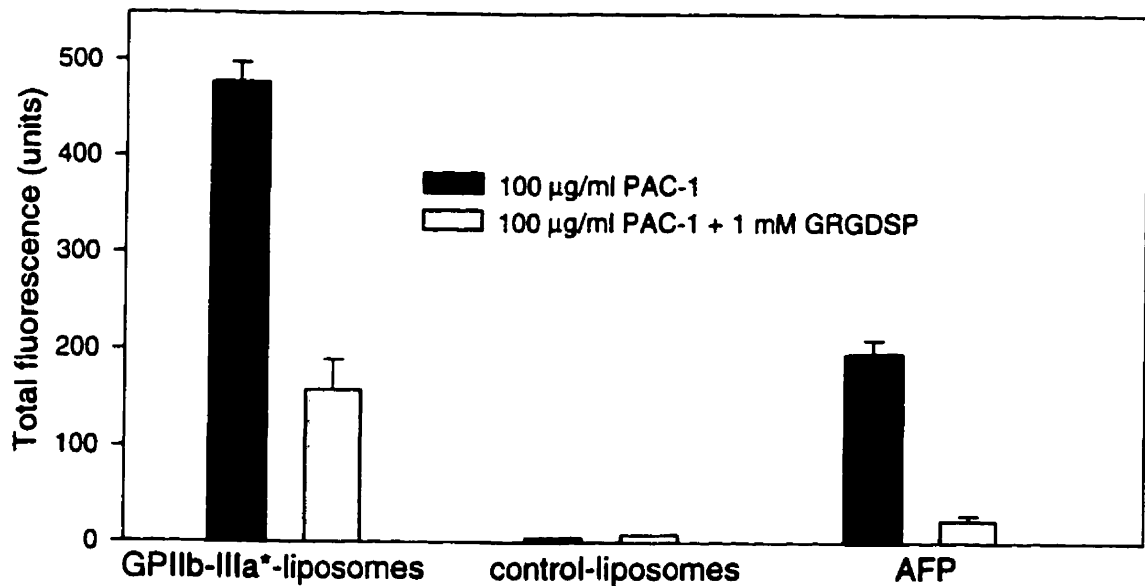
Receptor occupancy was determined by converting the specific fluorescence values of Figure 12b to # of Fg molecules bound (B), and then dividing by Fg_{max} .

Figure 13: Calcium-dependence of FITC-Fg binding to liposomes and platelets



Liposomes or activated, fixed platelets ($\sim 1000/\mu\text{l}$) were incubated with 100 nM FITC-Fg \pm 5 mM EDTA for 30 minutes at room temperature. Suspensions were read for 50 seconds on the FACScan to determine fluorescence. Results represent the mean of duplicate samples \pm SD.

Figure 14: Specificity of FITC-PAC-1 binding to liposomes and platelets



Liposomes or activated, fixed platelets ($\sim 1000/\mu\text{l}$) were incubated with 100 µg/ml FITC-PAC-1 \pm 1 mM GRGDSP for 30 minutes at room temperature. Suspensions were then diluted in buffer and read for 20 seconds on the FACScan to determine fluorescence. Results represent the mean of three separate experiments \pm SE.

Aggregation studies

After having established the Fg-binding properties of the GPIIb-IIIa*-liposomes, the vesicles were examined for their ability to undergo Fg-specific aggregation with stir. As illustrated by Figure 15a, there was a sharp drop in the proteoliposome count within the first minute of stirring the liposomes (with or without 500 nM Fg), while control-liposomes experienced minimal changes in cell number. Figure 15b indicates that Fg interactions with liposome GPIIb-IIIa were not necessary for this 'aggregation', as a large decrease in the cell count was observed even when the GPIIb-IIIa ligand-binding site was blocked by 1 μ M Ro. Although the liposome suspension shown in Figure 15b was stirred at a lower speed than the one in Figure 15a (250 vs. 1000 rpm), the longer time course should have allowed any Fg-dependent effects to manifest themselves, so the speed differential is not particularly relevant.

In contrast to these results, AFP at concentrations as low as 10 000/ μ l were seen to undergo Fg-specific aggregation with stir, as demonstrated by Figure 15c. In the absence of Fg there was only a slight change in cell number, but in the presence of 500 nM Fg the platelet count had decreased nearly 60% by 2 minutes (and ~ 80% by 5 minutes), a drop which was almost completely inhibited by preincubation with Ro. Higher platelet concentrations increased the rate but not the extent of aggregation: for AFP at 40 000/ μ l, PA was slightly above 80% by 2 minutes and remained virtually constant with time. Aggregation of platelet-rich plasma (PRP) stirred with 2 μ M ADP at 1000 rpm has also been shown to reach a maximum PA of more than 80%; this level of aggregation can be produced within 10 seconds by high concentrations of PRP (~ 500 000 cells/ μ l) [Frojmovic et al. 1983].

In order to better characterize the stir-induced decreases in proteoliposome or platelet number, unfixed samples from a few timepoints were examined using a light microscope. Figure 16a shows the aggregate distribution of GPIIb-IIIa*-liposomes stirred for 60 minutes in the presence or absence of Fg (\pm Ro). As can be seen, addition of 500 nM Fg leads to a slight reduction in the number of singlets accompanied by a small rise in the number of large aggregates (those containing more than five cells).

However, since the same trend was also observed in the presence of 1 μ M Ro, liposome aggregation does not appear to be due to an interaction between Fg and GPIIb-IIIa. On the other hand, AFP stirred with Fg initially form doublets but are soon recruited into sizeable aggregates, leading to a significant drop in singlet number; this is illustrated in Figure 16b. Preincubation with Ro almost completely blocked the formation of macroaggregates and partially suppressed the decrease in singlet count. As would be expected from the data presented in Figures 15a and 15b, the distribution of control-liposomes was virtually identical with or without Fg.

We postulated that the inability of GPIIbIIIa*-liposomes to undergo Fg-specific aggregation may have been due to the rapid saturation of the receptor at this Fg concentration (500 nM), illustrated in Figure 12b. As a result, liposomes were stirred in the presence of 100 nM Fg, which binds much more slowly to GPIIb-IIIa. However, despite the lower ligand concentration no Fg-GPIIb-IIIa-dependent aggregation was observed; as seen in Figure 17, there was very little decrease in liposome number with or without 1 μ M Ro. Furthermore, there does not appear to be a correlation between the changes in cell counts for the two Fg concentrations and the receptor occupancy (see Figure 12c). For the experiment of Figure 17 the cuvettes had been pre-siliconized, significantly reducing the non-specific loss of liposomes, as can be seen by comparison of the 500 nM curve with that of Figure 15a.

The loss of proteoliposomes with stir thus does not seem to be due to aggregation mediated by the Fg-GPIIb-IIIa interaction, but is likely caused by a combination of two different phenomena, which are only minimally seen with control-liposomes. The first of these is non-specific cell sticking to the sides of the cuvette in the absence of Fg, accounting for more than half of the drop in the liposome count; as shown in Figure 15a, this is further enhanced by Fg. The use of pre-siliconized cuvettes helped to minimize cell sticking, as seen in Figure 17. Non-specific aggregation in the presence of Fg (\pm Ro) - as suggested by Figure 16a - is another potential explanation for the stir-induced loss of proteoliposomes. This is a distinct possibility since some Fg-dependent aggregation was also observed for 'resting' GPIIb-IIIa⁰-liposomes with stir.

This group of liposomes exhibited high levels of non-specific FITC-Fg binding, as did OG-treated-liposomes. Exposure to detergent therefore appears to induce packing defects in the lipid bilayer, which enhance lipid-protein interactions [Blume & Cevc 1993]. Furthermore, phosphatidylcholine dispersions have been shown to undergo a conformational change and become more polar in the presence of Fg, allowing the protein to be inserted into the bilayer [Lis et al. 1976]. Upon association with the lipid membrane Fg could crosslink liposomes in a manner analogous to that seen for platelets; in addition, Fg may promote liposome attachment to the cuvette wall.

As described above, aggregometry is a useful technique for the generation of rapid and extensive platelet aggregation. However, flow patterns in the cuvette are complex and ill-defined, unlike the well-characterized hydrodynamic conditions associated with capillary tubes, the cone-and-plate viscometer, or a couette apparatus [Yung and Frojmovic 1982; Xia and Frojmovic 1994]. Low shear rates of $10\text{-}20\text{ s}^{-1}$ such as are found in the vortices of thrombotic vessels have been shown to promote platelet aggregation in vitro; for PRP activated with a high [ADP], microaggregation was maximal at G-values of about 30 s^{-1} , while formation of larger aggregates increased up to a G of 150 s^{-1} . We thus attempted to determine whether aggregation of proteoliposomes specifically mediated by the Fg-GPIIb-IIIa interaction could occur under laminar, low flow conditions generated by a micro-couette.

Figure 18 describes how counts of control- and GPIIb-IIIa*-liposomes changed when exposed to a shear rate of 50 s^{-1} . In the presence of 500 nM Fg the number of both types of vesicles fell over time, but this effect was much more pronounced for the proteoliposomes, which had dropped more than 30% by 10 minutes. As for the stir experiments, a similar effect was also seen after preincubation of the GPIIb-IIIa*-liposomes with $1\text{ }\mu\text{M}$ Ro or upon shearing GPIIb-IIIa⁰-liposomes together with Fg, and thus does not appear to be due to an interaction between Fg and activated GPIIb-IIIa. Microscopic examination of particles provided evidence of stir-type distributions for all experimental groups with regards to the number and size of aggregates. Unlike with stir, however, there was no loss of proteoliposomes sheared in the absence of Fg.

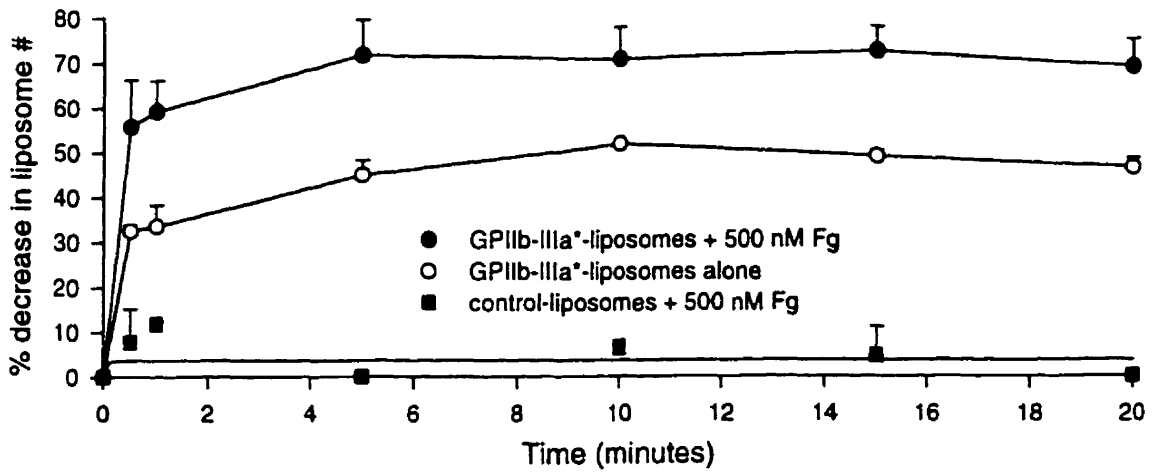
The above results contrast somewhat with those of Rybak, who likewise investigated the aggregability of GPIIb-IIIa-liposomes [Rybak 1986]. These vesicles were shown to undergo aggregation in the presence of 10 mM calcium after centrifugation with 1 mg/ml (~ 3 μ M) Fg for 10 minutes at 100 g; at such a high [Fg] the receptors would presumably have been completely saturated. Aggregation was enhanced by the addition of 5 μ g/ml Fn and 500 μ g/ml vWF, and was maximal when the liposomes were exposed to all three proteins as well as other liposomes containing TSP-1. However, quantitative determination of aggregate size could not be performed due to instability of the aggregates. Rybak also found that the vesicles bound to ADP-activated platelets in the presence of Fg and calcium; similarly, Baldassare et al. observed the Ca^{2+} -dependent binding of GPIIb-IIIa-liposomes to thrombin-stimulated platelets [Baldassare et al. 1985].

The binding of Fg to GPIIb-IIIa associated with other non-platelet environments has been reported to promote homotypic aggregation. Latex beads coated with platelet membranes were found to agglutinate when stirred with 50 μ g/ml (~ 150 nM) Fg and 4 mM Ca^{2+} at 800 rpm for 10 minutes; this was significantly inhibited by GRGDSP or the H12 peptide at a concentration of 2 mM, as well as by a 2 mM solution of the calcium chelator EGTA or a [Mg^{2+}] of 3 mM [Gawaz et al. 1996]. Coupling of GPIIb-IIIa to latex beads in our laboratory resulted in a PA of 42% upon stirring with 700 nM Fg at 1000 rpm for 2 minutes; this was almost completely blocked by preincubation with 1 mM GRGDSP [E Brown & M Frojmovic, unpublished data]. These beads also exhibited some specific aggregation with shear (350 s^{-1}) at the same [Fg] as for stir. Finally, Chinese hamster ovary (CHO) cells transfected with recombinant GPIIb-IIIa - known as A5 cells - were shown to form aggregates of 50 cells or more after gyrorotation with 500 nM Fg at 75 rpm for 15 minutes [Frojmovic et al. 1991a]. Under these conditions PA was ~ 80%, while in the presence of 1 mM GRGDSP it dropped to ~ 35%, and aggregation was completely inhibited by 5 mM EDTA. However, with stir these A5 cells exhibited no aggregation whatsoever, and only formed aggregates with shear at very low G-values [Frojmovic et al., unpublished observations].

It is thus clear that the Fg-GPIIb-IIIa interaction can specifically mediate particle aggregation. Although there may be several reasons why this was not seen with the GPIIb-IIIa*-liposomes, anchoring of the receptor is likely an important factor in promoting aggregate stability. As shown by the above studies, the Fg-dependent aggregates formed by the GPIIb-IIIa-liposomes of Rybak or the A5 cells of Frojmovic et al. were quite fragile. In contrast, the latex beads of Brown & Frojmovic or of Gawaz et al., having a much more rigid membrane than liposomes or CHO cells, were found to aggregate with both stir and shear. With regards to the GPIIb-IIIa*-liposomes, the bivalent binding of many Fg molecules to two receptors on the same vesicle, as suggested above, would have significantly diminished the proteoliposome aggregability. This is particularly relevant considering the high GPIIb-IIIa surface density of the liposomes used for the stir and shear experiments (preparations 3 and 4 from Table IV).

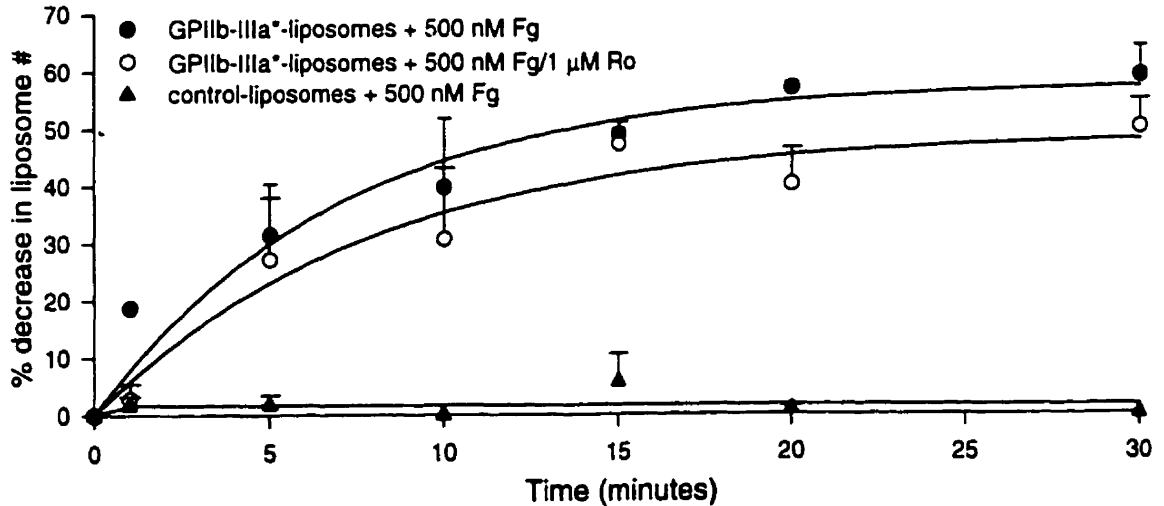
We proposed that the lack of specific GPIIb-IIIa*-liposome aggregation may have been linked to an inability to bind immobilized Fg. This was tested by using latex beads labelled with Fg (see below).

Figure 15a: Change in liposome # with stir at 1000 rpm in the presence or absence of 500 nM Fg



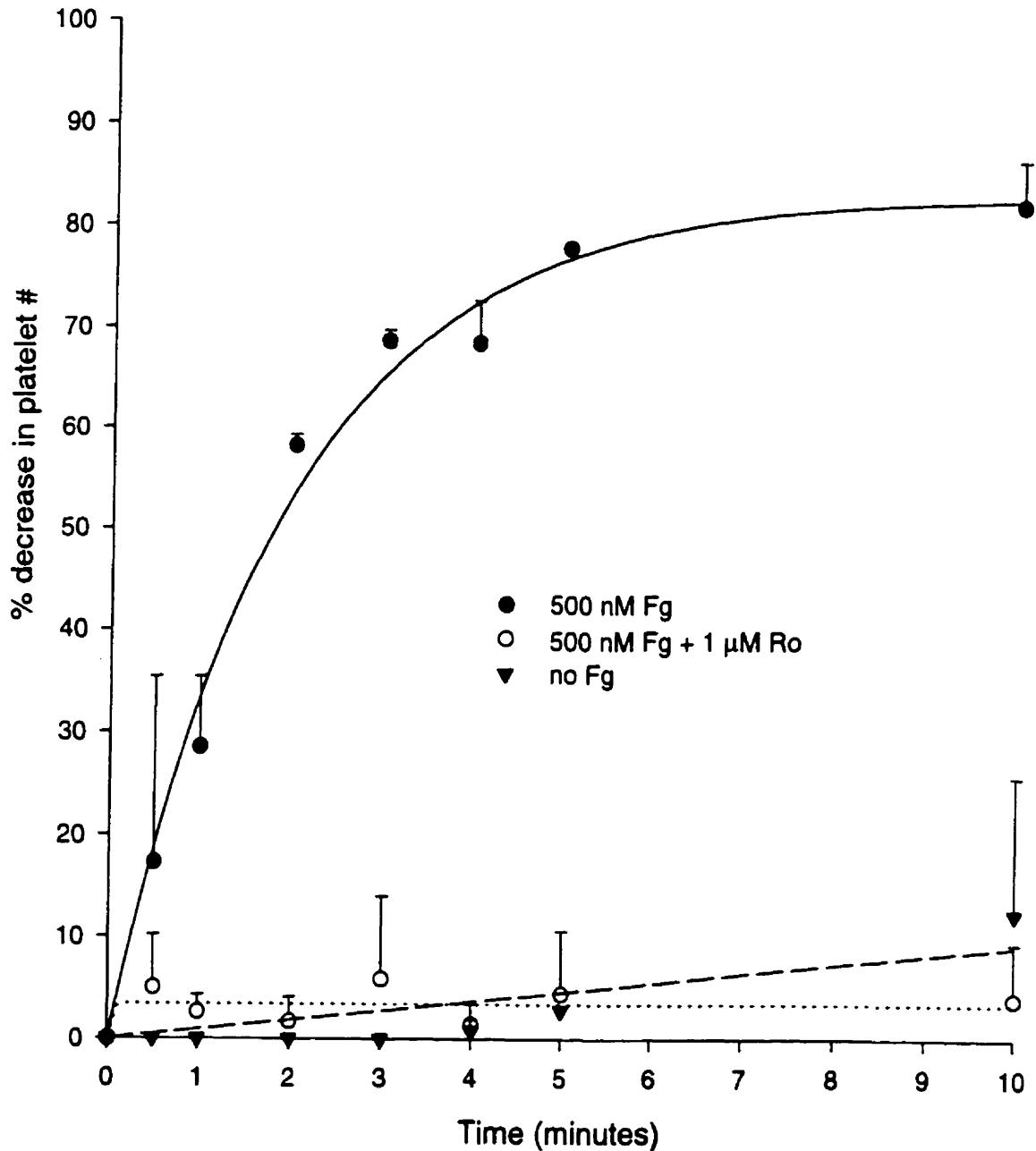
Liposomes in a glass cuvette (~ 15 000-20 000/ μ l) were stirred for 0-20 minutes at 1000 rpm in the presence or absence of 500 nM Fg. At certain timepoints subsamples were withdrawn and fixed in 4 volumes of 0.8% glutaraldehyde. Fixed samples were then diluted in buffer and read for 20 seconds on the FACScan to determine the cell count. Results are expressed as a percentage of the original cell count as described in the Methods section and represent the mean of duplicate samples \pm SD.

Figure 15b: Change in liposome # with stir at 250 rpm in the presence of 500 nM Fg \pm Ro



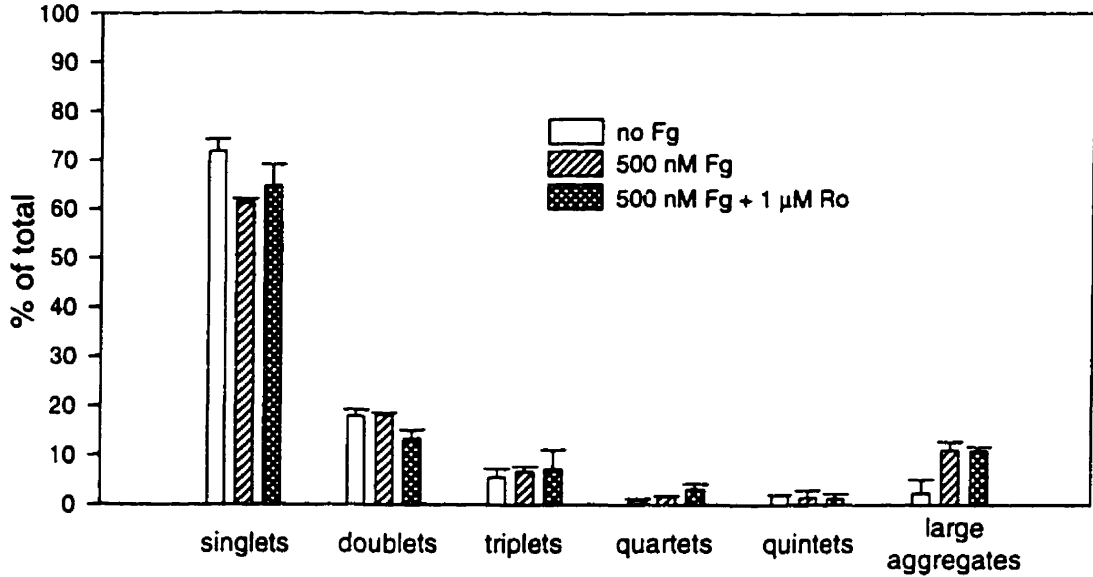
Liposomes in a glass cuvette (~ 15 000-20 000/ μ l) were stirred at 250 rpm for 0-30 minutes in the presence of 500 nM Fg \pm 1 μ M Ro. At certain timepoints subsamples were withdrawn and fixed in 4 volumes of 0.8% glutaraldehyde. Fixed samples were then diluted in buffer and read for 20 seconds on the FACScan to determine the cell count. Results are expressed as a percentage of the original cell count as described in the Methods section and represent the mean of three separate experiments \pm SE.

Figure 15c: Change in platelet # for AFP with stir at 1000 rpm



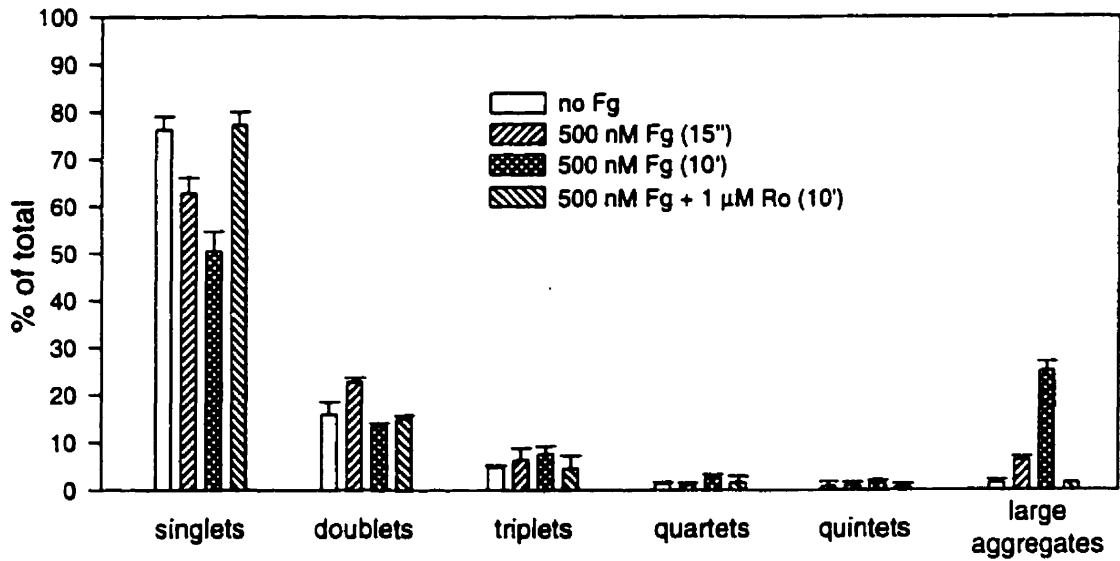
Activated, fixed platelets in a glass cuvette (~ 10 000/ μ l) were stirred at 1000 rpm for 0-10 minutes in the presence or absence of 500 nM Fg \pm 1 μ M Ro. At certain timepoints subsamples were withdrawn and fixed in 4 volumes of 0.8% glutaraldehyde. Fixed samples were then diluted in buffer and read for 20 seconds on the FACScan to determine the cell count. Results are expressed as a percentage of the original cell count as described in the Methods section and represent the mean of duplicate samples \pm SD.

Figure 16a: Singlet-aggregate distribution of GPIIb-IIIa*-liposomes with stir at 250 rpm



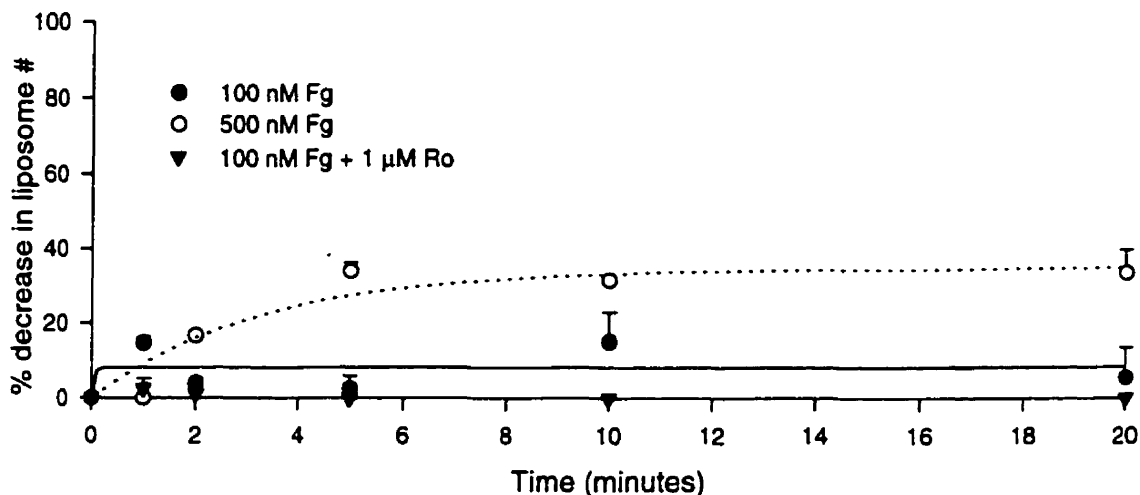
Liposomes in a glass cuvette (~ 15 000-20 000/μl) were stirred at 250 rpm for 60 minutes in the presence or absence of 500 nM Fg ± 1 μM Ro. Suspensions were then examined using a light microscope. Results represent the percentage of cells found as singlets or as multiplets of various sizes and are the mean of two separate measurements ± SD.

Figure 16b: Singlet-aggregate distribution of platelets with stir at 1000 rpm



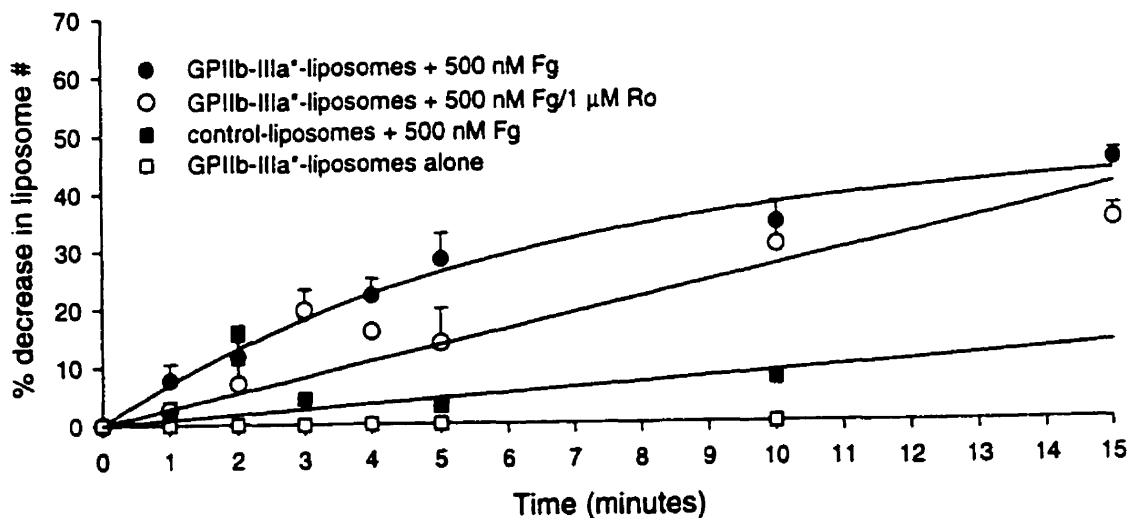
Activated, fixed platelets in a glass cuvette (~ 40 000/μl) were stirred at 1000 rpm for 0-10 minutes in the presence or absence of 500 nM Fg ± 1 μM Ro. At certain timepoints subsamples were withdrawn and examined using a light microscope. Results represent the percentage of cells found as singlets or as multiplets of various sizes and are the mean of two separate measurements ± SD.

Figure 17: Change in liposome # with stir at 1000 rpm in the presence of 100 nM Fg \pm Ro



Liposomes in a pre-siliconized glass cuvette ($\sim 15\ 000$ - $20\ 000/\mu\text{l}$) were stirred for 0-20 minutes at 1000 rpm in the presence of 100 or 500 nM Fg \pm 1 μM Ro. At certain timepoints subsamples were withdrawn and fixed in 4 volumes of 0.8% glutaraldehyde. Fixed samples were then diluted in buffer and read for 20 seconds on the FACScan to determine the cell count. Results are expressed as a percentage of the original cell count as described in the Methods section and represent the mean of duplicate samples \pm SD.

Figure 18: Change in liposome # with shear at 50 s⁻¹ in the presence or absence of 500 nM Fg \pm Ro

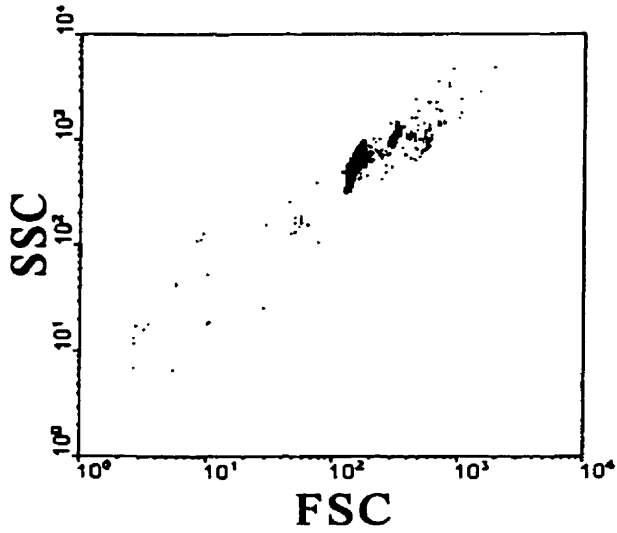


Liposomes ($\sim 10\ 000$ - $15\ 000/\mu\text{l}$) were sheared for 0-20 minutes at 50 s⁻¹ in the presence of 500 nM Fg \pm 1 μM Ro. At certain timepoints the couette was stopped; subsamples were withdrawn and fixed in 4 volumes of 0.8% glutaraldehyde. Fixed samples were then diluted in buffer and read for 20 seconds on the FACScan to determine the cell count. Results are expressed as a percentage of the original cell count as described in the Methods section and represent the mean of four separate experiments \pm SE.

Characterization of Fg- and Alb-beads

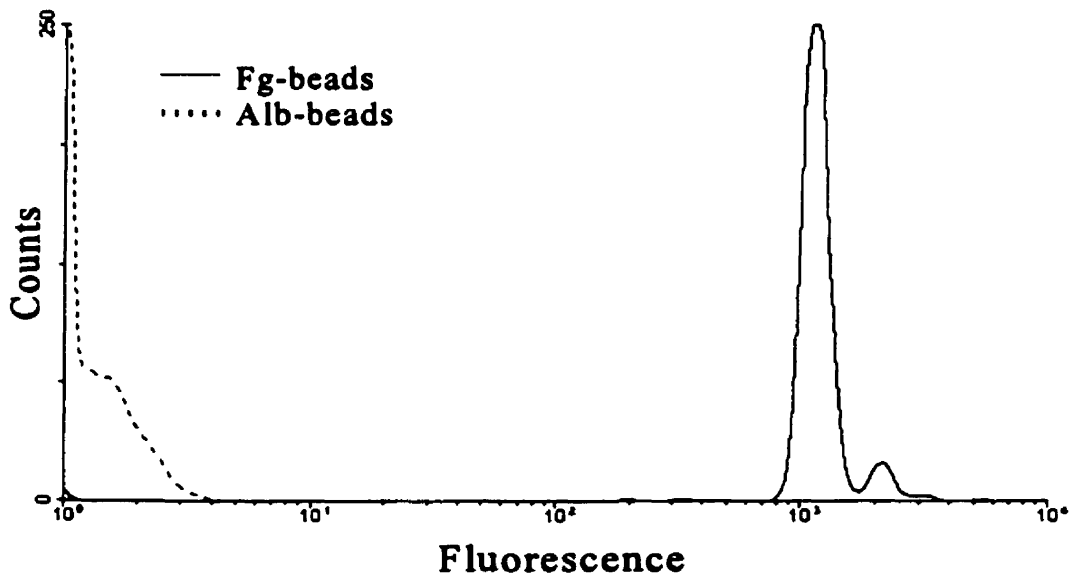
The FACScan scatter profile of Fg-coated latex beads (**Fg-beads**) is shown in Figure 19a, with an identical dot-plot seen for control albumin-coated beads (**Alb-beads**). Since the beads have diameters of about 4.3 μm , FSC and SSC values are significantly higher than for most liposomes or platelets, as can be seen by comparison to Figures 1a and 1b. Almost 90% of the Fg-bead population is present as unaggregated singlets. Figure 19b is a histogram depicting the fluorescence of Fg- and Alb-beads, with FI values of 1142 and 1.4 for these two groups. By using Eq. 1 to calculate the MESF and then dividing by the F:P ratio, this corresponds to an average of 65 000 fibrinogen molecules per Fg-bead.

Figure 19a: FACScan Fg-bead scatter profile



Fg-beads were diluted in buffer and read for 20 seconds on the FACScan.

Figure 19b: Fluorescence histograms of Fg- and Alb-beads



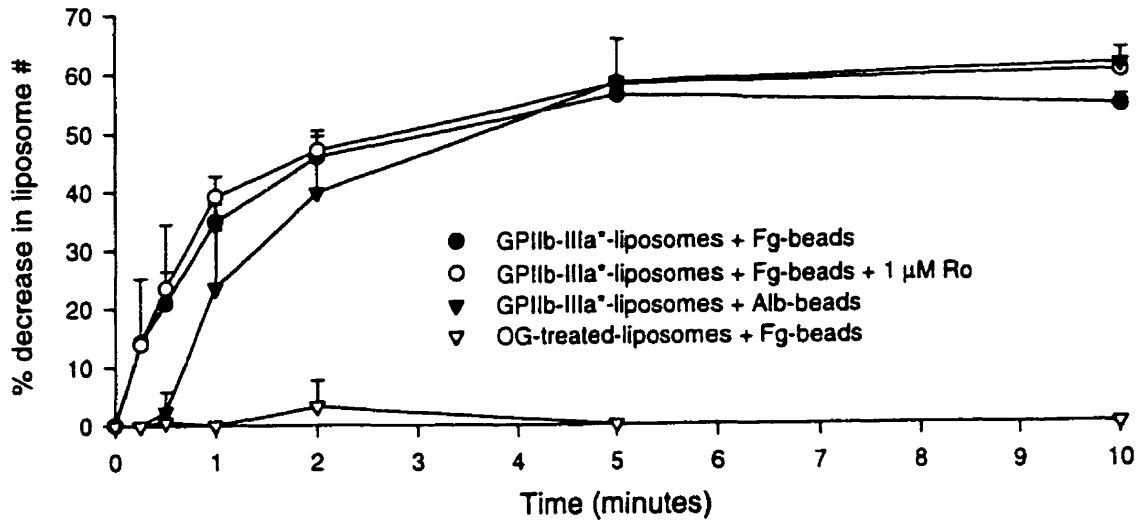
Beads were diluted in buffer and read for 20 seconds on the FACScan to determine fluorescence.

Co-aggregation of beads with liposomes or platelets

Although the above stir and shear experiments demonstrated that the proteoliposomes do not undergo Fg-GPIIb-IIIa specific aggregation, it was of interest to determine whether the activated receptor in liposomes could recognize and mediate binding to immobilized Fg with stir. This was tested by using Fg-coated latex beads known to bind soluble GPIIb-IIIa and to interact with activated platelets via GPIIb-IIIa [Q Liu & M Frojmovic, unpublished observations]. The distinct scatter profiles of liposomes and beads enabled separate tracking of both groups by FACScan analysis. Changes in the number of GPIIb-IIIa*- and OG-treated-liposomes with stir, in the presence of Fg- or Alb-beads, are shown in Figure 20a. The disappearance profile of the proteoliposomes was virtually the same whether they were stirred with Fg-beads \pm 1 μ M Ro, or with Alb-beads, reaching a maximum of 55-60% by 5 minutes; there was thus no specific co-aggregation mediated by the Fg-GPIIb-IIIa interaction. OG-treated liposomes, on the other hand, experienced no change in their number when stirred with Fg-beads. As seen in Figure 20b, Fg-beads exhibited substantial non-specific aggregation in the presence of the proteoliposomes \pm 1 μ M Ro (PA above 80%) or the OG-treated group (PA above 60%), while the Alb-beads showed no aggregation until 2 minutes and only reached a PA of 20% by 5 minutes.

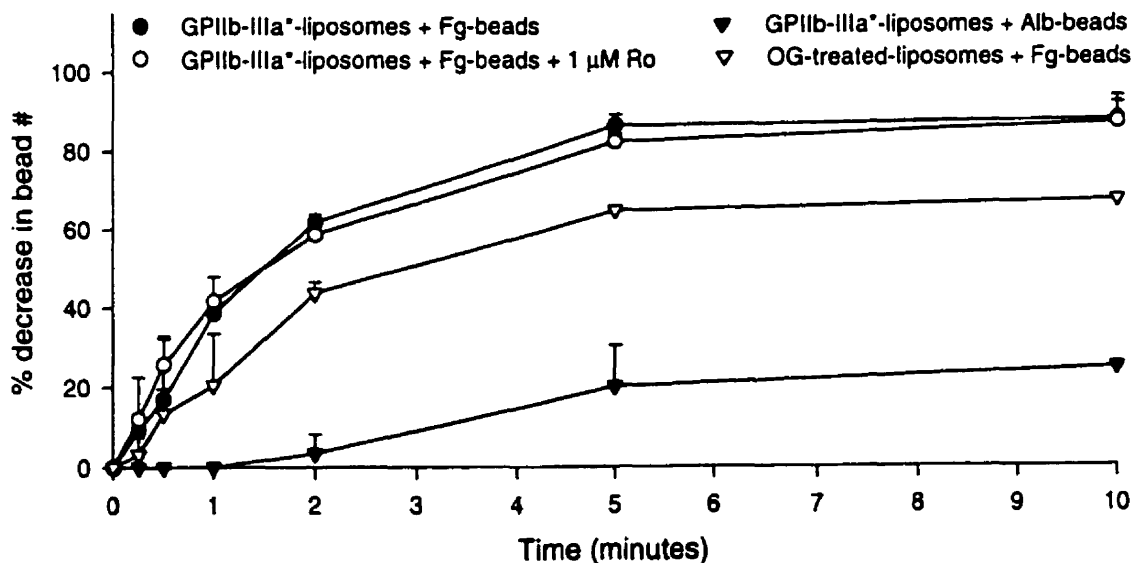
Like the liposomes, activated, fixed platelets could be distinguished from the beads on the basis of their scatter profile. As shown in Figure 21a, the platelets bound very well to Fg-beads, reaching a PA of 60% by 5 minutes. This co-aggregation was largely blocked by preincubation with 1 μ M Ro and was only minimally seen upon stirring with Alb-beads, illustrating the specificity of the Fg-GPIIb-IIIa interaction. When looking specifically at the beads similar results were observed, as depicted in Figure 21b: the very high aggregability of Fg-beads (above 80%) was decreased in the presence of Ro, while as above the Alb-beads demonstrated only limited aggregation.

Figure 20a: Change in liposome # with stir at 1000 rpm in the presence of Fg- or Alb-beads



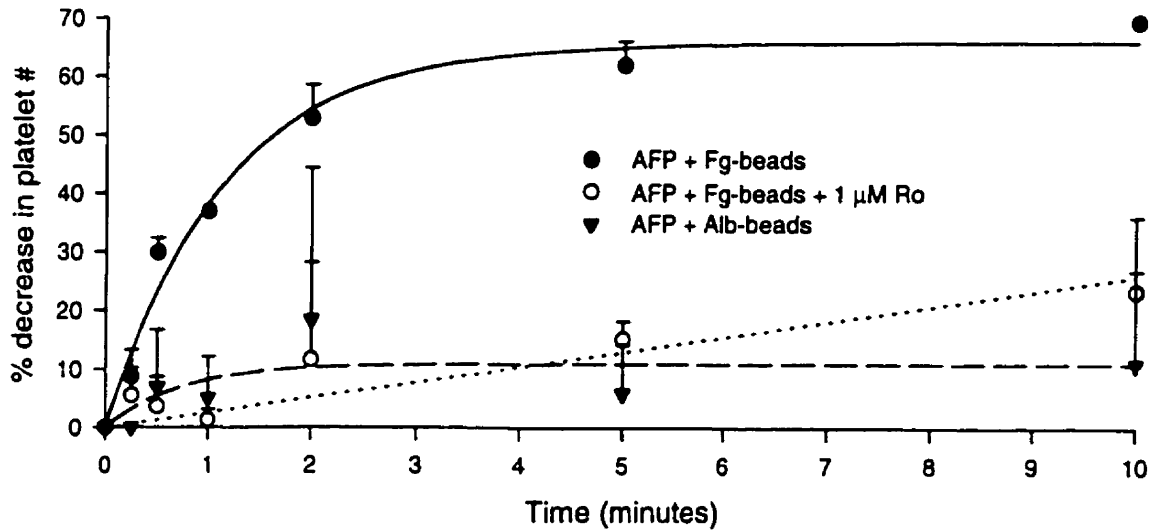
Liposomes (~ 20 000/μl) were stirred for 0-10 minutes at 1000 rpm in the presence of Fg- or Alb-beads (~ 10 000/μl) ± 1 μM Ro. At certain timepoints subsamples were withdrawn and fixed in 4 volumes of 0.8% glutaraldehyde. Fixed samples were then diluted in buffer and read for 20 seconds on the FACScan, followed by specific gating on liposomes. Results are expressed as a percentage of the original cell count as described in the Methods section and represent the mean of duplicate samples ± SD.

Figure 20b: Change in Fg- or Alb-bead # after 1000 rpm stir in the presence of liposomes



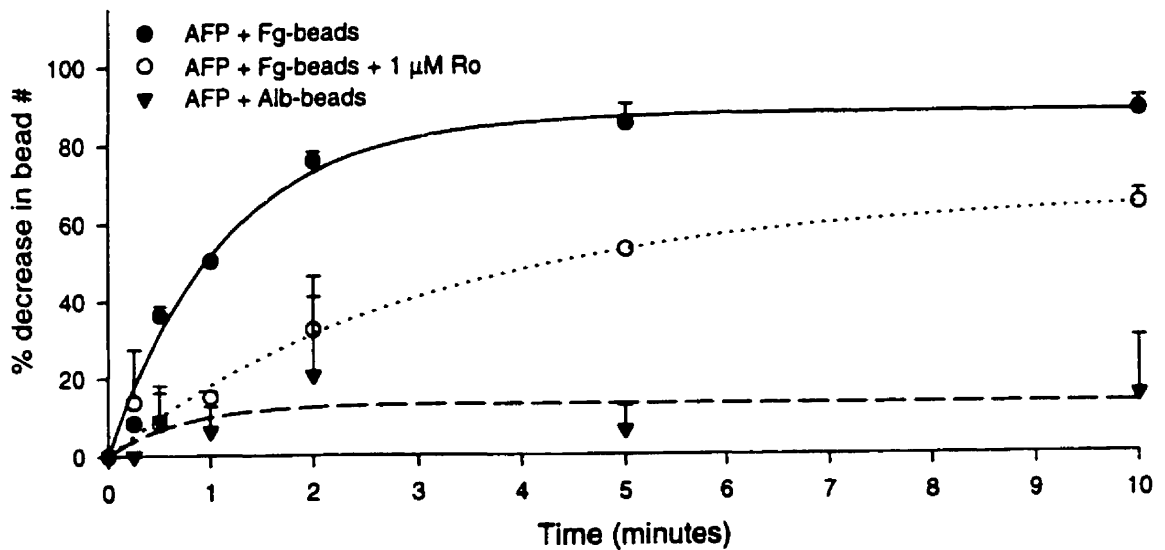
As described for Figure 20a, but with specific gating on beads instead of liposomes. Results are expressed as a percentage of the original bead count as described in the Methods section and represent the mean of duplicate samples ± SD.

Figure 21a: Change in platelet # after 1000 rpm stir in the presence of Fg- or Alb-beads



Activated, fixed platelets (~ 20 000/ μ l) were stirred for 0-10 minutes at 1000 rpm in the presence of Fg- or Alb-beads (~ 10 000/ μ l) \pm 1 μ M Ro. At certain timepoints subsamples were withdrawn and fixed in 4 volumes of 0.8% glutaraldehyde. Fixed samples were then diluted in buffer and read for 20 seconds on the FACScan, followed by specific gating on AFP. Results are expressed as a percentage of the original cell count as described in the Methods section and represent the mean of duplicate samples \pm SD.

Figure 21b: Change in Fg- or Alb-bead # after 1000 rpm stir in the presence of platelets



As described for Figure 21a, but with specific gating on beads instead of platelets. Results are expressed as a percentage of the original bead count as described in the Methods section and represent the mean of duplicate samples \pm SD.

Binding of mAb's to GPIIb-IIIa-bound Fg

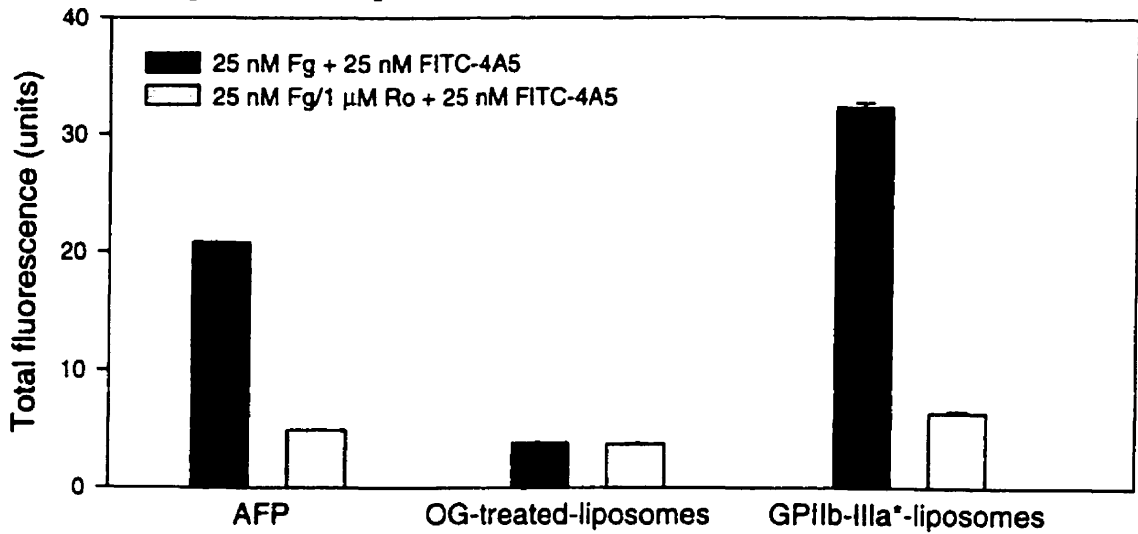
We hypothesized that the above lack of specific Fg-mediated aggregation of GPIIb-IIIa*-liposomes or co-aggregation with Fg-beads, despite evidence of specific binding of FITC-Fg to the receptor, was due to abnormal Fg binding. For example, the Fg bound to its receptor on liposomes may have been conformationally altered, or as described above, bivalently attached to two GPIIb-IIIa receptors such that the γ chain C-terminus required for normal crossbridging was inaccessible. To test these possibilities, the binding of two fluorescently labelled antibodies to Fg immobilized on GPIIb-IIIa-liposomes was investigated: **4A5**, which interacts with the Fg γ chain C-terminus (residues 400-411), and **anti-Fg-RIBS-I**, which associates with an epitope on Fg (γ residues 373-385) expressed upon binding to GPIIb-IIIa [Shiba et al. 1991; Zamarron et al. 1991].

Ligand concentrations of 25 nM - representing a receptor occupancy of approximately 24% as depicted in Figure 11b - were used in these assays to minimize platelet (and potential liposome) crosslinking by Fg before addition of antibody. The mAb concentrations used - 25 nM for 4A5 and 10 nM for anti-Fg-RIBS-I - had previously been shown in our laboratory to exhibit maximal binding to AFP-bound Fg at a concentration of 25 nM [Q Liu, unpublished data]. Figure 22a illustrates the equilibrium binding of FITC-4A5 to Fg immobilized on liposomes or platelets. As expected, there was good specific binding - inhibited by 1 μ M Ro - of the mAb to both GPIIb-IIIa*-liposomes and to AFP, indicating that the immobilized Fg still had free γ chain C-termini available for crosslinking to GPIIb-IIIa complexes on nearby cells. Fg attached to liposomes appeared to have a similar conformation as on platelets, with specific equilibrium binding of FITC-anti-Fg-RIBS-I observed for both cell types; this is shown in Figure 22b. No specific Fl was seen for OG-treated-liposomes in the presence of either antibody.

The equilibrium binding of these mAb's thus suggests that the Fg γ -terminus was sterically accessible on both liposomes and platelets. However, partial steric hindrance of this site on liposomes remained a possibility, and was evaluated by

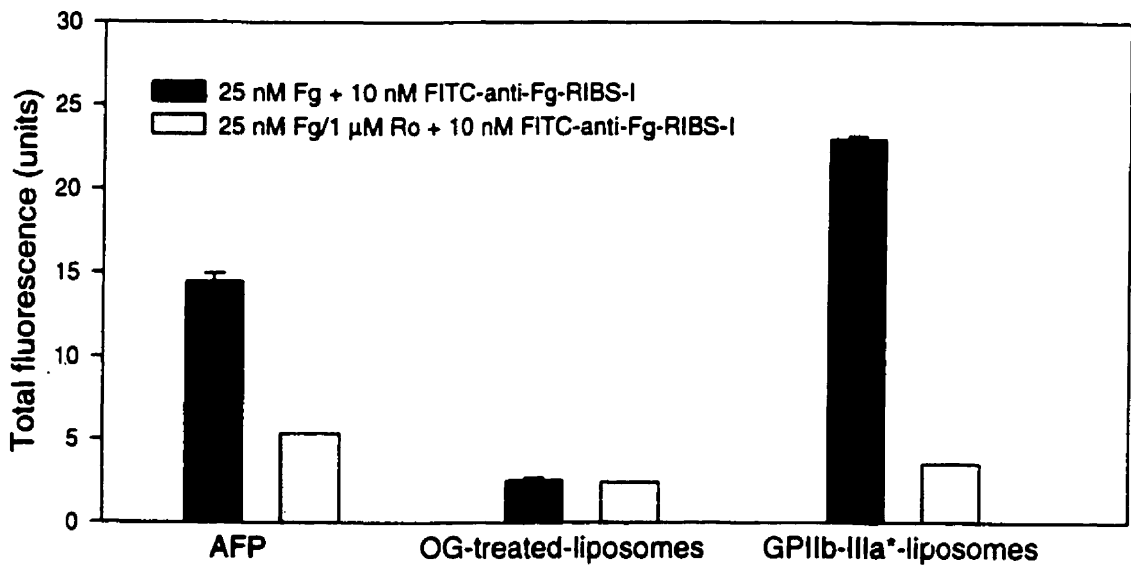
determining the binding kinetics of 4A5 to immobilized Fg. Such an approach has previously shown that PAC-1 binding to platelet GPIIb-IIIa is normal at equilibrium for varying pre-activation times (τ) with ADP, but that the V_{\max} decreases with increasing τ [Frojmovic et al. 1991b]. The time-dependence of 4A5 binding to immobilized Fg is depicted in Figure 23; Fg and mAb concentrations for this assay were as above. GPIIb-IIIa*-liposomes and AFP both had a $t_{1/2}$ of approximately 10 seconds and reached peak FI values by 2 minutes, while non-specific binding to OG-treated-liposomes was maximal after 15 seconds. As the V_{\max} and FI_{\max} of the proteoliposomes were both slightly less than twice those of the platelets (50.1 min^{-1} versus 27.1 min^{-1} and 18.5 units versus 9.4 units, respectively), the two groups had almost identical k_2 values (1.08 x $10^8 \text{ M}^{-1} \text{ min}^{-1}$ for the liposomes and 1.15 x $10^8 \text{ M}^{-1} \text{ min}^{-1}$ for the platelets). Steric hindrance of the Fg γ -terminus following ligand binding to GPIIb-IIIa*-liposomes thus appears unlikely.

Figure 22a: Specificity of FITC-4A5 binding to Fg immobilized on liposomes and platelets



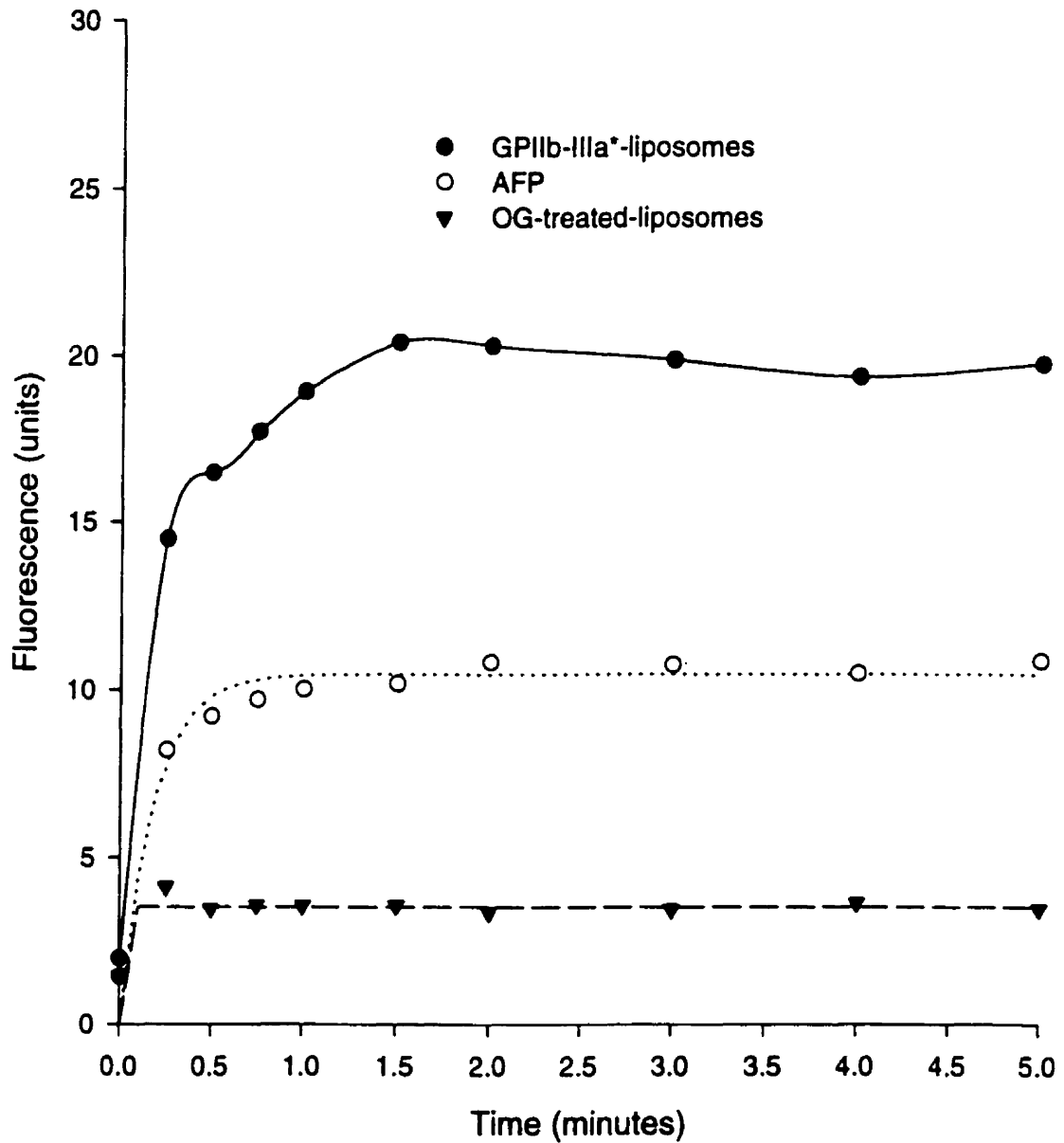
Liposomes or activated, fixed platelets ($\sim 1000/\mu$ l) were incubated with 25 nM Fg \pm 1 μ M Ro for 30 minutes at room temperature. Following dilution with buffer, 25 nM FITC-4A5 was added to the suspensions, which were incubated for another 5 minutes, further diluted, and read for 20 seconds on the FACScan to determine fluorescence. Results represent the mean of duplicate samples \pm SD.

Figure 22b: Specificity of FITC-anti-Fg-RIBS-I binding to Fg immobilized on liposomes and platelets



Liposomes or activated, fixed platelets ($\sim 1000/\mu$ l) were incubated with 25 nM Fg \pm 1 μ M Ro for 30 minutes at room temperature. Following dilution with buffer, 10 nM FITC-anti-Fg-RIBS-I was added to the suspensions, which were incubated for another 5 minutes, further diluted, and read for 20 seconds on the FACScan to determine fluorescence. Results represent the mean of duplicate samples \pm SD.

Figure 23: Time-dependence of FITC-4A5 binding to Fg immobilized on liposomes and platelets



Liposomes or activated, fixed platelets ($\sim 1000/\mu\text{l}$) were incubated with 25 nM Fg \pm 1 μM Ro for 30 minutes at room temperature. Following dilution with buffer, 25 nM FITC-4A5 was added to the suspensions, which were incubated for 0-5 minutes and read for 10 seconds at various timepoints on the FACScan to determine fluorescence.

CONCLUSIONS

Glycoprotein IIb-IIIa was incorporated into the bilayer of preformed large phospholipid/cholesterol vesicles by octyl glucoside-mediated membrane destabilization and subsequent detergent removal. These GPIIb-IIIa-liposomes were competent for fibrinogen binding, which was specific, saturable, time-dependent, and calcium-dependent, as is the case for Fg interactions with platelet GPIIb-IIIa. However, the liposomes bound Fg with a somewhat greater affinity than has been seen for platelets. Evaluation of GPIIb-IIIa-liposome immobilized Fg demonstrated the presence of free Fg γ chain C-termini available for crosslinking to adjacent vesicles.

Furthermore, liposome-immobilized Fg showed evidence of similar conformational changes upon binding to GPIIb-IIIa as occur for binding to platelets, as reported by a monoclonal antibody specific for a receptor-induced binding site on bound Fg.

In contrast to platelets, GPIIb-IIIa liposomes could not undergo specific co-aggregation with latex beads coupled to Fg. Although the liposomes did exhibit stir- and shear-induced aggregation in the presence of Fg, this aggregability was found to be non-specific, unlike the case for platelets. These results are consistent with studies done by other groups looking at Fg-GPIIb-IIIa-mediated aggregation in non-platelet systems. Such studies have demonstrated that centrifugation of GPIIb-IIIa-liposomes with Fg resulted in the formation of unstable aggregates, and that Chinese hamster ovary cells transfected with GPIIb-IIIa only aggregated under the near-static conditions of gyrorotation [Rybak 1986; Frojmovic et al. 1991a]. However, it has also been shown that latex beads coupled to GPIIb-IIIa underwent Fg-specific aggregation with both stir and shear [E Brown & M Frojmovic, unpublished data]. Receptor anchoring within the membrane or on the cell/particle surface may therefore be necessary for the formation of stable aggregates. As seen for platelets, the Fg-GPIIb-IIIa interaction is quickly stabilized by the binding of additional adhesive ligands to Fg and/or GPIIb-IIIa [Nurden 1994]; other important events are receptor clustering in the membrane, association with other membrane proteins like p24 [Slupsky et al. 1989], and

attachment to the actin cytoskeleton. Membrane lipids like palmitic acid and phosphatidic acid could also be involved in platelet aggregation [Schick 1994].

A number of experiments directly related to this project are worth pursuing. Firstly, it would be interesting to determine whether Fg immobilized on GPIIb-IIIa-liposomes could bind soluble GPIIb-IIIa under equilibrium conditions. This could be evaluated in a manner analogous to that used for 4A5 and anti-Fg-RIBS-I binding: allow unlabelled Fg to bind to the liposomes, add FITC-GPIIb-IIIa, and quantitate the fluorescence using the FACScan. Another simple flow cytometry assay would ascertain whether the GPIIb-IIIa reconstituted into liposomes undergoes the same type of conformational changes upon binding Fg as occur for the platelet receptor. This could be established by allowing Fg to bind to the liposomes, adding a fluorescently labelled anti-LIBS mAb like D3GP3 [Honda et al. 1996], and quantitating the fluorescence. It would also be worthwhile investigating whether the GPIIb-IIIa-liposomes could undergo Fg-specific aggregation under near-static conditions such as gyrorotation - as for the CHO cells [Frojmovic et al. 1991a] - or even diffusion, as has been previously observed for platelets [Longmire & Frojmovic 1990]. Finally, the possible extraction or 'fracture' of GPIIb-IIIa-Fg from the lipid bilayer during initiation of liposome cross-bridging in doublet formation, reported for red blood cell receptors not anchored via the cytoskeleton [Evans et al. 1991; Xia et al. 1994], could be explored with appropriate fluorescent labels and/or light-scattering techniques [Xia & van de Ven 1992].

Future GPIIb-IIIa-liposome studies may attempt to decrease bivalent Fg binding by way of a lower GPIIb-IIIa surface density; this could likely be accomplished by generating larger liposomes and/or by using a higher lipid:protein ratio. With regards to the liposomes themselves, it would be interesting to observe the effects of modifications in lipid bilayer composition on Fg binding and vesicle aggregation. This would not only help to elucidate the role of lipids in receptor function, but in addition may influence non-specific liposome aggregation and protein binding. For example, these processes may be reduced by lowering the bilayer phosphatidylserine content - as PS promotes aggregation in the presence of calcium [Grit & Crommelin 1993] - or by

the covalent attachment of molecules like polyethylene glycol [Blume & Cevc 1993]. However, generating liposomes with less bilayer packing defects - through better detergent removal - would presumably be the most effective means of decreasing non-specific adhesion and aggregation. It would also be desirable to develop a reconstitution technique which produces a higher yield of proteoliposomes than was seen for this project.

REFERENCES

- Agbanyo FR, Sixma JJ, de Groot PG, Languino LR, and Plow EF. Thrombospondin-platelet interactions: role of divalent cations, wall shear rate, and platelet membrane glycoproteins. *J Clin Invest* 92: 288-296, 1993.
- Altieri DC, Plescia J, and Plow EF. The structural motif glycine 190-valine 202 of the fibrinogen γ chain interacts with CD11b/CD18 integrin ($\alpha_M\beta_2$, Mac-1) and promotes leukocyte adhesion. *J Biol Chem* 268(3): 1847-1853, 1993.
- Bajt ML and Loftus JC. Mutation of a ligand binding domain of β_3 integrin: integral role of oxygenated residues in $\alpha_{IIb}\beta_3$ (GPIIb-IIIa) receptor function. *J Biol Chem* 269(33): 20913-20919, 1994.
- Baldassare JJ, Kahn RA, Knipp MA, and Newman PJ. Reconstitution of platelet proteins into phospholipid vesicles: functional proteoliposomes. *J Clin Invest* 75: 35-39, 1985.
- Bartlett GR. Phosphorus assay in column chromatography. *J Biol Chem* 234(3): 466-468, 1959.
- Bennett JS and Vilaire G. Exposure of platelet fibrinogen receptors by ADP and epinephrine. *J Clin Invest* 64: 1393-1401, 1979.
- Bennett JS. Mechanisms of platelet adhesion and aggregation: an update. *Hospital Practice (Office Edition)* 27(4): 124-140, 1992.
- Bergers JJ, Vingerhoeds MH, van Bloois L, Herron JN, Janssen LHM, Fischer MJE, and Crommelin DJA. The role of protein charge in protein-lipid interactions: pH-dependent changes of the electrophoretic mobility of liposomes through adsorption of water-soluble, globular proteins. *Biochemistry* 32: 4641-4649, 1993.
- Beumer S, IJsseldijk MJW, de Groot PG, and Sixma JJ. Platelet adhesion to fibronectin in flow: dependence on surface concentration and shear rate, role of platelet membrane glycoproteins GPIIb/IIIa and VLA-5, and inhibition by heparin. *Blood* 84(11): 3724-3733, 1994.
- Blume G and Cevc G. Molecular mechanism of the lipid vesicle longevity in vivo. *Biochim Biophys Acta* 1146: 157-168, 1993.
- Bonté F and Juliano RL. Interactions of liposomes with serum proteins. *Chem Phys Lipids* 40: 359-372, 1986.

Brass LF and Shattil SJ. Identification and function of the high affinity binding sites for Ca^{2+} on the surface of platelets. *J Clin Invest* 65: 626-632, 1984.

Brass LF. Ca^{2+} transport across the platelet plasma membrane. *J Biol Chem* 260(4): 2231-2236, 1985.

Brown CH III, Leverett LB, Lewis CW, Alfrey CP Jr, and Hellums JD. Morphological, biochemical, and functional changes in human platelets subjected to shear stress. *J Lab Clin Med* 86(3):462-471, 1975.

Brown E, Hooper L, Ho T, and Gresham H. Integrin-associated protein: a 50 kD-plasma membrane antigen physically and functionally associated with integrins. *J Cell Biol* 111: 2785-2794, 1990.

Calvete JJ. Clues for understanding the structure and function of a prototypic human integrin: the platelet glycoprotein IIb/IIIa complex. *Thromb Haemost* 72(1): 1-15, 1994.

Calvete JJ. On the structure and function of platelet integrin $\alpha_{IIb}\beta_3$, the fibrinogen receptor. *Proc Soc Exp Biol Med* 208: 346-360, 1995.

Charo IF, Nannizzi L, Phillips DR, Hsu MA, and Scarborough RM. Inhibition of fibrinogen binding to GPIIb-IIIa by a GP IIIa peptide. *J Biol Chem* 266(3): 1415-1421, 1991.

Charo IF, Kieffer N, and Phillips DR. Platelet membrane glycoproteins. In Colman RW, Hirsh J, Marder VJ, and Salzman EW (eds). Hemostasis and Thrombosis: Basic Principles and Clinical Practice, 3rd ed., pp. 489-507. Philadelphia: J.B. Lippincott Co., 1994.

Chen WJ, Goldstein JL, and Brown MS. NPXY, a sequence often found in cytoplasmic tails, is required for coated pit-mediated internalization of the low density lipoprotein receptor. *J Biol Chem* 265(6): 3116-3123, 1990.

Cheresh DA, Berliner SA, Vicente V, and Ruggeri ZM. Recognition of distinct adhesive sites on fibrinogen by related integrins on platelets and endothelial cells. *Cell* 58: 945-953, 1989.

Cierniewski CS, Krzeslowska J, Pawłowska Z, Witas H, and Meyer M. Palmitoylation of the glycoprotein IIb-IIIa complex in human blood platelets. *J Biol Chem* 264(21): 12158-12164, 1989.

Coller BS, Beer JH, Scudder LE, and Steinberg MH. Collagen-platelet interactions: evidence for a direct interaction of collagen with platelet GPIa/IIa and an indirect interaction with platelet GPIIb/IIIa mediated by adhesive proteins. *Blood* 74(1): 182-192, 1989.

Coller BS, Cheresch DA, Asch E, and Seligsohn U. Platelet vitronectin receptor expression differentiates Iraqi-Jewish from Arab patients with Glanzmann thrombasthenia in Israel. *Blood* 77(1): 75-83, 1991.

Coller BS, Anderson K, and Weisman HF. New antiplatelet agents: platelet GPIIb/IIIa antagonists. *Thromb Haemost* 74(1): 302-308, 1995.

Colman RW, Cook JJ, and Niewiarowski S. Mechanisms of platelet aggregation. In Colman RW, Hirsh J, Marder VJ, and Salzman EW (eds). Hemostasis and Thrombosis: Basic Principles and Clinical Practice, 3rd ed., pp. 508-523. Philadelphia: J.B. Lippincott Co., 1994.

Conforti G, Zanetti A, Pasquali-Ronchetti I, Quaglino D Jr, Neyroz P, and Dejana E. Modulation of vitronectin receptor binding by membrane lipid composition. *J Biol Chem* 265(7): 4011-4019, 1990.

Cramer EM, Berger G, and Berndt MC. Platelet α -granule and plasma membrane share two new components: CD9 and PECAM-1. *Blood* 84(6): 1722-1730, 1994.

Dedhar S and Hannigan GE. Integrin cytoplasmic interactions and bidirectional transmembrane signalling. *Curr Opin Cell Biol* 8: 657-669, 1996.

Diacovo TG, deFougerolles AR, Bainton DF, and Springer TA. A functional integrin ligand on the surface of platelets: intercellular adhesion molecule-2. *J Clin Invest* 94: 1243-1251, 1994.

Dixit VM, Haverstick DM, O'Rourke K, Hennessy SW, Broekelmann TJ, McDonald JA, Grant GA, Santoro SA, and Frazier WA. Inhibition of platelet aggregation by a monoclonal antibody against human fibronectin. *Proc Natl Acad Sci USA* 82: 3844-3848, 1985.

Doolittle RF, Everse SJ, and Spraggon G. Human fibrinogen: anticipating a 3-dimensional structure. *FASEB J* 10: 1464-1470, 1996.

Dorahy DJ, Thorne RF, Fecondo JV, and Burns GF. Stimulation of platelet activation and aggregation by a carboxyl-terminal peptide from thrombospondin binding to the integrin-associated protein receptor. *J Biol Chem* 272(2): 1323-1330, 1997.

D'Souza SE, Ginsberg MH, Burke TA, and Plow EF. The ligand binding site of the platelet integrin receptor GPIIb-IIIa is proximal to the second calcium binding domain of its α subunit. *J Biol Chem* 265(6): 3440-3446, 1990.

D'Souza SE, Ginsberg MH, Matsueda GR, and Plow EF. A discrete sequence in a platelet integrin is involved in ligand recognition. *Nature* 350: 66-68, 1991.

D'Souza SE, Haas TA, Piotrowicz RS, Byers-Ward V, McGrath DE, Soule HR, Cierniewski C, Plow EF, and Smith JW. Ligand and cation binding are dual functions of a discrete segment of the integrin β_3 subunit: cation displacement is involved in ligand binding. *Cell* 70: 659-667, 1994.

Du X, Plow EF, Frelinger AL III, O'Toole TE, Loftus JC, and Ginsberg MH. Ligands "activate" integrin $\alpha_{IIb}\beta_3$ (platelet GPIIb-IIIa). *Cell* 65: 409-416, 1991.

Elstad MR, La Pine TR, Cowley FS, McEver RP, McIntyre TM, Prescott SM, and Zimmerman GA. P-selectin regulates platelet-activating factor synthesis and phagocytosis by monocytes. *J Immunol* 155(4): 2109-2122, 1995.

Evans EA and Parsegian VA. Energetics of membrane deformation and adhesion in cell and vesicle aggregation. *Ann NY Acad Sci* 416: 13-33, 1983.

Evans E, Berk D, and Leung A. Detachment of agglutinin-bonded red blood cells. I. Forces to rupture molecular-point attachments. *Biophys J* 59: 838-848, 1991.

Farrell DH and Thiagarajan P. Binding of recombinant fibrinogen mutants to platelets. *J Biol Chem* 269(1): 226-231, 1994.

Fournier DJ, Kabral A, Castaldi PA, and Berndt MC. A variant of Glanzmann's thrombasthenia characterized by abnormal glycoprotein IIb/IIIa complex formation. *Thromb Haemost* 62(3): 977-983, 1989.

Fox JEB. The platelet cytoskeleton. *Thromb Haemost* 70(6): 884-893, 1993.

Frelinger AL III, Lam SCT, Plow EF, Smith MA, Loftus JC, and Ginsberg MH. Occupancy of an adhesive glycoprotein receptor modulates expression of an antigenic site involved in cell adhesion. *J Biol Chem* 263(25): 12397-12402, 1988.

Frelinger AL III, Cohen I, Plow EF, Smith MA, Roberts J, Lam SCT, and Ginsberg MH. Selective inhibition of integrin function by antibodies specific for ligand-occupied receptor conformers. *J Biol Chem* 265(11): 6346-6352, 1990.

Frelinger AL III, Du X, Plow EF, and Ginsberg MH. Monoclonal antibodies to ligand-occupied conformers of integrin $\alpha_{IIb}\beta_3$ (glycoprotein IIb-IIIa) alter receptor affinity, specificity, and function. *J Biol Chem* 266(26): 17106-17111, 1991.

Frojmovic MM and Milton JG. Human platelet size, shape, and related functions in health and disease. *Physiol Reviews* 62(1): 185-261, 1982.

Frojmovic MM, Milton JG, and Duchastel A. Microscopic measurements of platelet aggregation reveal a low ADP-dependent process distinct from turbidometrically measured aggregation. *J Lab Clin Med* 101: 964-976, 1983.

Frojmovic MM, Milton JG, and Gear AL. Platelet aggregation measured in vitro by microscopic and electronic particle counting. *Methods Enzymol* 169: 134-149, 1989.

Frojmovic MM, O'Toole TE, Plow EF, Loftus JC, and Ginsberg MH. Platelet glycoprotein IIb-IIIa ($\alpha_{IIb}\beta_3$ integrin) confers fibrinogen- and activation-dependent aggregation on heterologous cells. *Blood* 78(2): 369-376, 1991a.

Frojmovic M, Wong T, and van de Ven T. Dynamic measurements of the platelet membrane glycoprotein IIb-IIIa receptor for fibrinogen by flow cytometry. I. Methodology, theory and results for two distinct activators. *Biophys J* 59: 815-827, 1991b.

Frojmovic M and Wong T. Dynamic measurements of the platelet membrane glycoprotein IIb-IIIa receptor for fibrinogen by flow cytometry. II. Platelet size-dependent subpopulations. *Biophys J* 59: 828-837, 1991.

Frojmovic MM, Mooney RF, and Wong T. Dynamics of platelet glycoprotein IIb-IIIa receptor expression and fibrinogen binding. I. Quantal activation of platelet subpopulations varies with adenosine diphosphate concentration. *Biophys J* 67: 2060-2068, 1994.

Gailit J and Ruoslahti E. Regulation of the fibronectin receptor affinity by divalent cations. *J Biol Chem* 263(26): 12927-12932, 1988.

Gao AG, Lindberg FP, Finn MB, Blystone SD, Brown EJ, and Frazier WA. Integrin-associated protein is a receptor for the C-terminal domain of thrombospondin. *J Biol Chem* 271(1): 21-24, 1996.

Gartner TK, Amrani DL, Derrick JM, Kirschbaum NE, Matsueda GR, and Taylor DB. Characterization of adhesion of "resting" and stimulated platelets to fibrinogen and its fragments. *Thromb Res* 71: 47-60, 1993.

Gawaz M, Ott I, Reininger AJ, and Neumann FJ. Effects of magnesium on platelet aggregation and adhesion: magnesium modulates surface expression of glycoproteins on platelets in vitro and ex vivo. *Thromb Haemost* 72(6): 912-918, 1994.

Gawaz M, Ott I, Reininger AJ, Heinzmann U, and Neumann FJ. Agglutination of isolated platelet membranes. *Arterioscler Thromb Vasc Biol* 16: 621-627, 1996.

George JN and Nurden AT. Inherited disorders of the platelet membrane: Glanzmann Thrombasthenia, Bernard-Soulier syndrome, and other disorders. In Colman RW, Hirsh J, Marder VJ, and Salzman EW (eds). Hemostasis and Thrombosis: Basic Principles and Clinical Practice, 3rd ed., pp. 652-672. Philadelphia: J.B. Lippincott Co., 1994.

Gerrard JM. Platelet aggregation: cellular regulation and physiologic role. *Hospital Practice (Office Edition)*. 23(1): 89-108, 1988.

Gille J and Swerlick RA. Integrins: role in cell adhesion and communication. *Ann NY Acad Sci* 797: 93-106, 1996.

Ginsberg MH, Du X, O'Toole TE, Loftus JC, and Plow EF. Platelet integrins. *Thromb Haemost* 70(1): 87-93, 1993.

Gresham HD, Adams SP, and Brown EJ. Ligand binding specificity of the leukocyte response integrin expressed by human neutrophils. *J Biol Chem* 267(20): 13895-13902, 1992.

Grit M and Crommelin DJA. Chemical stability of liposomes: implications for their physical stability. *Chem Phys Lipids* 64: 3-18, 1993.

Hantgan RR, Francis CW, and Marder VJ. Fibrinogen structure and physiology. In Colman RW, Hirsh J, Marder VJ, and Salzman EW (eds). Hemostasis and Thrombosis: Basic Principles and Clinical Practice, 3rd ed., pp. 277-300. Philadelphia: J.B. Lippincott Co., 1994.

Harrison P, Wilbourn B, Debili N, Vainchenker W, Breton-Gorius J, Lawrie AS, Masse JM, Savidge GF, and Cramer EM. Uptake of plasma fibrinogen into the alpha granules of human megakaryocytes and platelets. *J Clin Invest* 84: 1320-1324, 1989.

Haskard DO. Adhesive proteins. In Bloom AL, Forbes CD, Thomas DP, and Tuddenham EGD (eds). Haemostasis and Thrombosis, 3rd ed., pp. 233-257. Edinburgh: Churchill Livingstone, 1994.

Hawiger J, Brass LF, and Salzman EW. Signal transduction and intracellular regulatory processes in platelets. *In* Colman RW, Hirsh J, Marder VJ, and Salzman EW (eds). Hemostasis and Thrombosis: Basic Principles and Clinical Practice, 3rd ed., pp. 603-628. Philadelphia: J.B. Lippincott Co., 1994.

Hawiger J. Mechanisms involved in platelet vessel wall interaction. *Thromb Haemost* 74(1): 369-372, 1995a.

Hawiger J. Adhesive ends of fibrinogen and its antiadhesive peptides: the end of a saga? *Semin Hematol* 32(2): 99-109, 1995b.

Hermanowski-Vosatka A, van Strijp JAG, Swiggard WJ, and Wright SD. Integrin modulating factor-1: a lipid that alters the function of leukocyte integrins. *Cell* 68: 342-352, 1992.

Hess S, Kanse SM, Kost C, and Preissner KT. The versatility of adhesion receptor ligands in haemostasis: morpho-regulatory functions of vitronectin. *Thromb Haemost* 74(1): 258-265, 1995.

Hettasch JM, Bolyard MG, and Lord ST. The residues AGDV of recombinant γ chains of human fibrinogen must be carboxy-terminal to support human platelet aggregation. *Thromb Haemost* 68(6): 701-706, 1992.

Hirsh J and Brain EA. Hemostasis and Thrombosis: a conceptual approach. New York: Churchill Livingstone, 1979.

Holmsen H. Platelet secretion and energy metabolism. *In* Colman RW, Hirsh J, Marder VJ, and Salzman EW (eds). Hemostasis and Thrombosis: Basic Principles and Clinical Practice, 3rd ed., pp. 524-545. Philadelphia: J.B. Lippincott Co., 1994.

Honda S, Tomiyama Y, Pelletier AJ, Annis D, Honda Y, Orchekowski R, Ruggeri Z, and Kunicki TJ. Topography of ligand-induced binding sites, including a novel cation-sensitive epitope (AP5) at the amino terminus, of the human integrin β_3 subunit. *J Biol Chem* 270(20): 11947-11954, 1995.

Hope MJ, Bally MB, Mayer LD, Janoff AS, and Cullis PR. Generation of multilamellar and unilamellar phospholipid vesicles. *Chem Phys Lipids* 40: 89-107, 1986.

Hu DD, Barbas CF III, and Smith JW. An allosteric Ca^{2+} binding site on the β_3 -integrins that regulates the dissociation rate for RGD ligands. *J Biol Chem* 271(36): 21745-21751, 1996.

Hughes PE, Diaz-Gonzalez F, Leong L, Wu C, McDonald JA, Shattil SJ, and Ginsberg MH. Breaking the integrin hinge: a defined structural constraint regulates integrin signaling. *J Biol Chem* 271(12): 6571-6574, 1996.

Hynes RO. Integrins: versatility, modulation, and signalling in cell adhesion. *Cell* 69: 11-25, 1992.

Ikeda Y, Handa M, Kawano K, Kamata T, Murata M, Araki Y, Anbo H, Kawai Y, Watanabe K, Itagaki I, Sakai K, and Ruggeri ZM. The role of von Willebrand Factor and fibrinogen in platelet aggregation under varying shear stress. *J Clin Invest* 87(4): 1234-1240, 1991.

Ikeda Y, Handa M, Kamata T, Kawano K, Kawai Y, Watanabe K, Kawakami K, Sakai K, Fukuyama M, Itagaki I, Yoshioka A, and Ruggeri ZM. Transmembrane calcium influx associated with von Willebrand Factor binding to GP Ib in the initiation of shear-induced platelet aggregation. *Thromb Haemost* 69(5): 496-502, 1993.

Israels SJ, McMillan EM, Robertson C, Singhroy S, and McNicol A. The lysosomal granule membrane protein, LAMP-2, is also present in platelet dense granule membranes. *Thromb Haemost* 75(4): 623-629, 1996.

Kamata T, Irie A, Tokuhira M, and Takada Y. Critical residues of integrin α_{IIb} subunit for binding of $\alpha_{IIb}\beta_3$ (glycoprotein IIb-IIIa) to fibrinogen and ligand-mimetic antibodies (PAC-1, OP-G2, and LJ-CP3). *J Biol Chem* 271(31): 18610-18615, 1996.

Kefalides NA. The biochemistry and molecular biology of extracellular matrix. In Colman RW, Hirsh J, Marder VJ, and Salzman EW (eds). Hemostasis and Thrombosis: Basic Principles and Clinical Practice, 3rd ed., pp. 745-761. Philadelphia: J.B. Lippincott Co., 1994.

Kehrel B. Platelet-collagen interactions. *Semin Thromb Hemost* 21(2): 123-129, 1995.

Knapp W, Dörken B, Rieber P, Schmidt RE, Stein H, and von dem Borne AEGK. CD Antigens 1989. *Blood* 74(4): 1448-1450, 1989.

Kouns WC, Wall CD, White MM, Fox CF, and Jennings LK. A conformation-dependent epitope of human platelet glycoprotein IIIa. *J Biol Chem* 265(33): 20594-20601, 1990.

Kroll MH, Hellums JD, McIntire LV, Schafer AI, and Moake JL. Platelets and shear stress. *Blood* 88(5): 1525-1541, 1996.

Languino LR, Duperray A, Joganic KJ, Fornaro M, Thornton GB, and Altieri DC. Regulation of leukocyte-endothelium interaction and leukocyte transendothelial migration by intracellular adhesion molecule 1-fibrinogen recognition. *Proc Natl Acad Sci USA* 92: 1505-1509, 1995.

Lawler J. Thrombospondins. In High KA and Roberts HR (eds). Molecular basis of thrombosis and hemostasis, pp. 621-638. New York: Marcel Dekker, 1995.

Legrand C, Thibert V, Dubernard V, Bégault B, and Lawler J. Molecular requirements for the interaction of thrombospondin with thrombin-activated human platelets: modulation of platelet aggregation. *Blood* 79(8): 1995-2003, 1992.

Legrand C, Morandi V, Mendelovitz S, Shaked H, Hartman JR, and Panet A. Selective inhibition of platelet macroaggregate formation by a recombinant heparin-binding domain of human thrombospondin. *Arterioscler Thromb* 14: 1784-1791, 1994.

Leung L and Nachman R. Molecular mechanisms of platelet aggregation. *Ann Rev Med* 37: 179-186, 1986.

Lis LJ, Kauffman JW, and Shriver DF. Raman spectroscopic detection and examination of the interaction of amino acids, polypeptides and proteins with the phosphatidylcholine lamellar structure. *Biochim Biophys Acta* 436: 513-522, 1976.

Loftus JC, O'Toole TE, Plow EF, Glass A, Frelinger AL III, and Ginsberg MH. A β_3 integrin mutation abolishes ligand binding and alters divalent cation-dependent conformation. *Science* 249: 915-918, 1990.

Loike JD, Sodeik B, Cao L, Leucona S, Weitz JI, Detmers PA, Wright SD, and Silverstein SC. CD11c/CD18 on neutrophils recognizes a domain at the N terminus of the A α chain of fibrinogen. *Proc Natl Acad Sci USA* 88: 1044-1048, 1991.

Longmire K and Frojmovic M. Long-range interactions in mammalian platelet aggregation. I. Evidence from kinetic studies in Brownian diffusion. *Biophys J* 58: 299-307, 1990.

Marcus AJ. Platelet lipids. In Colman RW, Hirsh J, Marder VJ, and Salzman EW (eds). Hemostasis and Thrombosis, pp. 472-485. Philadelphia: J.B. Lippincott Co., 1982.

Marguerie GA, Plow EF, and Edgington TS. Human platelets possess an inducible and saturable receptor specific for fibrinogen. *J Biol Chem* 254(12): 5357-5363, 1979.

Metzelaar MJ and Clevers MC. Lysosomal membrane glycoproteins in platelets. *Thromb Haemost* 68(4): 378-382, 1992.

Meyer D and Girma JP. Von Willebrand Factor: structure and function. *Thromb Haemost* 70(1): 99-104, 1993.

Mohri H, Tanabe J, Katoh K, and Okubo T. Identification of a novel binding site to the integrin $\alpha_{\text{Ib}}\beta_3$ located in the C-terminal heparin-binding domain of human plasma fibronectin. *J Biol Chem* 271(26): 15724-15728, 1996.

Montgomery RR and Collier BS. Von Willebrand Disease. In Colman RW, Hirsh J, Marder VJ, and Salzman EW (eds). Hemostasis and Thrombosis: Basic Principles and Clinical Practice, 3rd ed., pp. 134-168. Philadelphia: J.B. Lippincott Co., 1994.

Müller B, Zerwes HG, Tangemann K, Peter J, and Engel J. Two-step binding mechanism of fibrinogen to $\alpha_{\text{Ib}}\beta_3$ integrin reconstituted into planar lipid bilayers. *J Biol Chem* 268(9): 6800-6808, 1993.

Newman PJ. Platelet GPIIb-IIIa: molecular variations and alloantigens. *Thromb Haemost* 66(1): 111-118, 1991.

Newman PJ. Nomenclature of human platelet alloantigens: a problem with the HPA system? *Blood* 83(6): 1447-1451, 1994.

Niewiarowski S, Kornecki E, Budzynski AZ, Morinelli TA, and Tuszynski GP. Fibrinogen interaction with platelet receptors. *Ann New York Acad Sci* 408: 536-555, 1983.

Niewiarowski S, McLane MA, Kloczewiak M, and Stewart GJ. Disintegrins and other naturally occurring antagonists of platelet fibrinogen receptors. *Semin Hematol* 31(4): 289-300, 1994.

Niiya K, Hodson E, Bader R, Byers-Ward V, Koziol JA, Plow EF, and Ruggeri ZM. Increased surface expression of the membrane glycoprotein IIb/IIIa complex induced by platelet activation. Relationship to the binding of fibrinogen and platelet aggregation. *Blood* 70(2): 475-483, 1987.

Nurden AT. Human platelet membrane glycoproteins. In Bloom AL, Forbes CD, Thomas DP, and Tuddenham EGD (eds). Haemostasis and Thrombosis, 3rd ed., pp. 115-165. Edinburgh: Churchill Livingstone, 1994.

Nurden P, Humbert M, Piotrowicz RS, Bihour C, Poujol C, Nurden AT, and Kunicki TJ. Distribution of ligand-occupied $\alpha_{\text{Ib}}\beta_3$ in resting and activated human platelets determined by expression of a novel class of ligand-induced binding site recognized by monoclonal antibody AP6. *Blood* 88(3): 887-899, 1996.

Parise LV and Phillips DR. Reconstitution of the purified platelet fibrinogen receptor: fibrinogen binding properties of the glycoprotein IIb-IIIa complex. *J Biol Chem* 260(19): 10698-10707, 1985.

Parise LV and Phillips DR. Fibronectin-binding properties of the purified platelet glycoprotein IIb-IIIa complex. *J Biol Chem* 261(30): 14011-14017, 1986.

Parise LV, Helgerson SL, Steiner B, Nannizzi L, and Phillips DR. Synthetic peptides derived from fibrinogen and fibronectin change the conformation of purified platelet glycoprotein IIb-IIIa. *J Biol Chem* 262(26): 12597-12602, 1987.

Parsegian VA, Fuller N, and Rand RP. Measured work of deformation and repulsion of lecithin bilayers. *Proc Natl Acad Sci USA* 76(6): 2750-2754, 1979.

Parsegian VA and Rand RP. Membrane interaction and deformation. *Ann NY Acad Sci* 416: 1-12, 1983.

Paternostre MT, Roux M, and Rigaud JL. Mechanisms of membrane protein insertion into liposomes during reconstitution procedures involving the use of detergents. 1. Solubilization of large unilamellar liposomes (prepared by reverse-phase evaporation) by Triton X-100, octyl glucoside, and sodium cholate. *Biochemistry* 27: 2668-2677, 1988.

Pedvis LG, Wong T, and Frojmovic MM. Differential inhibition of the platelet activation sequence: shape change, micro- and macro-aggregation, by a stable prostacyclin analogue (Iloprost). *Thromb Haemost* 59(2): 323-328, 1988.

Peerschke EIB. Events occurring after thrombin-induced fibrinogen binding to platelets. *Semin Thromb Hemost* 18(1): 34-43, 1992.

Peerschke EIB. Bound fibrinogen distribution on stimulated platelets: examination by confocal scanning laser microscopy. *Am J Pathol* 147(3): 678-687, 1995.

Peterson DM, Stathopoulos NA, Giorgio TD, Hellums JD, and Moake JL. Shear-induced platelet aggregation requires von Willebrand Factor and platelet membrane glycoproteins Ib and IIb-IIIa. *Blood* 69(2): 625-628, 1987.

Philippeaux MM, Vesin C, Tacchini-Cottier F, and Piguet PF. Activated human platelets express β_2 integrin. *Eur J Haematol* 56: 130-137, 1996.

Philippot J, Mutaftschiev S, and Liautard JP. A very mild method allowing the encapsulation of very high amounts of macromolecules into very large (1000 nm) unilamellar liposomes. *Biochim Biophys Acta* 734: 137-143, 1983.

Phillips DR and Agin PP. Platelet membrane defects in Glanzmann's thrombasthenia: evidence for decreased amounts of two major glycoproteins. *J Clin Invest* 60: 535-545, 1977.

Phillips DR. Platelet membranes and receptor function. In Colman RW, Hirsh J, Marder VJ, and Salzman EW (eds). Hemostasis and Thrombosis, pp. 444-458. Philadelphia: J.B. Lippincott Co., 1982.

Phillips DR, Charo IF, Parise LV, and Fitzgerald LA. The platelet membrane glycoprotein IIb-IIIa complex. *Blood* 71(4): 831-843, 1988.

Phillips DR, Fitzgerald L, Parise L, and Steiner B. Platelet membrane glycoprotein IIb-IIIa complex: purification, characterization, and reconstitution into phospholipid vesicles. *Methods Enzymol* 215: 244-263, 1992.

Pidard D, Montgomery RR, Bennett JS, and Kunicki TJ. Interaction of AP-2, a monoclonal antibody specific for the human platelet glycoprotein IIb-IIIa complex, with intact platelets. *J Biol Chem* 258(20): 12582-12586, 1983.

Plow EF, Ginsberg MH, and Marguerie G. Regulation of platelet aggregation by inducible receptors for fibrinogen. In Conn PM (ed). The Receptors, vol. I, pp. 466-510. Orlando: Academic Press Inc., 1984.

Plow EF and Ginsberg MH. Cellular adhesion: GPIIb-IIIa as a prototypic adhesion receptor. *Prog Hemost Thromb* 9: 117-156, 1989.

Preissner KT and Jenne D. Structure of vitronectin and its biological role in haemostasis. *Thromb Haemost* 66(1): 123-132, 1991.

Prieto J, Eklund A, and Patarroyo M. Regulated expression of integrins and other adhesion molecules during differentiation of monocytes into macrophages. *Cellular Immunol* 156: 191-211, 1994.

Pytela R, Pierschbacher MD, Ginsberg MH, Plow EF, and Ruoslahti E. Platelet membrane glycoprotein IIb/IIIa: member of a family of Arg-Gly-Asp-specific adhesion receptors. *Science* 231: 1559-1562, 1986.

Rabhi-Sabile S, Thibert V, and Legrand C. Thrombospondin peptides inhibit the secretion-dependent phase of platelet aggregation. *Blood Coagulation and Fibrinolysis* 7: 237-240, 1996.

Ramsamooj P, Doellgast GJ, and Hantgan RR. Inhibition of fibrin(ogen) binding to stimulated platelets by a monoclonal antibody specific for a conformational determinant of GPIIIa. *Thromb Res* 58:577-592, 1990.

Rigaud JL, Pitard B, and Levy D. Reconstitution of membrane proteins into liposomes: application to energy-transducing membrane proteins. *Biochim Biophys Acta* 1231: 223-246, 1995.

Rivas GA and González-Rodríguez J. Calcium binding to human platelet integrin GPIIb/IIIa and to its constituent glycoproteins: effects of lipids and temperature. *Biochem J* 276: 35-40, 1991.

Ruf A and Patscheke H. Platelet-induced neutrophil activation: platelet-expressed fibrinogen induces the oxidative burst in neutrophils by an interaction with CD11c/CD18. *Br J Haematol* 90: 791-796, 1995.

Ruggeri ZM. New insights into the mechanisms of platelet adhesion and aggregation. *Semin Hematol* 31(3): 229-239, 1994.

Rybak ME. Glycoproteins IIb and IIIa and platelet thrombospondin in a liposome model of platelet aggregation. *Thromb Haemost* 55(2): 240-245, 1986.

Rybak ME, Renzulli LA, Bruns MJ, and Cahaly DP. Platelet glycoproteins IIb and IIIa as a calcium channel in liposomes. *Blood* 72(2): 714-720, 1988.

Rybak ME and Renzulli LA. A liposome based platelet substitute, the plateletsome, with hemostatic efficacy. *Biomater Art Cells Immob Biotech* 21(2): 101-118, 1993.

Saelman EUM, Nieuwenhuis HK, Hese KM, de Groot PG, Heijnen HFG, Sage EH, Williams S, McKeown L, Gralnick HR, and Sixma JJ. Platelet adhesion to collagen types I through VIII under conditions of stasis and flow is mediated by GPIa/IIa ($\alpha_2\beta_1$ - integrin). *Blood* 83(5): 1244-1250, 1994.

Savage B and Ruggeri ZM. Selective recognition of adhesive sites in surface-bound fibrinogen by glycoprotein IIb/IIIa on nonactivated platelets. *J Biol Chem* 266(17): 11227-11233, 1991.

Savage B, Shattil SJ, and Ruggeri ZM. Modulation of platelet function through adhesion receptors: a dual role for glycoprotein IIb-IIIa (integrin $\alpha_{IIb}\beta_3$) mediated by fibrinogen and glycoprotein Ib-von Willebrand Factor. *J Biol Chem* 267(16): 11300-11306, 1992.

Savage B, Bottini E, and Ruggeri ZM. Interaction of integrin $\alpha_{\text{IIb}}\beta_3$ with multiple fibrinogen domains during platelet adhesion. *J Biol Chem* 270(48): 28812-28817, 1995.

Savage B, Saldívar E, and Ruggeri ZM. Initiation of platelet adhesion by arrest onto fibrinogen or translocation on von Willebrand Factor. *Cell* 84: 289-297, 1996.

Scatchard G. The attraction of proteins for small molecules and ions. *Ann NY Acad Sci* 51: 660-672, 1949.

Schick PK. Megakaryocyte and platelet lipids. In Colman RW, Hirsh J, Marder VJ, and Salzman EW (eds). Hemostasis and Thrombosis: Basic Principles and Clinical Practice, 3rd ed., pp. 574-589. Philadelphia: J.B. Lippincott Co., 1994.

Schick PK, Wojenski CM, Bennett VD, and Ivanova T. The synthesis and localization of alternatively spliced fibronectin EIIIB in resting and thrombin-treated megakaryocytes. *Blood* 87(5): 1817-1823, 1996.

Schlossman SF, Bournsell L, Gilks W, Harlan JM, Kishimoto T, Morimoto C, Ritz J, Shaw S, Silverstein RL, Springer TA, Tedder TF, and Todd RF. CD Antigens 1993. *Blood* 83(4): 879-880, 1994.

Schnapp LM, Hatch N, Ramos DM, Klimanskaya IV, Sheppard D, and Pytela R. The human integrin $\alpha_8\beta_1$ functions as a receptor for tenascin, fibronectin, and vitronectin. *J Biol Chem* 270(39): 23196-23202, 1995.

Schwartz MA, Schaller MD, and Ginsberg MH. Integrins: emerging paradigms of signal transduction. *Annu Rev Cell Dev Biol* 11: 549-599, 1995.

Scotto AW, Goodwyn D, and Zakim D. Reconstitution of membrane proteins: sequential incorporation of integral membrane proteins into preformed lipid bilayers. *Biochemistry* 26: 833-839, 1987.

Semple SC, Chonn A, and Cullis PR. Influence of cholesterol on the association of plasma proteins with liposomes. *Biochemistry* 35: 2521-2525, 1996.

Shadle PJ, Ginsberg MH, Plow EF, and Baronides SH. Platelet-collagen adhesion: inhibition by a monoclonal antibody that binds glycoprotein IIb. *J Cell Biol* 99: 2056-2060, 1984.

Shattil SJ, Hoxie JA, Cunningham M, and Brass LF. Changes in the platelet membrane glycoprotein IIb-IIIa complex during platelet activation. *J Biol Chem* 260(20): 11107-11114, 1985.

Shattil SJ, Cunningham M, and Hoxie JA. Detection of activated platelets in whole blood using activation-dependent monoclonal antibodies and flow cytometry. *Blood* 70(1): 307-315, 1987.

Shattil SJ. Regulation of platelet anchorage and signaling by integrin $\alpha_{\text{IIb}}\beta_3$. *Thromb Haemost* 70(1): 224-228, 1993.

Shiba E, Lindon JN, Kushner L, Matsueda GR, Hawiger J, Kloczewiak M, Kudryk B, and Salzman EW. Antibody-detectable changes in fibrinogen adsorption affecting platelet activation on polymer surfaces. *Am J Physiol* 260: C965-C974, 1991.

Si-Tahar M, Pidard D, Balloy V, Moniatte M, Kieffer N, van Dorsselaer A, and Chignard M. Human neutrophil elastase proteolytically activates the platelet integrin $\alpha_{\text{IIb}}\beta_3$ through cleavage of the carboxyl terminus of the α_{IIb} subunit heavy chain: involvement in the potentiation of platelet aggregation. *J Biol Chem* 272(17): 11636-11647, 1997.

Sixma JJ. Interaction of blood platelets with the vessel wall. In Bloom AL, Forbes CD, Thomas DP, and Tuddenham EGD (eds). *Haemostasis and Thrombosis*, 3rd ed., pp. 259-285. Edinburgh: Churchill Livingstone, 1994.

Slupsky JR, Seehafer JG, Tang SC, Masellis-Smith A, and Shaw ARE. Evidence that monoclonal antibodies against CD9 antigen induce specific association between CD9 and the platelet glycoprotein IIb-IIIa complex. *J Biol Chem* 264(21): 12289-12293, 1989.

Smyth SS, Hillery CA, and Parise LV. Fibrinogen binding to purified platelet glycoprotein IIb-IIIa (integrin $\alpha_{\text{IIb}}\beta_3$) is modulated by lipids. *J Biol Chem* 267(22): 15568-15577, 1992.

Stamatatos L and Silvius JR. Effects of cholesterol on the divalent cation-mediated interactions of vesicles containing amino and choline phospholipids. *Biochim Biophys Acta* 905: 81-90, 1987.

Steiner B, Cousot D, Trzeciak A, Gillessen D, and Hadvary P. Ca^{2+} -dependent binding of a synthetic Arg-Gly-Asp (RGD) peptide to a single site on the purified platelet glycoprotein IIb-IIIa complex. *J Biol Chem* 264(22): 13102-13108, 1989.

Stryer L. *Biochemistry*, pp. 230-233. San Francisco: W.H. Freeman & Co., 1975.

Szoka F Jr and Papahadjopoulos D. Procedure for preparation of liposomes with large internal aqueous space and high capture by reverse-phase evaporation. *Proc Natl Acad Sci USA* 75(9): 4194-4198, 1978.

Szoka F Jr and Papahadjopoulos D. Comparative properties and methods of preparation of lipid vesicles (liposomes). *Ann Rev Biophys Bioeng* 9: 467-508, 1980.

Tandon NN, Holland EA, Kralisz U, Kleinman HK, Robey FA, and Jamieson GA. Interaction of human platelets with laminin and identification of the 67 kDa laminin receptor on platelets. *Biochem J* 274: 535-542, 1991.

Taylor D and Gartner T. A peptide corresponding to GPIIb_a 300-312, a presumptive fibrinogen gamma-chain binding site on the platelet integrin GPIIb/IIIa, inhibits the adhesion of platelets to at least four adhesive ligands. *J Biol Chem* 267: 11729-11733, 1992.

Tozer EC, Liddington RC, Sutcliffe MJ, Smeeton AH, and Loftus JC. Ligand binding to integrin subunit $\alpha_{IIb}\beta_3$ is dependent on a MIDAS-like domain in the β_3 subunit. *J Biol Chem* 271(36): 21978-21984, 1996.

Trikha M, Timar J, Lundy SK, Szekeres K, Tang K, Grignon D, Porter AT, and Honn KV. Human prostate carcinoma cells express functional $\alpha_{IIb}\beta_3$ integrin. *Cancer Res* 56: 5071-5078, 1996.

Tuszynski GP, Rothman VL, Murphy A, Siegler K, and Knudsen KA. Thrombospondin promotes platelet aggregation. *Blood* 72(1): 109-115, 1988.

Ugarova TP, Budzynski AZ, Shattil SJ, Ruggeri ZM, Ginsberg MH, and Plow EF. Conformational changes in fibrinogen elicited by its interaction with platelet membrane glycoprotein GPIIb-IIIa. *J Biol Chem* 268(28): 21080-21087, 1993.

van der Vieren M, le Trong H, Wood CL, Moore PF, St. John T, Staunton DE, and Gallatin WM. A novel leukointegrin, $\alpha_V\beta_2$, binds preferentially to ICAM-3. *Immunity* 3(6): 683-690, 1995.

Wagner CL, Mascelli MA, Neblock DS, Weisman HF, Collier BS, and Jordan RE. Analysis of GPIIb/IIIa receptor number by quantification of 7E3 binding to human platelets. *Blood* 88(3): 907-914, 1996.

Walsh PN. Platelet-coagulant protein interactions. *In* Colman RW, Hirsh J, Marder VJ, and Salzman EW (eds). Hemostasis and Thrombosis: Basic Principles and Clinical Practice, 3rd ed., pp. 629-651. Philadelphia: J.B. Lippincott Co., 1994.

Walter A and Siegel DP. Divalent cation-induced lipid mixing between phosphatidylserine liposomes studied by stopped-flow fluorescence measurements: effects of temperature, comparison of barium and calcium, and perturbation by DPX. *Biochemistry* 32: 3271-3281, 1993.

Wright SD, Weitz JI, Huang AJ, Levin SM, Silverstein SC, and Loike JD. Complement receptor type three (CD11b/CD18) of human polymorphonuclear leukocytes recognizes fibrinogen. *Proc Natl Acad Sci USA* 85: 7734-7738, 1988.

Wu C and Chung AE. Potential role of entactin in hemostasis: specific interaction of entactin with fibrinogen A α and B β chains. *J Biol Chem* 266(28): 18802-18807, 1991.

Xia Z and van de Ven TGM. Adhesion kinetics of phosphatidylcholine liposomes by evanescent wave light scattering. *Langmuir* 8: 2938-2946, 1992.

Xia Z and Frojmovic MM. Aggregation efficiency of activated normal or fixed platelets in a simple shear field: effect of shear and fibrinogen occupancy. *Biophys J* 66: 2190-2201, 1994.

Xia Z, Goldsmith HL, and van de Ven TG. Flow-induced detachment of red blood cells adhering to surfaces by specific antigen-antibody bonds. *Biophys J* 66: 1222-1230, 1994.

Xia Z, Wong T, Liu Q, Kasirer-Friede A, Brown E, and Frojmovic MM. Optimally functional fluorescein isothiocyanate-labelled fibrinogen for quantitative studies of binding to activated platelets and platelet aggregation. *Br J Haematol* 93(1): 204-214, 1996.

Yamada Y and Kleinman HK. Functional domains of cell adhesion molecules. *Curr Opin Cell Biol* 4: 819-823, 1992.

Yung W and Frojmovic MM. Platelet aggregation in laminar flow. I. Adenosine diphosphate concentration, time and shear rate dependence. *Thromb Res* 28: 361-377, 1982.

Zamarron C, Ginsberg MH, and Plow EF. A receptor-induced binding site in fibrinogen elicited by its interaction with platelet membrane glycoprotein IIb-IIIa. *J Biol Chem* 266(24): 16193-16199, 1991.

Zucker MB and Nachmias VT. Platelet activation. *Arteriosclerosis* 5: 2-18, 1985.